

**Palacký University Olomouc, Faculty of Science,
Department of Geoinformatics**

**Paris Lodron University Salzburg, Faculty of Natural Sciences,
Department of Geoinformatics**

MAPPING AND MONITORING SLUMS USING GEOINFORMATION TECHNOLOGIES

Diploma thesis

Author

Sheriff Oluwagbenga JIMOH

Supervisor (Palacký University Olomouc)

RNDr. Jan BRUS, Ph.D.

Co-supervisor (Paris Lodron University Salzburg)

Assoc. Prof. Stefan LANG, Ph.D.

**Erasmus Mundus Joint Master Degree Programme
Copernicus Master in Digital Earth
Specialization Track Geovisualization & Geocommunication
Olomouc, Czech Republic, 2021**



Palacký University
Olomouc



With the support of the
Erasmus+ Programme
of the European Union

ANNOTATION

The main objective of this study is to map and monitor slums using geoinformation technologies with more focus on the comparison of GIS and image analysis methods, of remotely sensed imagery (i.e. pixel-based, object-based and deep learning) and their algorithms (maximum likelihood, random trees, support vector machine and U-Net classifier) thereby choosing the optimal algorithm for slum mapping. Two study areas were chosen for this thesis: Lagos Mainland LGA (Nigeria) and Vila Andrade district (Brazil). The dataset used are Sentinel-2 imagery of the two study areas, drone imagery of Lagos Mainland LGA, orthophoto of Vila Andrade district and their respective administrative boundaries. This study adopted the different methods within the overall strategy supervised image classification where classification schema was created with five classes (slums, non-slums, vegetation, water and roads). Training samples were selected from each imagery which were then used to train the algorithms for the classification proper. The classification results for all dataset were assessed using the site-specific accuracy assessment including error matrix. The results were published as Web Map Service (classification results) and WFS (the administrative boundaries) using Geoserver to aid their usage in the web application environment. The web application was developed with a leaflet software and VS code editor to visualize the results. The results of this study showed that the SVM algorithm outperformed other algorithms within the pixel and object-based methods, although the object-based SVM performed better with an overall accuracy of 68% over the pixel-based SVM (63.1%). The RT algorithm for both pixel and object-based methods had 58.4% and 52.8% accuracy, followed by the ML algorithm with an overall accuracy of 49.8% and 38.7% for both methods. The deep learning U-Net algorithm had an overall accuracy of 60%.

KEYWORDS

Deep learning, Drone, GIS, Informal settlements, LIDAR, Maximum likelihood, Object-based image analysis, Orthophoto, Pixel-based analysis, Random trees, Remote sensing, Sentinel-2 imagery, Support vector machine, Urbanization.

Number of pages: 62

Number of appendixes: 13

DECLARATION

This thesis has been composed by *Sheriff Oluwagbenga JIMOH* for the Erasmus Mundus Joint Master's Degree Program in Copernicus Master in Digital Earth for the academic year 2020/2021 at the Department of Geoinformatics, Faculty of Natural Sciences, Paris Lodron University Salzburg, and Department of Geoinformatics, Faculty of Science, Palacký University Olomouc.

Hereby, I declare that this piece of work is entirely my own, the references cited have been acknowledged and the thesis has not been previously submitted to the fulfilment of the higher degree.

20/05/2021, Olomouc

Sheriff Oluwagbenga JIMOH

ACKNOWLEDGMENTS

I would like to appreciate the selfless and unrelenting efforts of my supervisors, RNDr. Jan Brus, Ph.D. and Assoc. Prof. Stefan Lang, Ph.D. Your guidance, mentorship, and support from the beginning of the project until the end paved the way for me to achieve this thesis. I am very honoured to have chosen both of you as my supervisors and I enjoyed our collaboration.

My heartfelt gratitude goes to the Head of departments of both universities (Paris Lodron University Salzburg and Palacky University Olomouc); Prof. Josef Strobl and Prof. Vit Vozenilek, respectively for your fatherly guidance and assistance throughout the master programme. It was well appreciated, and I would never take it for granted.

My appreciation extends to the lecturers and the entire staffers of both universities for the warm reception, knowledge impartment and total support. I learnt a lot from your lectures, seminars, workshops and practical classes.

To my CDE cohort, I profoundly appreciate you guys. Your diverse ideas and innovative mindsets made the master programme very distinct and enjoyable. I'm glad to have had the opportunity to meet and collaborated with you all, and I look forward to more collaboration in future endeavours.

I would like to thank my wife, Mrs Habibat Jimoh, for her perseverance and endurance during my studies abroad. Your confidence in me and words of encouragement took me this far, and I will forever cherish you.

To my family and friends who impacted my life in one way or another during my study, even though you were thousands of miles away, I give thanks to you all.

Palacký University Olomouc

Faculty of Science

Academic year: 2020/2021

ASSIGNMENT OF DIPLOMA THESIS

(project, art work, art performance)

Name and surname: Sheriff Oluwagbenga JIMOH
Personal number: R200663
Study programme: N0532A330010 Geoinformatics and Cartography
Field of study: Geoinformatics and Cartography
Work topic: Mapping and Monitoring Slums Using Geoinformation Technologies
Assigning department: Department of Geoinformatics

Theses guidelines

The aim of the thesis is to develop a test methodology for mapping and monitoring slums primarily using open data. The student will explore the possibility of mapping slums within cities by using satellite imagery, geophysical datasets, and complementary data. The partial aim is to use identical input data, comparing the performance of different algorithms to monitor slums and determine which algorithm provides the optimal results. The result will be maps, graph and optimal workflow of mapping and monitoring slums in the context of spreading the epidemic. The student will attach all the collected datasets and all the animations to the thesis in digital form. The student will create a website about the thesis following the rules available on the department's website and a poster about the diploma thesis in A2 format. The student will submit entire text (text, attachments, poster, outputs, input and output data) in digital form on a storage medium and the text of the thesis in two bound copies to the secretary of the department.

Extent of work report: max 50 pages
Extent of graphics content: as needed
Form processing of diploma thesis: printed
Language of elaboration: English

Recommended resources:

- KOHLI, D., A. STEIN AND R. SLIUZAS Uncertainty analysis for image interpretations of urban slums. *Computers, Environment and Urban Systems*, 2016, 60, 37-49.
- MACHADO, R. P. P. AND J. C. PEDRASSOLI Remote sensing applications to identify and analyze slums over the Sao Paulo Metropolitan Area: a two case studies methodologies comparison.
- OLAJUYIGBE, A. E., S. A.-A. ADEGBOYEGA AND I. OJEABUO Household-Based Mapping of Slum Severity Using Satellite Imageries and GIS Technology: Example from Ondo Core Area, Nigeria. *Ife Research Publications in Geography*, 2016, 13(1), 1-18.
- RANGUELOVA, E., B. WEEL, D. ROY, M. KUFFER, et al. Image based classification of slums, built-up and non-built-up areas in Kalyan and Bangalore, India. *European journal of remote sensing*, 2019, 52(sup1), 40-61.
- RIBEIRO, S., M. JARZABEK-RYCHARD, J. CINTRA AND H.-G. MAAS Describing the vertical structure of informal settlements on the basis of lidar data a case study for favelas (slums) in Sao Paulo city. *ISPRS Annals of Photogrammetry, Remote Sensing & Spatial Information Sciences*, 2019, 4.
- WURM, M. AND H. TAUBENBÖCK Detecting social groups from space Assessment of remote sensing-based mapped morphological slums using income data. *Remote Sensing Letters*, 2018, 9(1), 41-50.
- VOŽENÍLEK, V. *Diplomové práce z geoinformatiky*. Edition ed. Olomouc: Vydavatelství Univerzity Palackého, 2002.

Supervisors of diploma thesis: **RNDr. Jan Brus, Ph.D.**
Department of Geoinformatics

Date of assignment of diploma thesis: **November 9, 2020**

Submission deadline of diploma thesis: **May 6, 2021**

UNIVERZITA PALACKÉHO V OLOMOUCI
PŘÍRODOVĚDECKÁ FAKULTA
KATEDRA GEOINFORMATIKY
17. listopadu 50, 771 46 Olomouc

L.S.

doc. RNDr. Martin Kubala, Ph.D.
Dean

prof. RNDr. Vít Voženílek, CSc.
Head of Department

Olomouc December 14, 2020

CONTENT

LIST OF ABBREVIATIONS	X
INTRODUCTION	X
1 OBJECTIVES.....	12
2 METHODOLOGY.....	13
2.1 Study Area	13
2.2 Data	15
2.2.1 Satellite Imagery	15
2.2.2 Drone imagery of Makoko and environs	16
2.2.3 Orthophoto of Vila Andrade	16
2.2.4 Administrative Boundaries of the Study Areas	16
2.3 Methods Adopted	17
2.3.1 Software Used	17
2.3.2 Workflow diagram	17
3 STATE OF THE ART	18
3.1 Background.....	18
3.2 Slum Mapping and Monitoring Approaches	18
3.2.1 Survey and Census-Based Approach	18
3.2.2 Participatory-Based Approach	19
3.2.3 GIS and Image Analysis Approach	20
3.2.3.1 Methods in the GIS and Image Analysis Approach	21
3.2.3.2 Review and Comparison of the methods in GIS and RS Approach....	24
4 PROCEDURES	26
4.1 Data acquisition	26
4.1.1 Acquisition of Sentinel-2 imagery from Open Access Hub	26
4.1.2 Drone mission of Makoko and environs	28
4.1.3 Acquisition of Vila Andrade Orthophoto	28
4.1.4 Downloading the administrative boundaries	30
4.2 Processing and Analysis.....	31
4.2.1 Image Mosaicing	31
4.2.2 Image Classification	31
4.2.3 Classification Wizard in ArcGIS Pro	31
4.2.4 Supervised Classification (Pixel and Object-Based).....	32
4.2.4.1 Classification schema and classes.....	34
4.2.4.2 Image Segmentation	34
4.2.4.3 Selection of training samples.....	34
4.2.4.4 Training and applying the algorithms (classifiers)	35
4.2.4.5 Maximum Likelihood (ML) Algorithm	35
4.2.4.6 Random Trees (RT) Algorithm.....	36
4.2.4.7 Support Vector Machine (SVM) Algorithm.....	37
4.2.4.8 Class Merging.....	37
4.2.5 Deep Learning (DL) Classification in ArcGIS Pro.....	38

4.2.5.1	U-Net Model	38
4.3	Reference or Ground truth Dataset	39
4.4	Classification accuracy assessment	40
4.5	Slum Change Monitoring	41
5	WEB APPLICATION DEVELOPMENT	42
5.1	Setting up PostgreSQL/PostGIS database	42
5.2	Publishing Web Services on Geoserver	43
5.2.1	Web App Creation on Leaflet	44
6	RESULTS	47
6.1	Results of the pixel-based classification	47
6.2	Results of the object-based classification	49
6.3	Results of the deep learning classification	51
6.4	Comparison of Algorithms	52
6.4.1	Comparison of algorithms in the classification of Lagos Mainland Sentinel-2 imagery	52
6.4.2	Comparison of algorithms in the classification of Vila Andrade Sentinel-2 imagery	52
6.4.3	Comparison of algorithms in the classification of Makoko & environs Drone imagery	53
6.4.4	Comparison of algorithms in the classification of Vila Andrade orthophoto	53
6.4.5	Comparison of processing time used by the algorithms	54
6.5	Result of the Slum change monitoring	55
6.6	Pixel Counts Calculation	57
7	DISCUSSION	59
8	CONCLUSION	61
	REFERENCES AND INFORMATION SOURCES	
	ATTACHMENTS	

LIST OF ABBREVIATIONS

Abbreviation	Meaning
ANN	Artificial Neural Network
ASTER	Advanced Spaceborne Thermal Emission and Reflection Radiometer
CBERS 2B	China–Brazil Earth Resources Satellite 2B
CNN	Convolutional Neural Network
CPU	Central Processing Unit
DBMS	Database Management System
DEM	Digital Elevation Model
DSM	Digital Surface Model
DTM	Digital Terrain Model
DL	Deep Learning
EO	Earth Observation
ESA	European Space Agency
Esri	Environmental Systems Research Institute
GDEM	Global Digital Elevation Model
GEE	Google Earth Engine
GI	Geographic Information
GIS	Geographic Information System
GPU	Graphics Processing Unit
GPS	Global Navigation System
HRC	High Resolution Camera
LIDAR	Light Detection and Ranging
LGA	Local Government Area
LR	Logistic Regression
MLB	Machine Learning Based
ML	Maximum Likelihood
NGOs	Non-Governmental Organizations
OBIA	Object Based Image Analysis
OSM	OpenStreetMap
RADAR	Radio Detection and Ranging
RT	Random Trees
RGB	Red Green Blue (Colour Model)
RS	Remote Sensing
SDI	Shack / Slum Dwellers International
SRTM	Shuttle Radar Topography Mission
STS	Spectral, Textural and Structural
SVM	Support Vector Machine
UAV	Unmanned Aerial Vehicle
UN	United Nations
USGS	United States Geological Survey
VHR	Very High Resolution
WFS/WMS	Web Feature Service / Web Map Service

INTRODUCTION

Many cities in developed, developing, and under-developed countries face the challenges of meeting the social, environmental, and economic needs of the huge proliferation of global urbanization. Urban settlements continue to witness an abrupt increase in population worldwide due to the migration of people from rural settlements and the rise in the fertility rate. According to the United Nations, the world urban population experienced a speedy growth from 1960 (when it was 1 billion) to 4.4 billion in 2020. Today, 55% of the world's population lives in urban areas and it has been estimated that this figure will increase to 68% by 2050 (United Nations, 2019).

The developing and under-developed countries are the most affected due to lack of adequate resources (such as electricity, affordable housing, good roads, water system, sanitation, etc.) to cater for the cities' current dwellers. The continual increase in the number of people living in such cities mounted more pressure on these available resources. One of the biggest challenges faced with the huge increase in global urbanization is the irrepressible growth of slums. Within the urban population, over 1 billion people live in slums and the proportion of slum dwellers is expected to grow rapidly in the nearest decades (UN-Habitat, 2003).

Slums are regarded as informal settlements characterized by an over-crowded population, poor structural quality of housing, clumsy and compacted shelters, inadequate basic amenities, uncondusive environments, poor and unsafe living conditions. In the traditional sense, slums are housing areas that are once desired and respected but become deteriorated due to the migration of the original dwellers to better parts of the city. Still, today, slums are categorized as informal settlements, which have become the most visible reflection of urban poverty in cities worldwide (UN-Habitat, 2007). In different parts of the world, slums have different sizes and shapes depending on the regions' diverse attributes, although they still possess similar features and trends. Due to the clumsiness and bad living conditions of the slum dwellers, the inhabitants are prone to various outbreaks and contagious diseases.

Most of the world's largest slums are found in megacities, particularly in Africa, Latin America and Asia. Lack of spatial and attribute information about the slums such as slum extents, size, geographic location, number of houses and the population of slum dwellers, etc. hindered planning, development, and proper management of cities, thus deprived the dwellers of some adequate services, infrastructures and amenities for life sustainability. In some cases, the slums are not existing in the master plan of the urban settlements (Ottavianni, 2020).

However, geospatial technologies bridged the information gap, hence enabling the concerned bodies to make well-informed decisions on improving the living conditions of the slum dwellers. Government agencies, international organizations (such as UN-Habitat etc.), NGOs (such as SDI, LiveInSlums etc.) support slum dwellers through various international cooperation projects and developments programmes. To achieve such projects, it is necessary to gather adequate information about the slums (locations, types etc.) and the dwellers (population density); hence geoinformation technology is pertinent.

Several types of research have been carried out on slum mapping, detection and monitoring using traditional approaches, with the most recent studies being carried out with OBIA (Object-Based Image Analysis), machine and deep learning algorithms using either supervised or unsupervised image classification. Some of these researches adopted either land surveying data, EO (Earth Observation) data (such as optical, multispectral and radar satellite imagery), LIDAR (Light Detection and Ranging) data or UAV

(Unmanned Aerial Vehicle) data to distinguish slums areas in urban settlements while other researches employed combinations of two or more data sources (Hofmann, 2001; Ayo, 2020; Tesfay, 2018; Leonita *et al.*, 2018; Reuß, 2017; Mahabir et al., 2018b).

This research tends to map and monitor slums from imagery using different algorithms and then select the best-performed algorithm with optimal result. It was observed that within the significant number of researches carried out on slum mapping and monitoring using Geographic Information (GI), very few demonstrated different spatial algorithms, this is the main motivation for this study.

Over time, GIS and remote sensing have proved to be efficient tools and techniques for mapping and monitoring slums using different techniques and methods. With the continual advancement in technology, existing methods are witnessing continuous refinement and new methodologies are also being invented to facilitate faster processing time with more accurate result.

1 OBJECTIVES

The main aim of the diploma thesis is to map and monitor slums using geoinformation technologies. The main aim was divided into sub-goals which are:

- i. To develop a test methodology for mapping and monitoring slums primarily using open data.
- ii. To explore the possibility of mapping slums within cities by using imagery, geophysical datasets, and complementary data.
- iii. To compare the performance of different methodologies for identifying slums and determine which algorithm provides the optimal results.
- iv. To contribute towards curbing disease outbreaks.

Practically, different methodologies (algorithms) that were already embedded into geospatial software (ArcGIS Pro) will be employed. The data will be inputted into this software while applying the methodologies to determine the best algorithms that give an optimal and accurate result.

Furthermore, the work outputs will be maps displaying the results from the algorithms, graphs, and optimal workflow of mapping and monitoring slums in spreading the epidemic.

The result, therefore, will serve the following benefits:

- i. Create a set of best practice guidelines for selecting the most suitable techniques for mapping slums in a selected location.
- ii. To support the achievement of Sustainable Development Goals (SDGs) No. 11 of the United Nations.
- iii. To contribute towards curbing disease outbreaks in slum areas.
- iv. Serve the need for benchmarking framework for evaluating slum mapping algorithms.

2 METHODOLOGY

This chapter presents the study areas selected for the thesis, the description of imagery, the description of the methodologies adopted in this study, the software used, and the work process that led to achieving the objectives.

2.1 Study Area

The study areas are Lagos Mainland local government area (Lagos), Nigeria and Vila Andrade district (Sao Paulo), Brazil. These cities were chosen based on their difference in slum types, relief characteristics and most importantly, data availability.

Lagos Mainland is a local government in Lagos State, Nigeria (see fig 2). It represents a continual growing urbanized area of the state with an estimated population of 317,980 inhabitants (Wikipedia, 2020). Communities in Lagos mainland includes Akoka, Abule-nla, Ebute-metta, Iddo-otto, Iwaya, Makoko (slum) and Yaba. Lagos mainland is a true reflection of the proliferation of urban growth within the Lagos metropolis with Lagos state being regarded as the fastest growing and most populated city in Africa with a population of 14,862,111 people (WorldPopulationReview, 2021).

The highlight of the slum in Lagos Mainland LGA

Makoko is a localized community located on the coast of Lagos mainland, Nigeria (see fig 1). It is regarded as a water-front settlement and one of Africa's largest floating and most unique inner-city slums with a third of the community built on stilts in a lagoon off the Lagos mainland while the rest is built on land (Ottavianni, 2020). Makoko is sometimes described as the “Venice of Africa” (Methu, 2014). Emeka & Ifeyinwa, 2020 described Makoko as the world’s largest floating city which is home to about 85,000 people; however there is no official record of the dwellers as the area was not counted during the 2006 census (the most recent population census carried out by the Nigerian Government). Due to the nature of its environment, dwellers are subjected to living in difficult conditions due to a lack of infrastructures and basic amenities. For a long time, Makoko used to be a blank spot on the map even though it is at the centre of Lagos until recently when Code for Africa, a civic tech and data journalism initiative, partnered with the local community to create the first bottom-up, crowdsourced map of Makoko (Ottavianni, 2020).



Fig 1 Makoko Slum in Lagos Mainland Local Government, Nigeria (Ravine News, 2018).

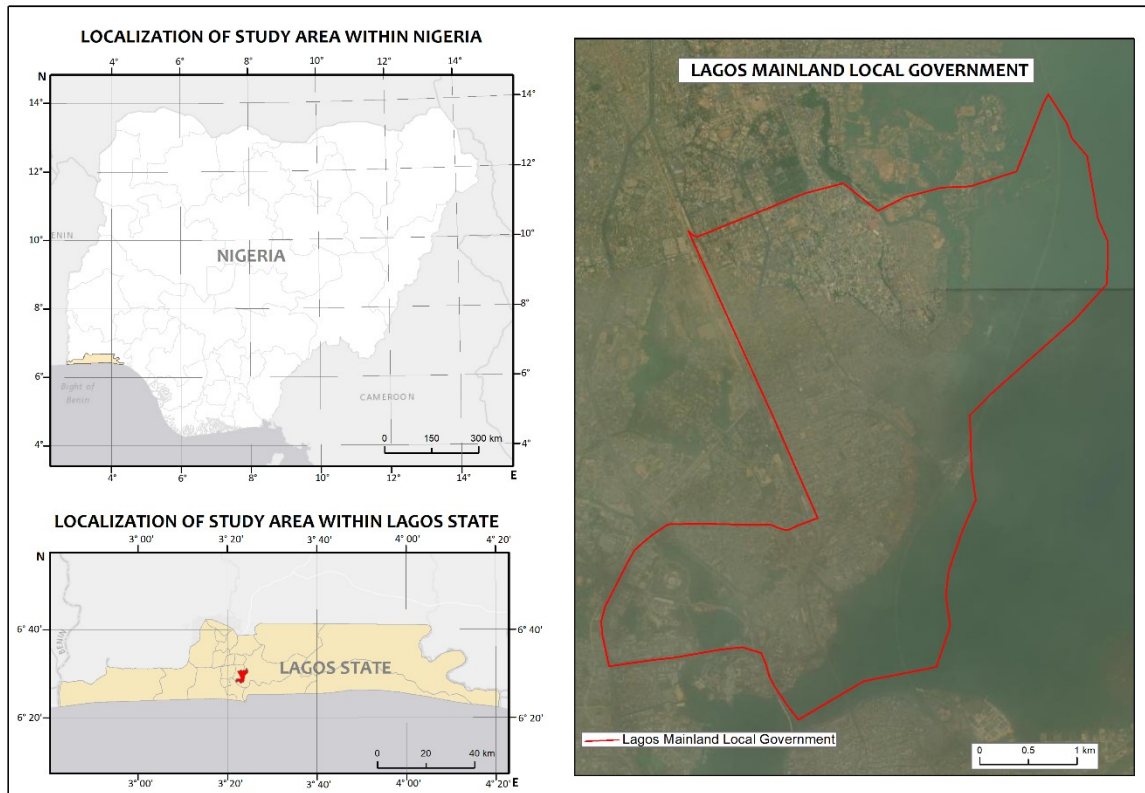


Fig 2 Study Area 1 (Lagos Mainland local government, Nigeria) (Source: Author)

Vila Andrade is a district in Sao Paulo city situated in the South of the city and domiciliated by the growing urban dwellers (see fig 4). The inhabitants are both high and low-income families representing one of the districts with the largest socioeconomic disparity (Wikipedia, 2021c). It has a population of 127,015 (2010 population census) with an area of 10.3 km². Notable communities in Vila Andrade are Panamby and Paraisópolis (one of the largest slum in the city).

The highlight of the slum in Vila Andrade

Paraisópolis is a favela (slum) in the Vila Andrade district with a population of 42,826 inhabitants based on the population census of 2010 (the most recent Brazillian Government population census). However, there has been a huge increase in the number of dwellers living in the slum presently (see fig 3). The slum neighbourhood occupies an area of 798,695m² (Wikipedia, 2021a). According to Vilicic et al., 2009, the slum originated in the 1920s from an allocation of 2,200 small plots (10m x 50m of regular blocks and 10m wide in streets), but at present, there are 17,730 households in Paraisópolis.



Fig 3 Paraisópolis Slum in Vila Andrade District, Brazil ((Arantxa H., 2019)

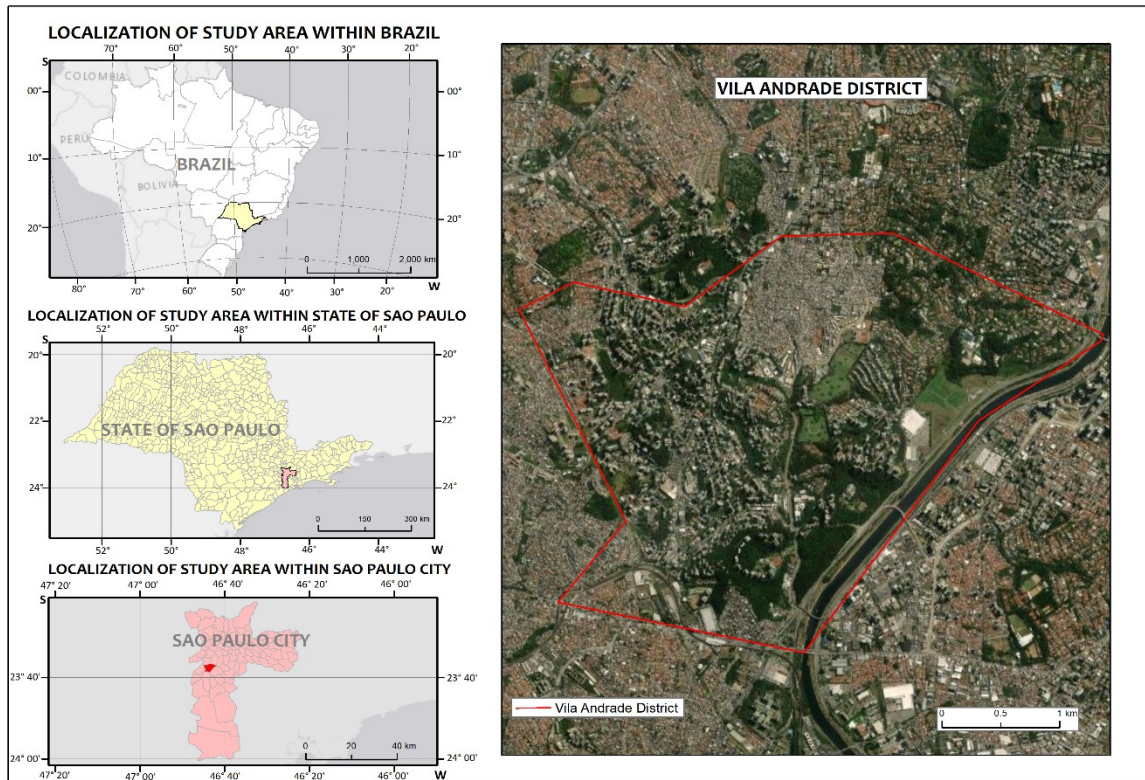


Fig 4 Study Area 2 (Vila Andrade district, Brazil) (Source: Author)

2.2 Data

2.2.1 Satellite Imagery

Many studies have utilized the Sentinel-2 imagery of the Copernicus programme for slum mapping and monitoring (Ayo, 2020). Sentinel-2 is an optical spaceborne (multispectral instrument) constellation of two polar-orbiting satellites (Sentinel 2A and 2B) positioned in the same sun-synchronous orbit. Some of the advantages of Sentinel-2 are its provision of free and open very high resolution (VHR) imagery and the availability of EO data in spatial (10m), spectral (13 bands) and temporal resolution (5 days at the equator) (ESA, 2013).

For this study, three bands (B2, B3, B4) out of the 13 available bands which provide a spatial resolution of 10m were used. The data were downloaded from the Copernicus open access hub website. During the downloading section, quality and minimal cloud cover imagery were selected since optical imagery has limitation of cloud covers (see fig 5). Table 1 shows the imagery acquisition dates and the band combinations used.



Fig 5 Section view of the Sentinel-2 (L), drone imagery (M) and Makoko orthophoto (R) used for this study

Table 1 Sentinel-2 imagery acquisition dates and the band combination used.

Study Area	Acquisition date	Band Combination Used	Spatial Resolution
Lagos Mainland	26-12-2020	4,3,2	10m
Vila Andrade	07-11-2020	4,3,2	10m

2.2.2 Drone imagery of Makoko and environs

Unmanned Aerial Vehicles (UAVs) also known as drone are gradually becoming popular for slum mapping hence a good source of information for mapping applications in general. Some studies have utilized UAVs for slum mapping due to their ability to capture very high spatial resolution imagery and the availability of low-cost drones; however, most drones are limited in terms of coverage area (provision of imagery over small areas) (Sliuzas et al., 2017). The drone imagery of Makoko was acquired using the DJI Mavic Pro drone on the 24th of January 2021 to demonstrate its effectiveness in mapping slums and test the algorithms on imagery from different data sources. Fig 5 shows the section view of the acquired drone imagery of Makoko and environs (see table 2 for attribute information).

Table 2 Attribute information about the acquired drone imagery.

Study Area	Acquisition date	Bands	Spatial Resolution
Makoko and environs	24/01/2021	4	4.9cm

2.2.3 Orthophoto of Vila Andrade

Orthophoto of Sao Paulo is openly accessible and freely available from the GeoSampa web portal (Grohmann, 2019). GeoSampa is a digital platform of the Sao Paulo city that housed various datasets covering the city, such as administrative boundary, old maps, DSM, DTM, orthophoto, and other spatial datasets. The orthophoto derived from LIDAR data was downloaded in image tiles and were later mosaiced with the ArcGIS Pro software (see fig 5 for a section of the orthophoto).

2.2.4 Administrative Boundaries of the Study Areas

Having accurate data that shows the extent of an area, be it a parcel, district, municipality, region, country or global level, is essential to support spatial analysis. The boundaries of the world countries are currently available on many web portals and GADM is one such platform. GADM is an open-access web portal that served as a repository for administrative boundaries of all countries at different levels depending on the subdivision of each country. Based on the countries of the study areas, Nigerian administrative boundary is available in three (3) levels due to its subdivision (federal, state and local government), while Brazil has four (4) subdivision levels (federal, state, municipality and district). The boundaries of both countries were downloaded and stored in the project folder directory for further analysis.

2.3 Methods Adopted

The software employed and the workflow diagram developed during this study were explained in this section.

2.3.1 Software Used

The following software was employed for this study. ArcGIS Pro for processing and analysis, PostgreSQL/PostGIS served the purpose of spatial database for vector data, Geoserver for publishing of data as Web Feature Service (WFS) and Web Map Service (WMS), Leaflet for web application development, Visual Code Studio as the code editor during the implementation of the web application, Microsoft Excel and Microsoft Word for graphical representation of analysis and thesis documentation respectively. ArcGIS Pro is a highly robust desktop GIS software built and developed by Esri with the capability of advanced spatial analysis, data visualization and data maintenance in 2D, 3D, and 4D (Esri, 2021a). Due to its robustness and integration of numerous workflows embedded into the software for various applications, it suits the need for the analysis required for this study. The application of the softwares were analyzed in chapter 4 and 5.

2.3.2 Workflow diagram

The procedure ranged from data acquisition, processing & analysis and web application development. Fig 6 shows the workflow diagram used for this thesis.

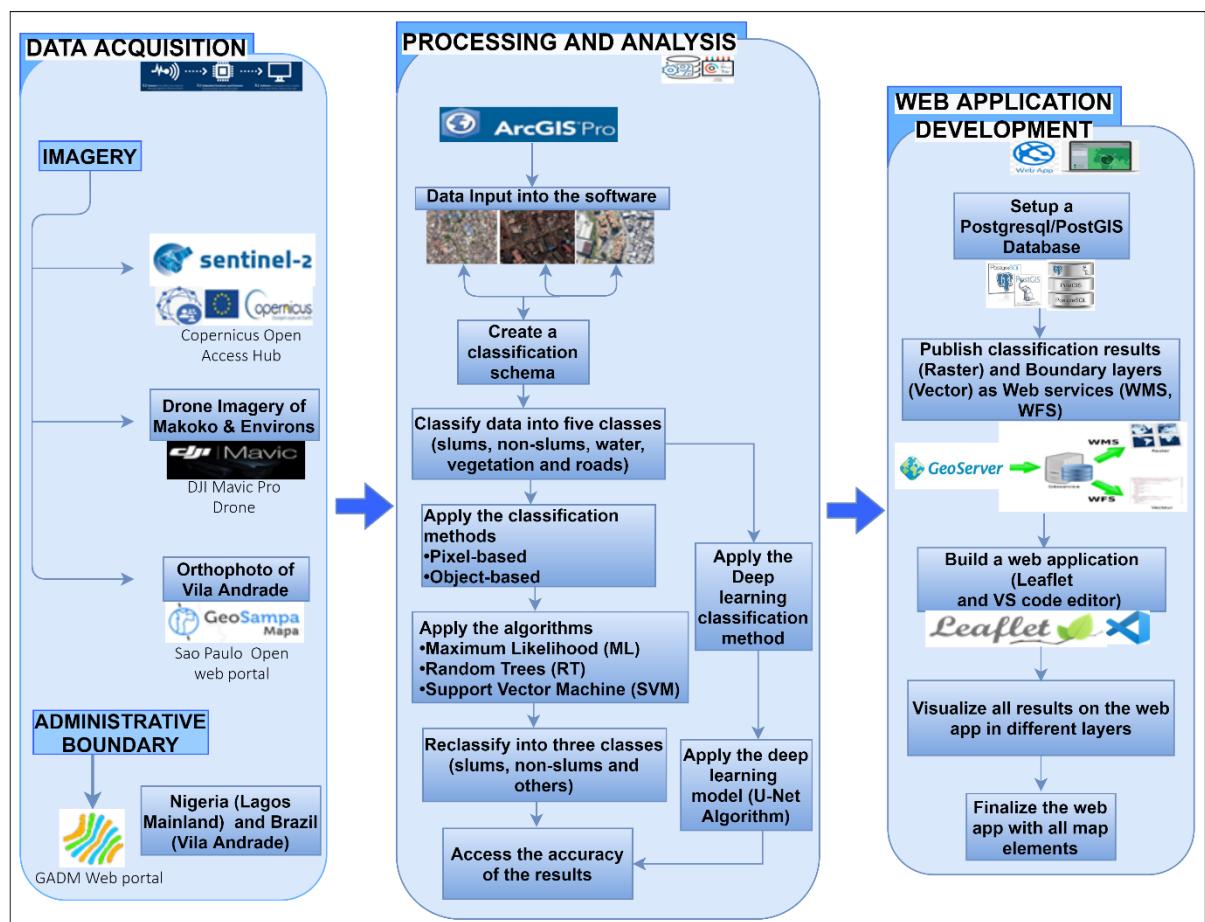


Fig 6 Thesis workflow diagram (Source: Author)

3 STATE OF THE ART

This section deals with the theoretical and conceptual approaches on slum mapping and review of different techniques used by different researchers in their studies to detect and map slums in cities.

3.1 Background

The continual growth of slums within urban settlements poses a lot of threats worldwide. It is pertinent to monitor, manage and devise a mechanism to control this rapid growth to address the issue of land use and land tenure system within urban areas. Due to the nature of the slums, it often affects the development of the cities.

Generally, slum monitoring can be achieved only with access to reliable information about the slums and the inhabitants, which involves using the correct techniques to obtain spatial and other related information about the slums coupled with meaningful analysis. UN-Habitat, 2003 reiterated the importance of reliable spatial and attribute data about slums which in turn would facilitate the formation of the right policies and programs for slum upgrading and eradication.

Several studies have demonstrated slum mapping and monitoring using various techniques. This study tends to evaluate the performance of some of these techniques, hence determining the best-performed algorithm for mapping slums.

3.2 Slum Mapping and Monitoring Approaches

Slum identification, mapping, and monitoring have been achieved mainly by three approaches, as proved by many studies. These approaches are survey and census-based, participatory based, and GIS / Image analysis approach of remotely sensed imagery (Kohli et al., 2011). Due to the different slum types and complexities in different parts of the world, precisely knowing the best approach to map each slum will afford the concerned bodies and government organizations to make the right decision.

It is pertinent to explore all three approaches distinctively, although this study evaluates the performance of the various techniques in the GIS / Image analysis approach.

3.2.1 Survey and Census-Based Approach

Survey and census-based approach is a concept which involves gathering of census data (such as demographic, infrastructure, social and economic data of the people living in a particular region) for planning and formulating policies that would boost the development of the area in consideration and provide the necessary infrastructure for the inhabitants (i.e. serves as a cornerstone for mapping of poverty or deprivation) (Mahabir et al., 2018a). Such data can be available at country level (local, state, county, municipality, federal etc.), continent level (Eurostat) or global level (World Bank) depending on the data source and its mode of acquisition.

Weeks *et al.*, 2007 created a slum index using census data of Accra, Ghana (study area). The index was based on the UN-Habitat slum indicators, which help in qualitatively evaluate the concentration of slums in different areas. The created slum index was used to successfully identify and locate the worst slums in Accra based on slum characteristics. As a result, high correlations were found between the slum index, neighbourhoods' socio-economic characteristics, and certain land cover metrics derived from very high resolution (VHR) satellite imagery.

Roy *et al.*, 2018 utilized a survey-based approach to collect data for studying the socio-economic and demographic variables of slums in Bangalore, India. The data was collected using questionnaires, and 267,894 data points were collected from 242 questions for 1,107 households. The survey covered about 36 slums within Bangalore city. This research concluded that such a dataset could be useful for interdisciplinary research on spatial and temporal dynamics of urban poverty, focusing on rapid urbanization in cities.

Exploratory factor analysis was adopted by Roy *et al.*, 2019 to determine the Slum Severity Index (SSI) of Mexico City from a census survey of Mexico to measure the shelter deprivation levels of households from 1990 to 2010. The result highlighted a huge variance in housing conditions and showed a significant SSI decrease between 1990 and 2000 resulting from policy reforms but an increase in SSI was found between 2000 to 2010.

Mahabir *et al.*, 2018a while comparing survey / census-based data with remotely sensed data, highlighted several limitations of census data for slum mapping and monitoring. First, it is labour intensive, consumes time, and require substantial financial resources. Second, slum dwellers are usually reluctant in engaging in the census and household surveys due to fright of eviction by concerned authorities once they can be located. Third, even if there is up-to-date census data, the lack of rigorous quality control implemented in some countries mostly affect reliance on such data for slum mapping and developing policies necessary to reduce slum populations. Fourth, it has an issue of long temporal gaps between census data gathering campaigns. Lastly, census statistics are mostly available at the neighbourhood level or aggregated city without the necessary information about the varying size, housing quality and density of slums.

3.2.2 Participatory-Based Approach

This approach involves mapping the slums with the cooperation and active participation of the slum dwellers. It involves acquiring both spatial and attribute data about the slums. The participatory approach began in the late 1970s due to the introduction of a new research approach known as “Rapid Rural Appraisal (RRA)” (Shekhar, 2014).

The slum mapping of all urban areas in Indonesia was achieved using the participatory (survey) based slum mapping (SBSM) approach, which was completed in 2017 (Leonita *et al.*, 2018). A study carried out by Shekhar, 2014 demonstrated mapping of Borabainagar slum in Kalaburagi city (India) using a participatory approach. Borabainagar slum dwellers participated actively in the community mapping and a slum map was created with the aid of a GPS (Global Navigation System) survey. 3D map was therefore created from the 2D map with development of spatial decision support system (SDSS) also achieved. This study highlighted the importance of a participatory approach for mapping slums and the relevance of the SDSS and 3D scenes for proper planning of slums and making a well-informed decision.

Code for Africa partnered with the local community to create the Makoko map (Ottavianni, 2020). The project involved training 32 persons as drone pilots to engage in the community drone mapping of Makoko which happened to be a near-blank spot on the urban map of Lagos, Nigeria. High-resolution images were captured from the drone mission, which were then stitched together into shapefiles with labelling done by the local community using Open Data Kit. The created open-source map which is available in the OSM database (OpenStreetMap) will serve as a benchmark to improve the living condition of the dwellers (Ottavianni, 2020).

Even though the participatory approach can be employed to acquire the necessary data required for slum planning and development, it is labour-intensive, time-consuming, and not suitable for mapping large areas (e.g. cities) due to its limited spatial coverage (Kohli et al., 2011).

3.2.3 GIS and Image Analysis Approach

The availability and applicability of satellite imagery for solving real-life issues make this approach very ideal for slum mapping and monitoring. GIS and remote sensing (RS) have over time served as a solution-driven tool and operational technique for processing satellite data, thereby enabling proper mapping and monitoring of slums and making accurate slum predictions.

Since the late 1990s, satellite imagery with a spatial resolution of one to four metres has enabled the acquisition of numerous data over slum areas, facilitating the comparison of inter and intra heterogeneity between different slums. In recent time, advancements in technology have led to the availability of very high spatial and temporal satellite imagery with a sub-meter resolution that enables more detailed spatial analysis and is very suitable for studying the urban landscape and slum areas at a finer scale (Mahabir et al., 2018a). VHR imagery shows a detailed representation of the physical elements of a landscape, hence capturing the physical characteristics of slum areas (Kuffer et al., 2016).

Commercial satellite sensors such as IKONOS (the first commercial satellite launched in September 1999 (Dare & Fraser, 2001)), Pleiades, Quickbird, Worldview, SPOT, etc. with VHR imagery has been employed over the years to map slums. Some commercial sensors are designed to simultaneously provide multispectral (MS) and panchromatic (PAN) imagery. For instance, Pleiades being an optical spaceborne twin satellite (Pleiades 1A and 1B) can acquire multispectral (2m resolution) and panchromatic imagery (0.5m resolution) in a package (Astrium, 2012). It is important to note that commercial sensors have their limitations, such as high cost (to some degree) and global coverage (some of the satellites only provides imagery at the country level, e.g. Resourcesat satellites (Mundhe, 2019)).

The increasing availability of VHR imagery from free satellite sensors (e.g. Sentinels, Landsat) has paved the way for open access to satellite data globally in high spatial and temporal resolution. Free data are therefore available from optical sensors (10m resolution) and radar sensors (5m resolution) for studying and mapping the dynamics of slums (Kuffer et al., 2016). Due to the variation in slum morphology, types and characteristics, slum monitoring from satellite imagery might be challenging however adopting the right methods to monitor slums will bridge the challenge (Kohli et al., 2016).

Visual interpretation has been utilized to extract information about the dynamics of slums from VHR imagery (Sliuzas et al., 2008). Mundhe, 2019 integrated different datasets (satellite data {Resourcesat-2}, ASTER GDEM, topographic maps, demographic data etc.) to identify and map slums in Pune city, India. Visual interpretation, image rectification, enhancement and classification were adopted to extract the slum areas from the satellite imagery. Combining such datasets enabled comprehensive analysis for the study.

In general, Mahabir et al., 2018a identified the three processing steps that have been used to map slums from satellite data which are detection (locating the feature of interest and basically the first step of image classification), delineation (recognizing the spatial extent of real-world objects) and characterization (labelling of features as per the class

they belong). From the methods employed and reported in the literature, the author further pointed out seven categories of studying the spatial properties of slums. These categories are multi-scale, image texture analysis, landscape analysis, object-based image analysis (OBIA), building feature extraction, data mining and socio-economic measures.

3.2.3.1 Methods in the GIS and Image Analysis Approach

Having gone through various researches that demonstrated the different methods in GIS and image analysis for mapping slums, it is very important to have a review of some of these methods to observe their performances and results.

Pixel-Based classification method

Pixel is the basic unit of a satellite image. Pixel-based classification involves analyzing individual image pixels based on their spectral information in the image (Richards, 2013). Image classification in a pixel-based approach works in the manner of pixel by pixel and that one pixel can solely be associated with one class. For decades, pixel-based methods have been the conventional method applied for image interpretation and classification before the introduction of other image classification approaches (Mo et al., 2007). Being a traditional classification approach, some of its notable limitations are the non-applicability of spatial information for image classification and its inability to illustrate the heterogeneity of complex urban environments (salt and pepper effect) on VHR imagery (Shekhar, 2012; Makinde et al., 2016). A typical workflow process of pixel-based classification is as shown in fig 7.

A study carried out by Ranguelova et al., 2018 utilized pixel-based classification for detecting slum areas from VHR satellite imagery (RGB bands) of two cities (Bangalore and Kalyan) in India based on three classes of urban areas (slums, built up and non-built up). Their study applied standard computer vision for the classification while image tiles were trained using the multi-class SVM classifier. The result showed the potentiality of pixel-based computer vision for mapping slums; however the authors expressed a need to obtain ground checks of slum locations to avoid false positives that sometimes occur in image classification.

Comparing pixel and object entails dealing with spectral properties versus the combination of spatial, spectral and temporal properties of real-world entities. Myint et al., 2011 compared per-pixel and object-based classification of urban land cover from VHR data (Quickbird imagery of central region of Phoenix city, Arizona). The study evaluated the effectiveness of using only spectral information (per-pixel) for delineating urban land cover. The maximum likelihood classifier used resulted in an overall accuracy of 67.60% however, using object-based (membership functions and nearest neighbour) classifier had an accuracy of 90.40%. It was demonstrated with this study that the per-pixel method seems not very efficient for urban land cover classification, as was concluded by the authors. Makinde et al., 2016 also found out for their study that pixel-based produced less accuracy over OBIA with overall accuracies of 84.64% and 94.47% obtained respectively while carrying out image classification of Eti-Osa Lagos, Nigeria from Rapid-eye imagery.

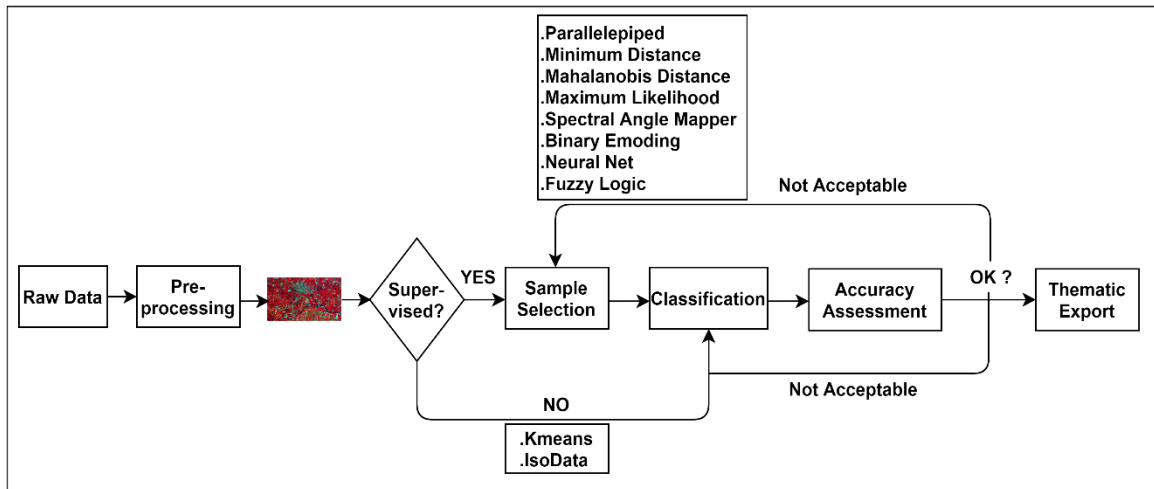


Fig 7 Traditional pixel-based image classification workflow (Mo et al., 2007).

Object-Based Image Analysis (OBIA) method

OBIA combines spatial concepts with signal processing for either automated or semi-automated image analysis which operates on objects rather than on pixels (Lang & Blaschke, 2006). OBIA concept is built upon the older concepts of segmentation, edge detection, feature extraction, and classification used for decades in RS image analysis; hence, OBIA facilitates making an accurate distinction within objects or groups of objects that is not possible with the traditional image analysis. To achieve wider OBIA application, it is vital to understand and integrate real-world entities' philosophical and ontological aspects (Blaschke, 2010).

Variables can be categorized and defined as shape (size and compactness), spectral (standard deviation and mean value of a particular spectral band) and neighbourhood (mean difference of an object compared to darker objects) (Addink and Van Coillie, 2010). Availability of VHR imagery has shifted a new paradigm for OBIA and boosted its image analysis capabilities; however a good understanding of image interpretation (expert knowledge) is pertinent.

Hofmann, 2001 introduced an approach based on multi-scale image segmentation (image segmentation, class hierarchy and image classification) to detect informal settlements from VHR IKONOS imagery of Cape Town, South Africa. The study adopted the eCognition developer software due to its object-based capabilities. Thus, the author concluded that this approach is well suited for generating image objects even with the complexity and structural differences that existed with different informal settlements. Also, the result of the image segmentation shows the accurate depiction of real-world objects. Mo et al., 2007 proposed a new OBIA system (see fig 8 and 9) that integrates traditional image processing system (pixel), GIS (vector) and data mining technology (intelligent computing) for image interpretation. This system facilitates interpreting images from pixels to segments with the final result being the thematic information.

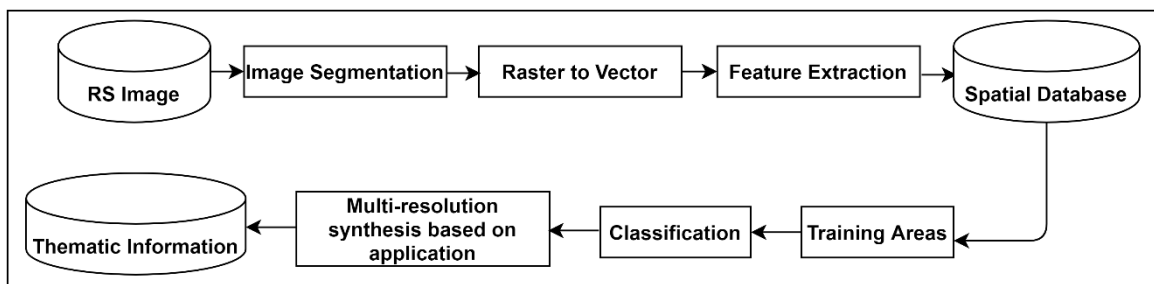


Fig 8 General framework of object-oriented image system introduced by Mo et al., 2007

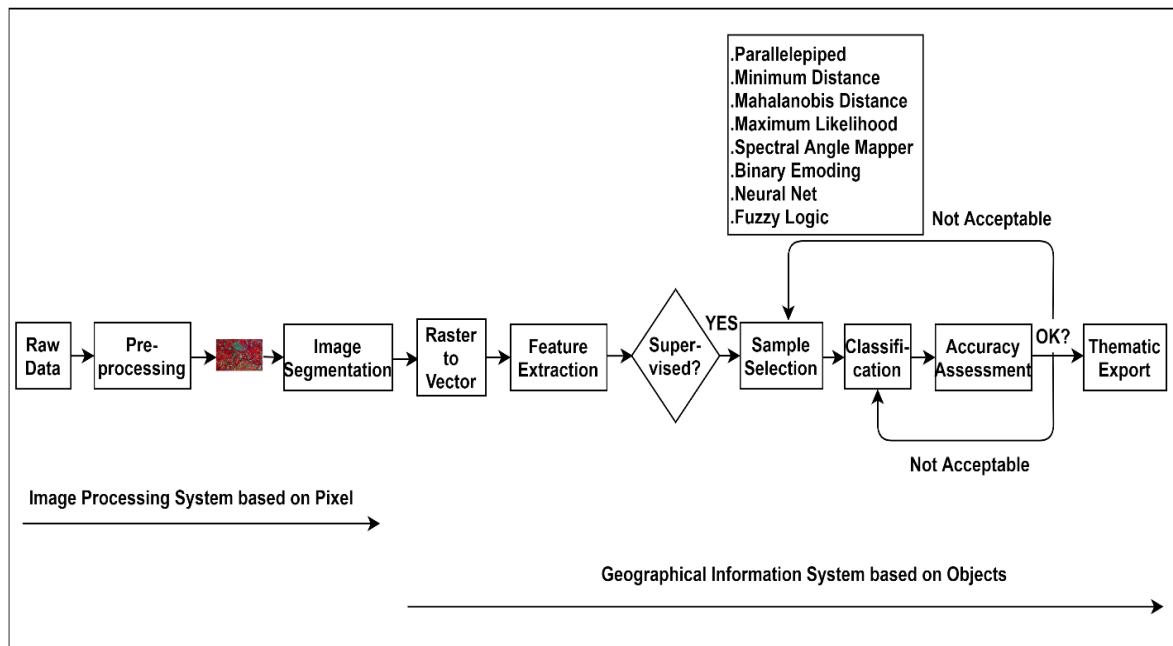


Fig 9 Framework of the RS image intelligent interpretation system by Mo et al., 2007

Mapping and detection of slum based on the structure of the built environment was carried out by Kohli et al., 2016. Spatial and textural metrics derived from Quickbird satellite imagery were adopted to delineate the slum within Pune city, India. The authors combined the processes of image segmentation, hierarchical classification and expert knowledge (local slum ontology). The classification result showed 80.8% for land cover classification and 60% was achieved when comparing the obtained slum classification with the reference data due to large variations. Their study produced possible results and therefore very useful for mapping slum that has similar morphology.

A study carried out by Tesfay, 2018 compares OBIA one-class support vector machine (SVM) with expert-based classification in identifying Addis Ababa city slum from GeoEye-1 imagery. To determine the best value of parameters for the SVM algorithms, both manual (extensive manual trial) and automatic fine-tuning (cross-validation grid search) were applied, whereas a decision tree was used for the expert-based classification. The author's result showed higher accuracy in the one class SVM manual tuning (97.7% {subset1}, 92% {subset 2}) than the one class SVM automatic tuning and expert-based classification. Due to this result, the author concluded that the one class SVM with manual tuning requires less computing time and effort than the expert system.

Machine Learning-Based (MLB) method

The proliferation of research, development, and innovation in artificial intelligence and machine learning has enabled its full potential for image interpretation and mapping urban landscapes. With more researches being carried on ANN, CNN and other AI and ML algorithms, the future of the MLB method for slum detection and mapping look very promising.

Recently, many studies have shown the capability of the MLB method for mapping and monitoring slums from satellite imagery which allows training of datasets (algorithms) and applying the trained algorithms to detect and map slums from VHR imagery taken into consideration the spectral, geometry, structure, texture of the features of interest (Ayo, 2020; Leonita et al., 2018; Duque et al., 2017). Ayo, 2020 combined OSM data with Sentinel-2 imagery to classify and monitor slums in Kampala and Dar es Salaam using

MLB (CNN) approach. The study achieved an accuracy of 90.3% with an optimally trained CNN algorithm. Leonita et al., 2018 compared the MLB approach with SBSM previously used to map all Indonesian slums in 2017. Using two MLB algorithms, SVM and RF, an accuracy of 88.5% was achieved with the SVM. The author concluded that it would be difficult to use the SBSM result to embark upon slum upgrading however, MLB result would suit this purpose due to its ability to deal with big data.

Reuß, 2017 in his research, adopted texture parameters and ML to detect favelas in Rio de Janeiro and Sao Paulo cities of Brazil. This study used Sentinel-2, CBERS 2B HRC, and Orbview 3 imagery for the analysis. The texture parameter was calculated from the imagery, while the RF classifier was used for the image classification. The author concluded that this approach has good accuracy and high capability to detect favelas in cities, considering the characteristics of the slum morphology and works perfectly when mapping morphology differences of different settlement forms.

Using spectral, textural and structural (STS) features derived from VHR imagery to detect urban slums demonstrated promising and high accuracy. Duque et al., 2017 used STS features as input data. It evaluated the performance of three ML algorithms (LR, SVM and RF) for classifying urban settlements (slum and non-slum areas) of three different cities (Buenos Aires (Argentina), Recife (Brazil) and Medellin (Colombia)). The study concluded that SVM achieved the optimal accuracy (F2-scores over 0.81) and thence established that the uniqueness within cities prevents using a unified classification model.

Current and future slum identification and prediction are crucial to enable the seeming control of urban growth and its development. Ibrahim et al., 2018 proposed a Multinomial Logistic Regression (MNL) and Artificial Neural Networks (ANN) model algorithms based on spatial statistics and ML to identify and predict slums. Street intersections data was the conventional input data for the proposed model. The model was applied in five different cities in Egypt (Alexandria, Greater Cairo, Hurghada and Minya) and India (Mumbai). The model showed high accuracy and validity for predicting informal settlements. The author proposed this method due to its simplicity of using minimal data (yet produces very accurate result) as an alternative to either supervised or unsupervised ML models that may require multiple input data.

3.2.3.2 Review and comparison of the methods in GIS and Image analysis Approach

Several reviews have been carried out on researches that adopted GIS and image analysis slum mapping approach. A critical review done by Mahabir et al., 2018a concluded that most studies are mainly centralized on a small geographical area and majorly applied a single method (i.e. image texture and OBIA). The author, therefore, recommends combining volunteer geographic information with geosensor networks to develop a comprehensive framework that can address the challenges in the existing methods hence helps to determine the best methods for slum mapping, monitoring and detection.

Kuffer et al., 2016 reviewed the different remote sensing approaches for mapping slums over the last 15 years (i.e. 2000 - 2015). The authors analyzed 87 papers that used satellite imagery for mapping slums. The analysis was based on four dimensions (contextual factors, physical slum characteristics, data and requirements, and slum extraction methods). Lots of hypotheses were observed in the results of these different studies (reviewed papers), ranging from the extracted information levels (area or object-

based), applied indicator sets (small or large) and the methods adopted. Although the methods that have been used to map slums from VHR satellite imagery are diverse, the most used technique within 2000 – 2015 was object-based image analysis (OBIA) (32.2%). Aside OBIA, visual image interpretation (17.2%), pixel-based image classification (12.6%) and machine learning (ML) (12.6%) were also used (see table 3). According to the authors, OBIA effectively extracts information in the area and object-based for mapping slums from a localized point of view.

Table 3 Frequency of methods versus main focus for slum mapping using VHR imagery (Kuffer et al., 2016).

METHODS									
		Contour Model	Machine Learning	Object-Based Approach	Pixel-Based Approach	Statistical Model	Texture/Morphology	Visual Image Interpretation	Total number (%)
FOCI	Analysis of types of slum area	0	1	1	0	1	1	2	6 (6.9)
	Correlation with socio-economic indicators	0	0	1	3	0	0	1	5 (5.7)
	Identification of slum areas	0	8	15	3	2	9	11	48 (55.2)
	Extraction of objects	4	0	7	0	0	1	1	13 (14.9)
	Land use/land cover mapping	0	2	4	5	1	3	0	15 (17.2)
	Total number (%)	4 (4.6)	11(12.6)	28 (32.2)	11 (12.6)	4 (4.6)	14 (16.1)	15 (17.2)	87 (100)

4 PROCEDURES

This chapter expands in detail the achievement of the data acquisition, processing and analysis in the thesis workflow diagram as shown in section 2.3.2.

4.1 Data acquisition

The data acquisition section highlights the process of acquiring the necessary data used for this study. The imageries were acquired from their available platforms taking into consideration the location (chosen study areas), acquisition time and spatial resolution.

4.1.1 Acquisition of Sentinel-2 imagery from Open Access Hub

The Copernicus Sentinel programme is commissioned by the European Union (EU) and operated by the European Space Agency (ESA). It allows access to free and open imagery of the Earth in different spectral bands and spatial resolutions. The programme has successfully launched optical and radar satellites which orbit the earth and gather information within days depending on the satellite mission. Optical satellite imagery (Sentinel-2) was used due to its ability to acquire data in multispectral bands, which fits the need of this study.

The Copernicus Open Access Hub (<https://scihub.copernicus.eu/>) is a platform where Sentinel imagery are readily and freely available for download. Sentinel-2 imagery of the study areas acquired as explained in fig 10 – 12. The numbering on the figures highlights the steps followed for the imagery acquisition.

1. Open hub was used to have access to the Sentinel-2 imagery through the interactive graphical user interface.
2. The download was accessed by logging into the portal with the user account details.
3. The rectangle symbol was clicked from the right side panel and the study area was zoomed into to facilitate acquiring the correct imagery.
4. The study area was highlighted.
5. The sensing period (date) and imagery type (Sentinel-2) were populated in the search section.
6. The search button was clicked, and all available imageries were displayed. Navigation was done to the veracious imagery and was then downloaded. The imagery was carefully selected for download concerning minimal cloud cover. Importantly, the imagery was free from any correction (atmospheric, radiometric, etc.); so no corrections were applied after download.

This process was followed to download the imagery of Lagos Mainland and Vila Andrade.

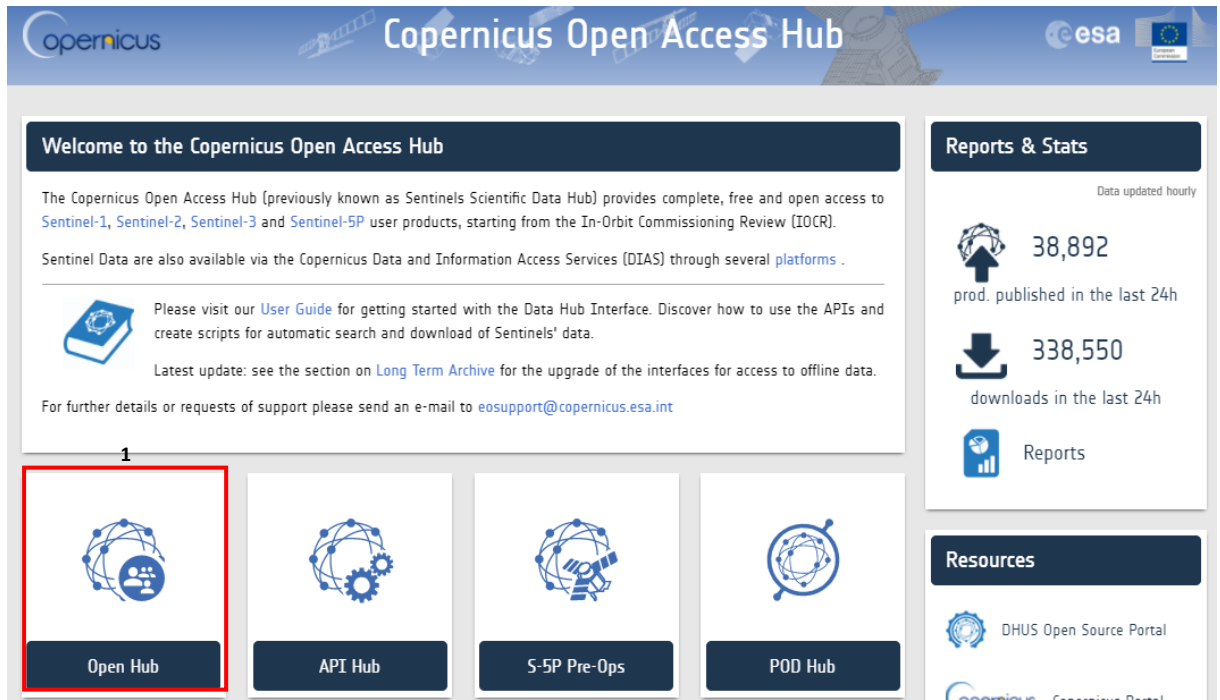


Fig 10 The homepage of the Copernicus open access hub (Source: Author)

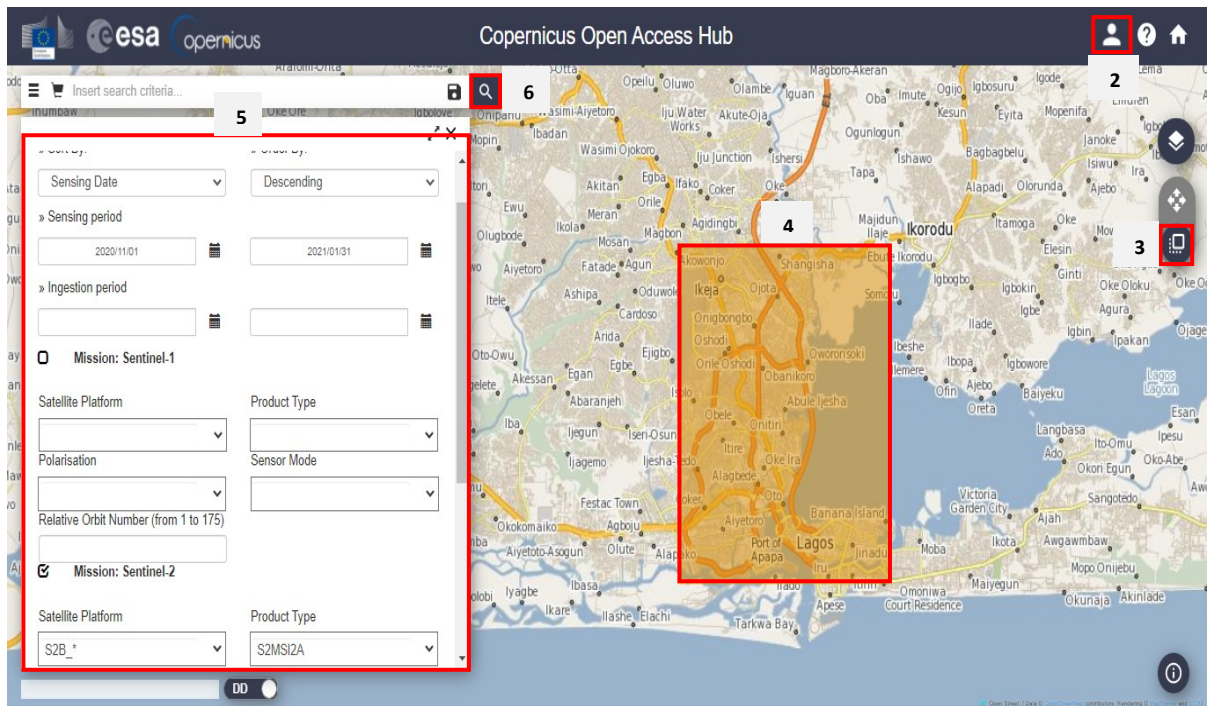


Fig 11 Searching the S-2 Lagos Mainland (Study area 1) on the open access hub portal (Source: Author)

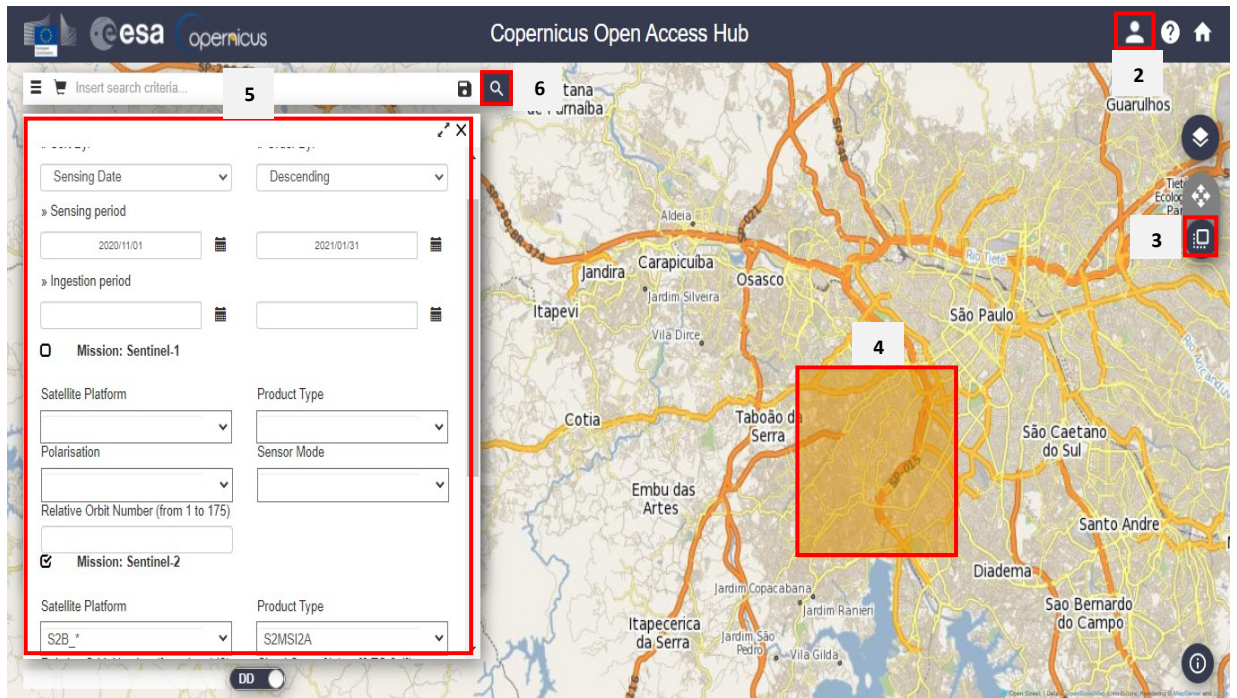


Fig 12 Searching the S-2 Vila Andrade (Study area 2) on the open access hub portal (Source: Author)

4.1.2 Drone mission of Makoko and environs

The drone imagery was essential to test the algorithms on different imagery while also considering very high spatial resolution imagery. The drone mission was intended to cover Lagos Mainland (study area 1). Still, due to persistent restrictions and security concern, the drone pilot was restricted to capture Makoko and the surrounding part of the urban area (i.e. Makoko and environs). DJI Mavic Pro drone was used for the acquisition and the images were acquired on the 24th of January, 2021. The drone was flown at an altitude of 150m, covered 236 hectares and successfully captured 1,493 images.



Fig 13 Sample of the drone images of the buildings in Slum (L) and Urban areas (R)

4.1.3 Acquisition of Vila Andrade Orthophoto

The orthophoto of Vila Andrade was freely available at the Geo Sampa web portal (http://geosampa.prefeitura.sp.gov.br/PaginasPublicas/_SBC.aspx#). The web portal served as a repository for Sao Paulo city's geospatial dataset (orthophoto, old maps, etc.) The imagery dataset can be retrieved in tiles (see fig 15). The orthophoto has a spatial



Fig 16 Sample of the orthophoto of the buildings in Slum (L) and Urban areas (R)

4.1.4 Downloading the administrative boundaries

The administrative boundaries of the study areas were downloaded from GADM web portal (<https://gadm.org/index.html>). The web portal provides free access to administrative and subdivision boundaries of world countries in both shapefile and Geopackage format. The download was achieved by launching the homepage on the web browser and navigation was done to the data page by clicking on data (shown in red) on the homepage. The homepage and the data page is as shown in fig 17. Nigeria and Brazil were chosen simultaneously from the list of countries and the boundaries were downloaded in shapefile format (see fig 18) as this format is best suited for ArcGIS Pro.

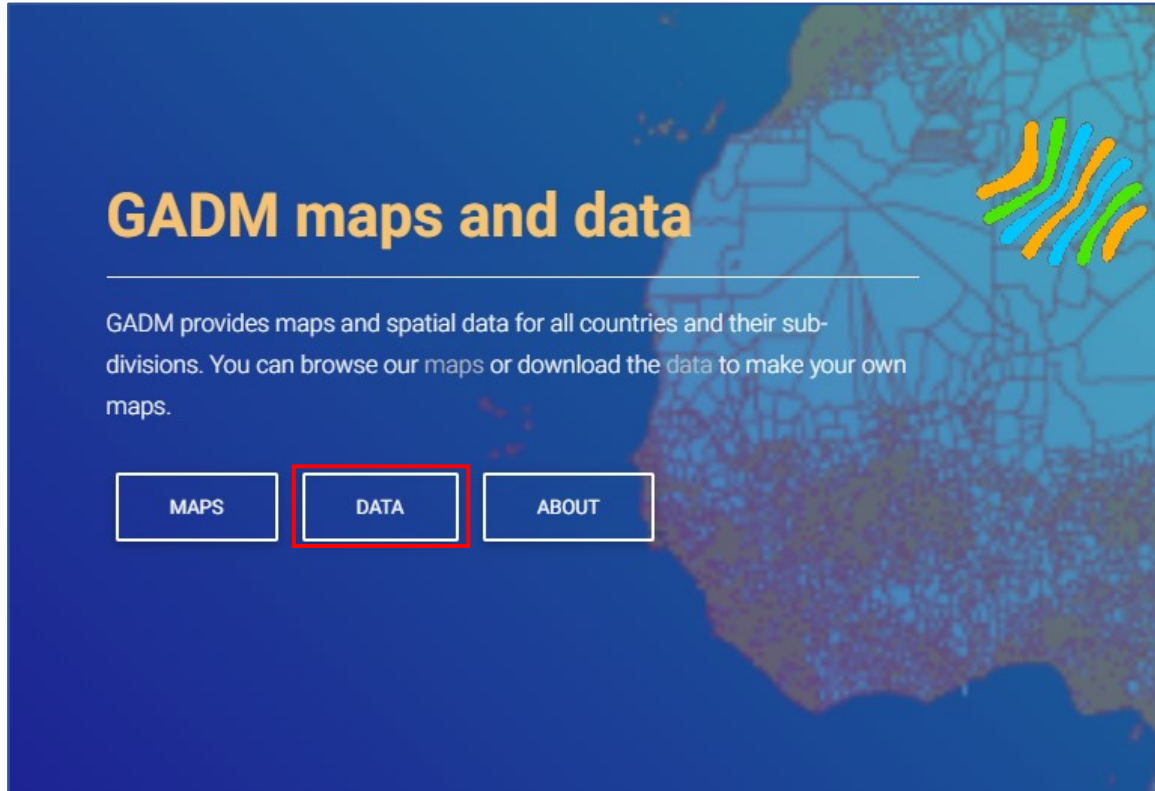


Fig 17 GADM homepage (Source: Author)



Fig 18 Selection of study areas in shapefile format from GADM web portal (Source: Author)

4.2 Processing and Analysis

After the data acquisition process, the imagery (Sentinel-2, Drone and Orthophoto) were processed individually in ArcGIS Pro software. This process involved image mosaicing, image segmentation and image classification (pixel-based, object-based and deep learning based). This chapter explains the processes involved in the classification leading to evaluating the GIS and RS method and algorithms for slum mapping.

4.2.1 Image Mosaicing

The drone images of Makoko & environs and tiled orthophoto of Vila Andrade were mosaiced respectively to foster further analysis (see fig 21). The drone images were mosaiced with Agisoft Metashape software by the drone operator due to his better understanding of the terrain. The downloaded tiled orthophoto of Vila Andrade were merged with the aid of the mosaic tool in the ArcGIS Pro software.

4.2.2 Image Classification

Image classification involves extracting information (e.g. land cover classes) from multiband remotely sensed imagery (Esri, 2021d). As such, it is very crucial when carrying out digital image analysis. It entails classifying the features in an image considering the objects or the land cover types that these features represent in real life. Using imagery to map slums requires image classification. Since slums are majorly situated within urban environment, image classification is essential to delineate the slum areas from other land covers (non-slums, vegetation etc.).

4.2.3 Classification Wizard in ArcGIS Pro

ArcGIS Pro software has an in-built step for image classification called “Classification Wizard”. The classification wizard has an integrated and comprehensive workflow involving series of steps for classifying imagery (Esri, 2021d). Noteworthy, the classification methods in this workflow are supervised and unsupervised classifications, whereas pixel-based and object-based are the classification types (see fig 19). Both methods contained the two classification types. For this study, the supervised classification was used because it involves providing training samples to achieve the classified result, which suits the purpose of this study. The pixel-based and object-based classification workflow were as shown in fig 22.

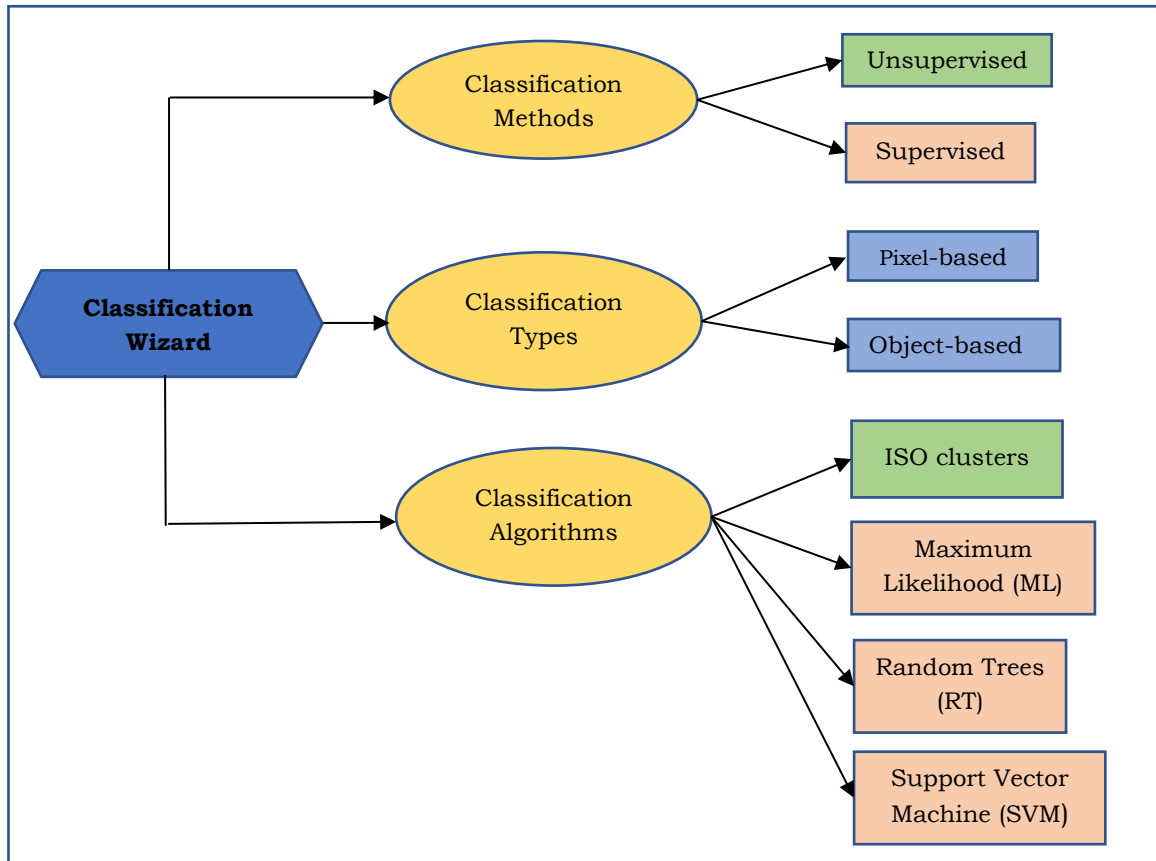


Fig 19 The classification wizard structure in ArcGIS Pro (Source: Author)

4.2.4 Supervised Classification (Pixel and Object-Based)

The supervised classification involves guiding the image processing software (algorithms) with training sample selection and classes division to aids its classification. Therefore, it can also be referred to as human-guided classification. The user’s knowledge about image classification is very paramount in the sense that the user would select sample pixels or objects that represent specific features in the image and the algorithms (classifiers) uses the selected sample pixels as a reference to classify other pixels or objects in the image (Mapasyst, 2019). Importantly, the classification result is highly dependent on the training samples provided for the classifiers (Esri, 2021d). The classification processes carried out in this study for the pixel and object-based methods were explained in this section.

Four ArcGIS Pro project workspaces (i.e. slum mapping 1 – 4) were created for the classifications. The administrative boundary and the imagery were added to the individual project workspaces. Due to the extent of the Sentinel-2 imagery and orthophoto, it was necessary to clip them to the extent of the study areas (see fig 20). The clipping was achieved by running the “extract by mask tool” in the geoprocessing panel of the ArcGIS Pro and the result of the process was saved in the content pane of the project.

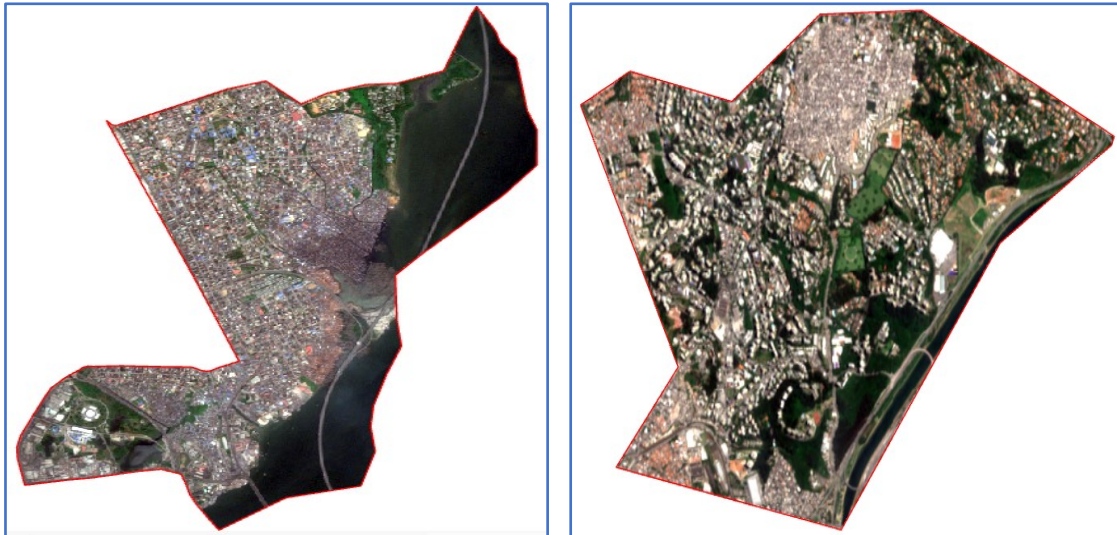


Fig 20 Clipped Sentinel-2 imagery of Lagos mainland (L) and Vila Andrade (R)

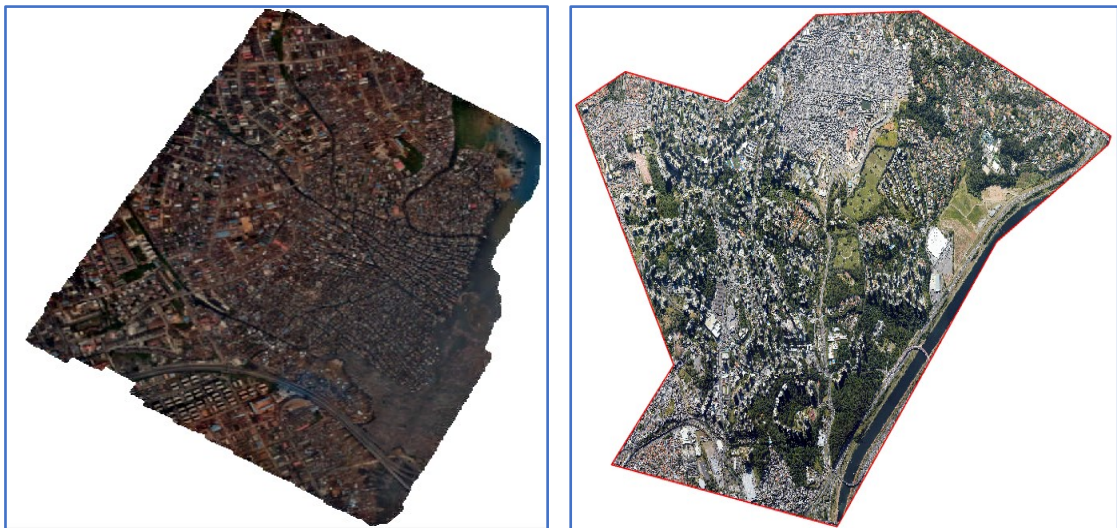


Fig 21 The mosaiced drone imagery (L) and orthophoto (R)

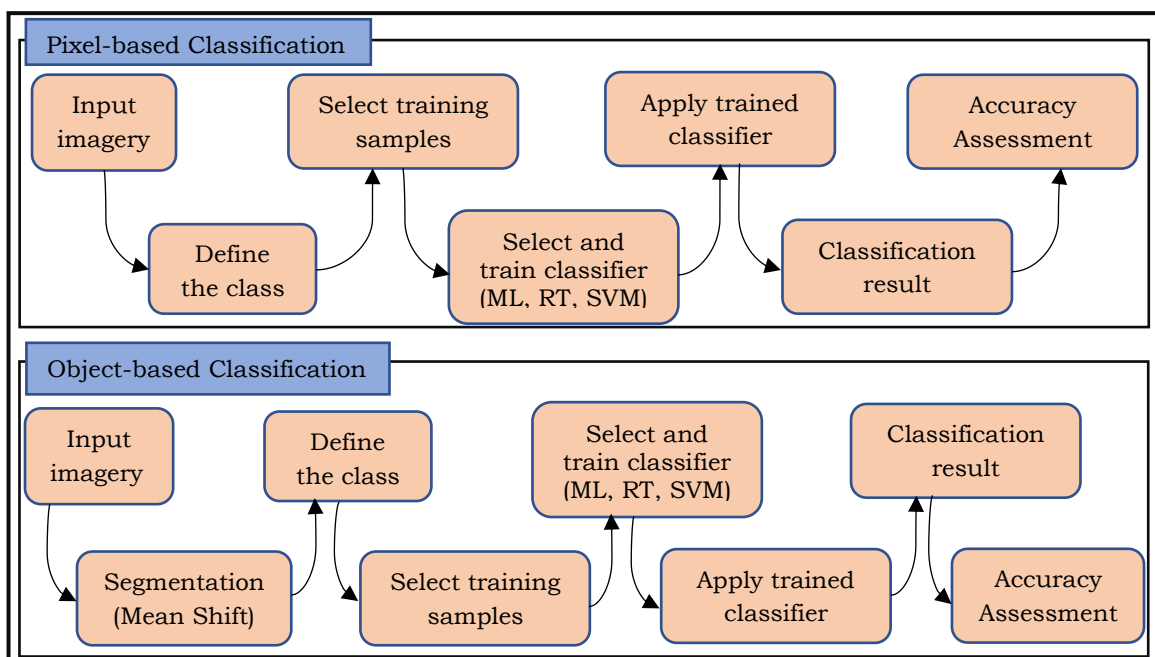


Fig 22 Pixel and object-based classification workflow (Source: Author)

4.2.4.1 Classification schema and classes

The classification schema specifies the number of classes necessary for the classification and it houses the classes. For this study, a classification schema was generated and saved as an Esri classification schema format (.ecs) on the computer system. Furthermore, five classes were created for the classification, namely slum area (buildings), non-slum areas (buildings), water, vegetation and roads as shown in fig 23.

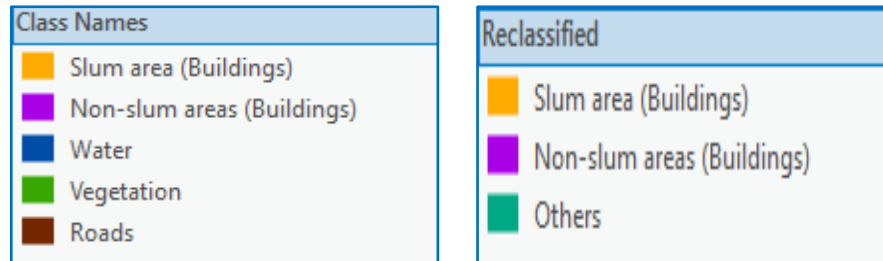


Fig 23 The five classes (L) and the reclassified three classes (R) (Source: Author)

4.2.4.2 Image Segmentation

Image segmentation is necessary for the object-based method because it facilitates finding image object primitives, which are the basic processing units used for classification (Yan, 2003). In reality, an image object provides considerably more information when comparing it to a single pixel. The principle of segmentation is to produce image objects either as small as possible or as large as necessary, depending on the purpose of usage and the parameters adopted for the segmentation. When segmenting an image, neighbouring pixels that have similar colour and shape are grouped.

The mean-shift segmentation (i.e. the segmentation process) has been integrated into the classification wizard workflow. Image segmentation was carried out during the classification with the object-based method. Mean shift segmentation works by calculating the local density gradient of homogenous image pixels. The gradient calculations are executed repetitively to identify all similar pixels from the pixels of an image (Zhou et al., 2011). In ArcGIS Pro, the result of the segmentation is based on the values (between 1 to 20) assigned to the spatial (closeness between features), spectral (difference in spectral characteristics of features) details and the minimum segment size (values are between 1 to 9999) during the segmentation process.

To achieve the segmentation, the spectral detail was assigned value 15; 5 was assigned to the spatial detail while the minimum segment size was 20. For the pixel-based method, segmentation was not carried out as it was not part of its workflow. The pixel-based method classifies image based on spectral detail only (Richards, 2013).

4.2.4.3 Selection of training samples

The principal objective of this section is to gather a set of statistics that depict the spatial and spectral response pattern of the feature type (classes) for the image classification. Training data are typically the image pixels that denote the spatial and spectral information of land cover classes which the user selects in the case of supervised classification for training the algorithms. For optimum classification result, training samples must be complete and properly represent the land cover class it intends to classify, i.e. training sample for each class must be distinctive and cut across all spectral variability for such class and sufficiently represented in the training set statistics adopted for the classification (Mather, 1987; Lillesand et al., 2000).

Training samples for the classes were selected with the aid of the training samples manager in the classification tools. The samples were applied to both pixel and object-based classification methods. To carefully delineate slums areas from non-slum areas, it was necessary to select the samples based on a pattern. As described in section 2.1, the major part of the slum area in Lagos Mainland (study area 1) is situated on water. Therefore the selected samples in study area 1 followed the pattern of slum buildings on water, slum buildings on land and the building clusters. The training samples of the slum area in Vila Andrade (Study area 2) were selected based on roof types and building morphology. Non-slum (buildings) are usually not clustered hence the training samples were picked in this manner. The other three classes (water, vegetation, roads) were selected based on their true representation. The training samples were saved in shapefile format in the project folder (i.e. LagosMainland_TS.shp, Makoko_TS.shp, Vila_Andrade_TS.shp). Fig 24 shows the selected training samples for the study areas.

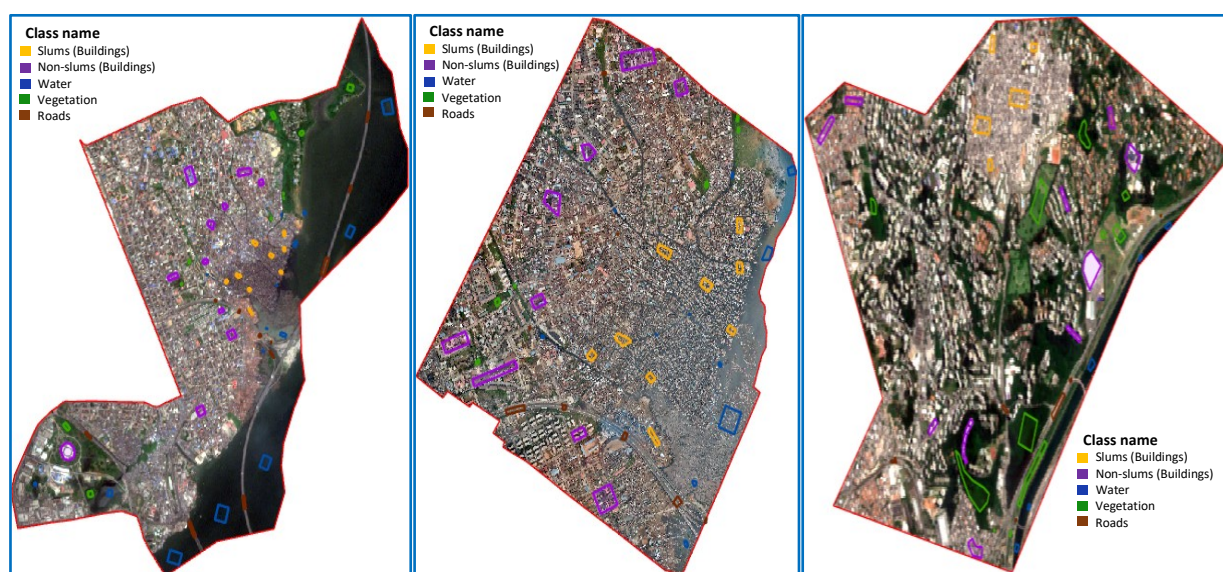


Fig 24 The selected training samples for the classification process (Source: Author)

4.2.4.4 Training and applying the algorithms (classifiers)

After selecting the training samples, the three algorithms (maximum likelihood, random trees and support vector machine) for the supervised classification were trained with the training samples and were applied to the imagery. The working principles of the algorithms are further explained in detail, although they have been integrated into the classification wizard of the ArcGIS Pro software.

4.2.4.5 Maximum Likelihood (ML) Algorithm

The maximum likelihood algorithm is a traditional parametric technique and one of the widely used algorithms (classifiers) for supervised image classification (Tucker et al., 2004). Myint et al., 2011 stated that ML is based on the assumption that a pixel belongs to a specific class and such assumptions are the same for all classes. To achieve an accurate result with the ML algorithm, the training samples representing each class have to be similar and follow a normal distribution (Esri, 2021d). The ML algorithm operates by computing weighted distances (likelihood) and it follows the Bayesian equation as expressed below (ERDAS, 1999).

$$D = (\ln(a_c) - [0.5 \ln(|Cov_c|)]) - [0.5(X - M_c)] T (Cov_c^{-1})(X - M_c)$$

Where: D = likelihood (weighted distance);

\ln = the natural logarithm function; c = a specific class;

a_c = percent assumption that any candidate pixel is a member of class c (usually has its default as 1.0 or is inserted from a priori knowledge);

X = the candidate pixel's measurement vector;

M_c = mean vector of the class sample c ; T = transposition function;

Cov_c = the covariance matrix of the pixel of the class sample c ;

$|Cov_c|$ = the determinant of Cov_c ; Cov_c^{-1} = the inverse of Cov_c .

For this study, the training of algorithms and the classification were achieved concurrently. Using the classification schema of five classes (see fig 23), the ML algorithm was applied to classify the imagery after properly trained the algorithm with the training samples. The pixel-based classification was achieved and afterwards, the object-based classification was carried out. The classification process followed the sequence of classifying the study area 1 (Lagos Mainland Sentinel-2 and drone imagery) followed by the study area 2 (Vila Andrade Sentinel-2 imagery and orthophoto).

4.2.4.6 Random Trees (RT) Algorithm

The random tree, which is regarded and often used in many texts as random forest or decision tree algorithm (classifier) is one of the possible approaches for image classification, which is known for resisting overfitting (Esri, 2021d). A random tree is a group of classification trees where each tree contributes a single vote to the actualization of the classification result from the input or sample data (Guo et al., 2011). Random tree utilizes a random subset of input features, hence facilitating error reduction due to generalisation (Rodriguez-galiano et al., 2012).

Safavian & Landgrebe, 1991 stated that the RT algorithm split up very complex image classification problems into a series of simpler decisions hoping that the final result would correspond with the desired (expected) result. Fig 25 shows a typical random tree diagram where $C(t)$ is the subset of classes that is accessible from node t , $F(t)$ is the feature subset that is used at node t and $D(t)$ is the decision rule that is utilized at node t .

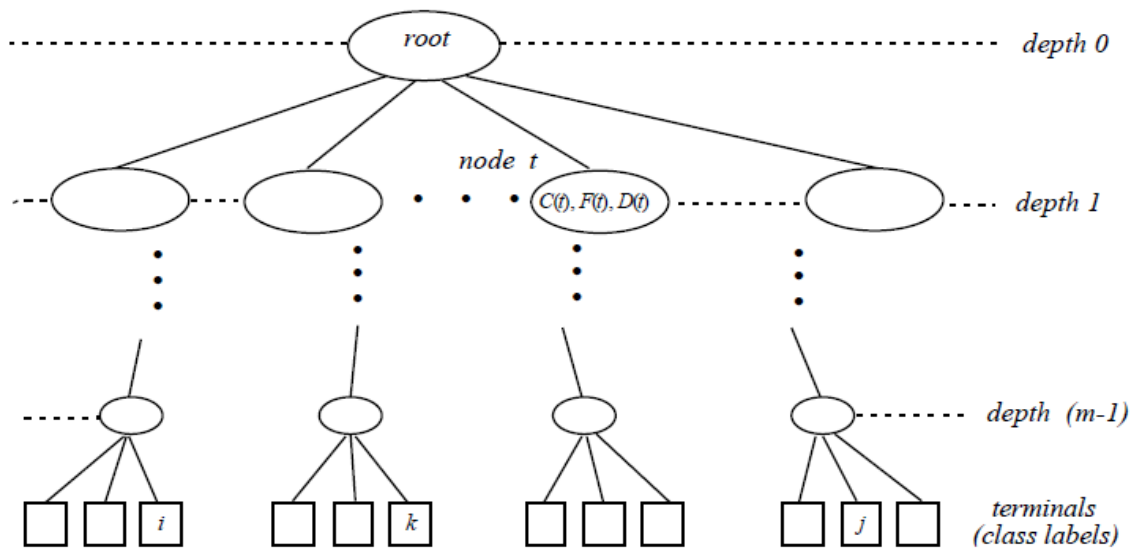


Fig 25 Sample of a generic random tree (Safavian & Landgrebe, 1991)

The random trees algorithm was trained and applied using the same training samples from the maximum likelihood. The same classification process was followed as explained in the maximum likelihood process.

4.2.4.7 Support Vector Machine (SVM) Algorithm

Support vector machine algorithm has gained a lot of recognition and gone through many evolutions since it was first introduced in 1963 by Vapnik and Chervonenkis (Vapnik V. N et al., 1971). SVM is a supervised learning technique applied for classification, regression and outlier detection (Scikit-learn, 2020). Basically, it is one of the most widely used algorithms in science and technology, especially in remote sensing. In principle, SVMs works by constructing a hyperplane or set of a hyperplane in a high dimensional space.

Simply put, SVMs are linear binary classifiers that designate to a class a given test sample from one of the two possible labels (Mountrakis et al., 2011). It is majorly aimed at establishing decision boundaries in the feature space, thereby classifying data points that belong to different classes and, therefore, mapping the input space into a high dimensional feature space (see fig 26a). SVMs minimizes the error of generalization by creating a supreme hyperplane within two classes (Raghavendra et al., 2014). Fig 26b demonstrate a classification problem from a simple linear SVM where there exist two classes in a two-dimensional input space.

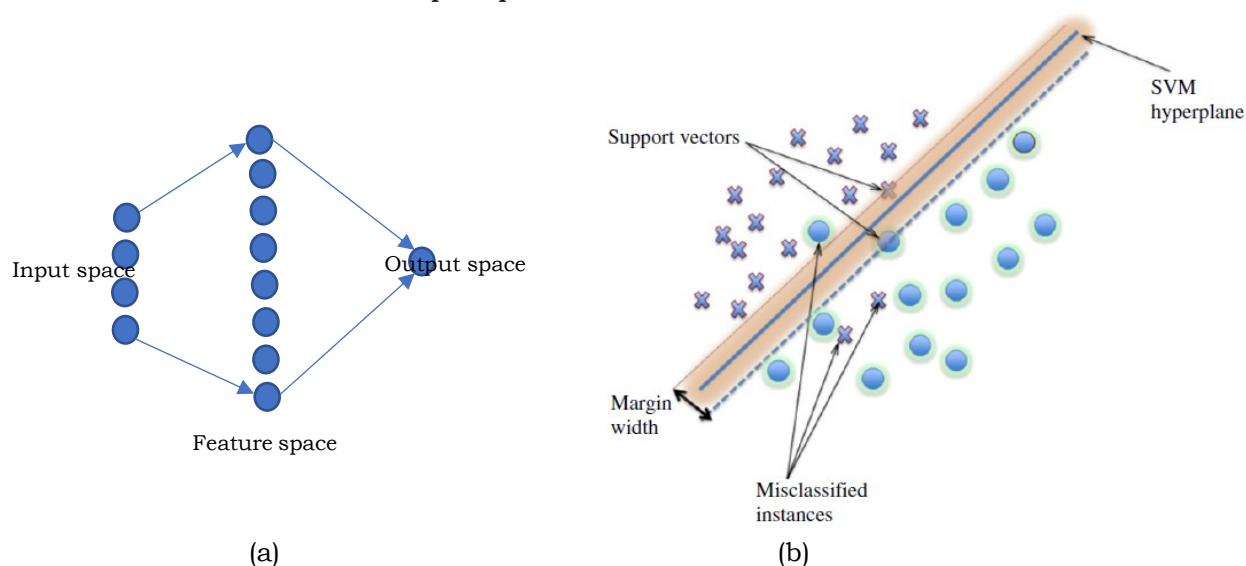


Fig 26 Sample of a linear support vector machine (Raghavendra et al., 2014; Mountrakis et al., 2011)

In ArcGIS Pro, the SVM algorithm has been integrated into the classification wizard. After properly selecting training samples that were used by the ML and RT algorithms, the SVM algorithm was therefore trained and applied for the classification which followed the same process as that of the ML and RT algorithms. The results of the classification for all imagery were achieved in five classes accordingly.

4.2.4.8 Class Merging

Some classes were merged to distinctively distinguish slum areas from other classes and to accomplish simplified results in the classification. Water, vegetation and roads were merged into a superclass named “Others” (see fig 23). After the merging process, a classified result was achieved that displayed three classes (slums {buildings}, non-slums {buildings} and others).

4.2.5 Deep Learning (DL) Classification in ArcGIS Pro

The deep learning classification has a separate workflow in ArcGIS Pro. The process involved preparing the training data, training the deep learning model (U-Net algorithm), and classifying the imagery with the trained model. This classification was carried out on the drone imagery and the orthophoto. Two project workspaces were created for this analysis and both datasets were added to the individual workspace. The drone imagery was firstly classified, followed by the orthophoto. Fig 27 presents the deep learning workflow employed for classifying the imagery.

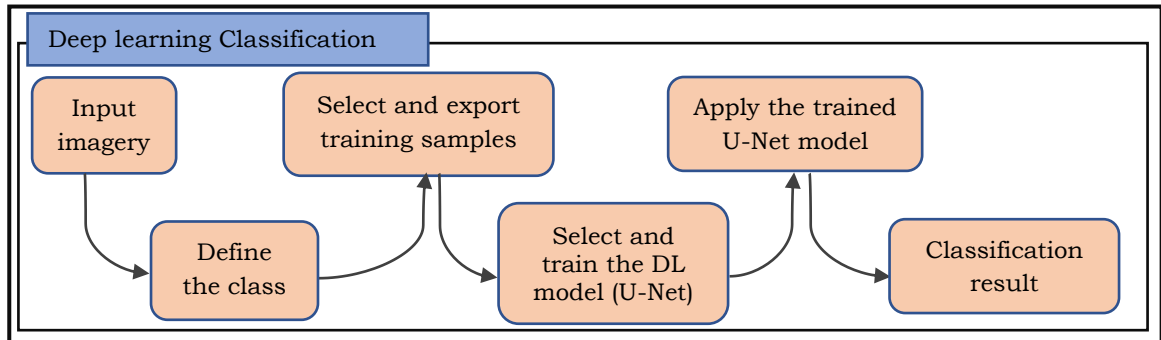


Fig 27 Deep learning classification workflow (Source: Author)

4.2.5.1 U-Net Model

The U-Net, built as a convolutional neural network (CNN) was invented in 2015 by Ronneberger et al. for biomedical image segmentation (Wikipedia, 2021b). CNNs are established on translation invariance and their basic elements (i.e. activation functions, convolution and pooling) function on local input regions, which rely only on relative spatial coordinates (Shelhamer et al., 2017).

In image classification, U-Net worked with the principle that the image is the input data and output is one label. It classifies every pixel and ensures that the input and output share the same size, although it localises and differentiates their borders (Jeremy Zhang, 2019). According to SankeSara, 2019, U-Net utilises a new loss weighting scheme for every pixel which helps to generate higher weight at the boundary of segmented objects. A typical U-Net architecture is presented in fig 28.

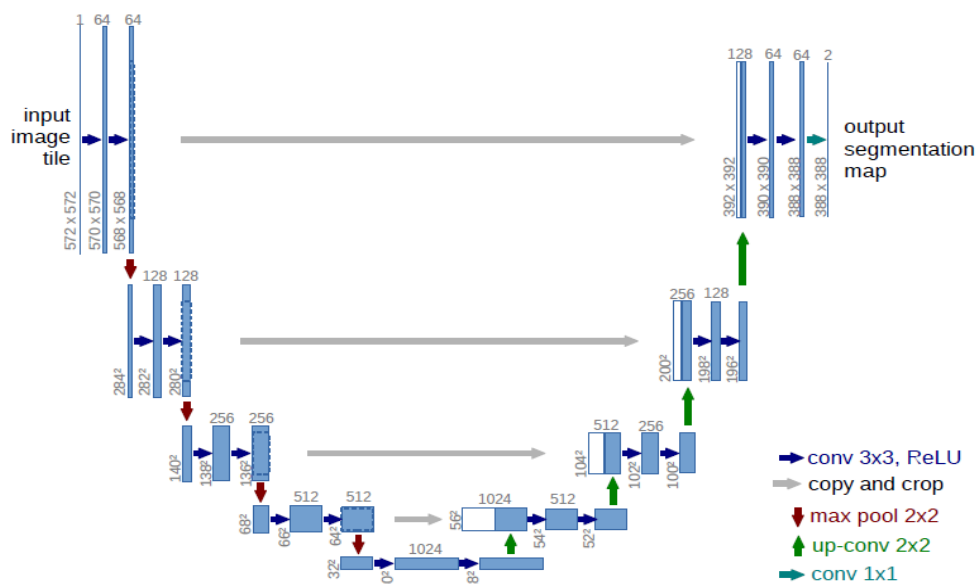


Fig 28 U-Net architecture (Ronneberger et al., 2015)

The workflow of the deep learning classification has been integrated into the ArcGIS Pro software. The training samples that were used for the pixel and object-based classification were employed for the deep learning classification. The training samples were exported as training data using the label objects for the deep learning tool in the classification tool panel to train the deep learning model. U-Net classifier which is a pixel classification model was chosen because it requires fewer parameters for image classification (Esri, 2021c).

The model was trained and ran for 20 epochs (see fig 29). After the training process, the “classify pixels using deep learning tool” was used to classify the imagery. This enabled deploying the trained model (i.e. “Mak_DL_TModel.emd” as in the case of study area 1 (Lagos Mainland)) to classify the imagery. This process was followed to classify the orthophoto.

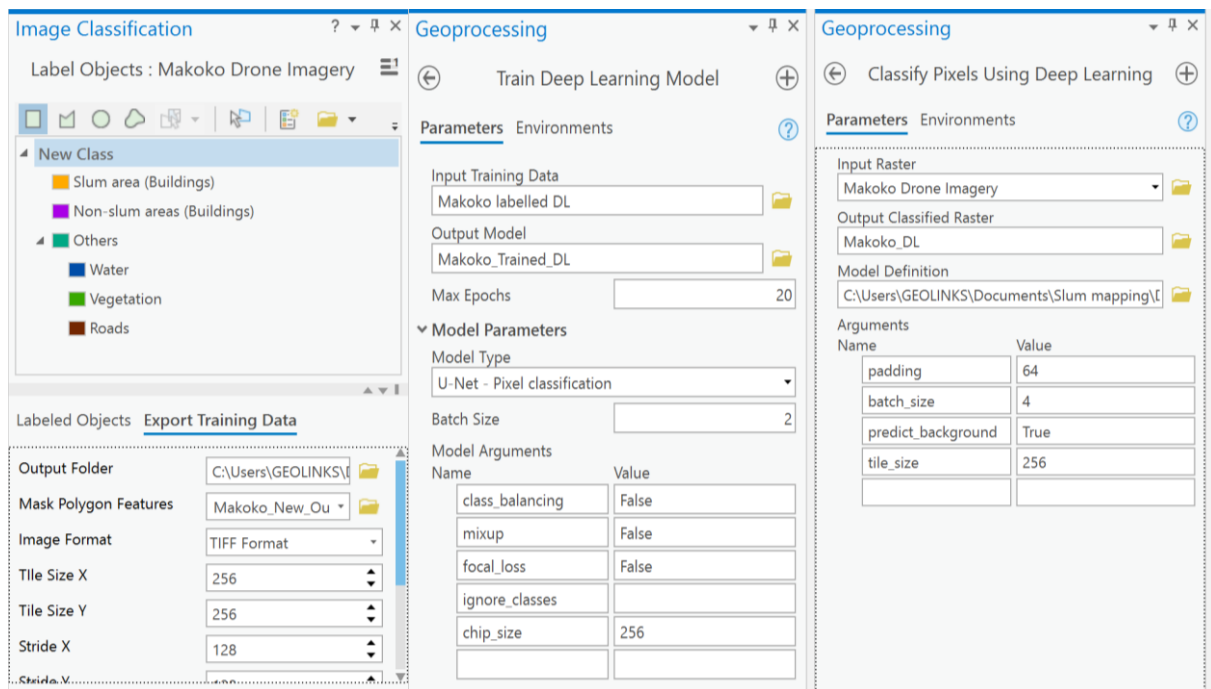


Fig 29 The deep learning classification process for the Makoko drone imagery (Source: Author)

4.3 Reference or Ground truth Dataset

Having a reference or ground truth data is paramount for image classification as this enabled checking the accuracy of the classification result. Reference data can be a raster dataset, polygon feature class (shapefile) or point feature class (shapefile) (Esri, 2021b). In this study, the polygon feature class was used to ensure that the reference data covers the entire study area. The reference data of the study areas were acquired by expert knowledge and visual interpretation from the VHR drone imagery, orthophoto and Esri world imagery. A new project workspace named “Slum Mapping Reference Data” was created in ArcGIS Pro and the imagery was added to the workspace. A polygon feature class (shapefile) was created, which was loaded in the content pane accordingly and in the attribute table of the feature class, new fields were created, namely “Classname” and “Classvalue” which housed the classes (slum area (buildings), non-slum areas (buildings), water, vegetation and roads) and their classification schema values.

“Create feature tool” was clicked and the classes were digitized based on visual perception and saved accordingly as shown in fig 30. This process was followed to achieve the reference data for the study areas. In the case of Lagos Mainland, the drone imagery

could not cover the entire area. Hence the Esri world imagery was used to digitize the missing areas. After the digitizing process, a new field was created in the attribute table of each reference data. The “water, vegetation and roads” features were merged and named as “Others” in this field.

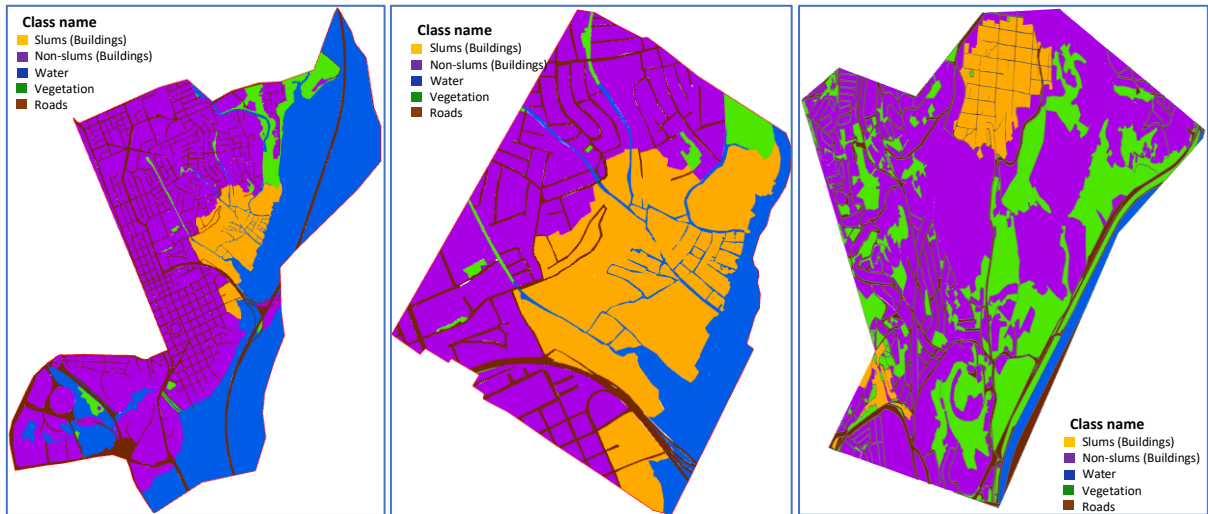


Fig 30 The reference dataset for the study areas (Source: Author)

4.4 Classification accuracy assessment

Accuracy assessment is the final process of image classification (Patil et al., 2012). In principle, accuracy assessment is the degree of correctness of a classification. By definition, it is the degree of conformity of the derived image classification to the ground truth or the reality (Foody, 2002). To ensure that any classification result is accurate to some degree, it is evident to carry out evaluation and accuracy assessment.

In ArcGIS Pro, image classification accuracy can be accessed using the site-specific accuracy assessment including the confusion matrix, which is also called an error matrix. A confusion matrix states the relationship between the classified image and the reference data samples with the result displayed as a square array of numbers in rows and columns (Foody, 2002). The rows indicate the classes from which the information categories are classified, while the columns display the information categories (Patil et al., 2012). The confusion matrix is given by the user accuracy, producer accuracy and kappa statistics (Esri, 2021b). The user accuracy shows the omission errors or false positives. The producer accuracy expresses the commission errors or false negatives and kappa statistics display the overall assessment of the classification accuracy. The accuracy is represented from 0 to 1, with 1 denoting that the accuracy is 100 percent. Table 4 displayed a sample of the confusion matrix table in ArcGIS Pro where P_Accuracy is the producer accuracy, U_Accuracy denotes the user accuracy and Kappa means the kappa statistics.

Table 4 Sample of the result of confusion matrix accuracy assessment.

ClassValue	C_100	C_101	C_102	Total	U_Accuracy	Kappa
C_100	20	8	3	31	0.645161	0
C_101	12	23	7	42	0.547619	0
C_102	0	4	23	27	0.851852	0
Total	32	35	33	100	0	0
P_Accuracy	0.625	0.657143	0.69697	0	0.66	0
Kappa	0	0	0	0	0	0.488491

In the ArcGIS Pro image classification wizard, there exist the accuracy assessment tool where the assessment was carried out. For this study, 100 random points were selected for each assessment. The equalized stratified random sampling strategy was selected, which allows the points to be distributed equally amongst each class. The reference data in section 4.3 was inputted into the reference data panel of the workflow in each case. This process was carried out for all the classification results of three classes (after class merging). The accuracy assessment results were further analysed in section 6.4 where the comparison of algorithms was explained.

4.5 Slum Change Monitoring

To achieve the objective of providing a test methodology for monitoring the growth of slum areas in spreading the epidemic, change detection was carried out. The slum change detection was accomplished for the two study areas within one (1) year (i.e. before the emergence of Covid-19 and a year after) to evaluate how the pandemic has affected the migration of people within the slum areas. The first sets of Sentinel-2 imagery used for the analysis were downloaded as explained in section 4.1.1 while the Sentinel-2 imagery used for the classification process in chapter 4 was adopted as the second sets (see table 5).

Table 5 Set of Sentinel-2 imagery used for the change detection.

First sets of Sentinel-2 imagery			
Study Area	Acquisition date	Band Combination Used	Spatial Resolution
Lagos Mainland	01-01-2020	4,3,2	10m
Vila Andrade	08-12-2019	4,3,2	10m
Second sets of Sentinel-2 imagery			
Study Area	Acquisition date	Band Combination Used	Spatial Resolution
Lagos Mainland	26-12-2020	4,3,2	10m
Vila Andrade	07-11-2020	4,3,2	10m

The object-based classifications SVM result from initial classifications were retained for the second sets because it was more reliable than the results from other algorithms (see section 6.4). In that case, the first sets of Sentinel-2 imagery were classified with the object-based method (SVM algorithm) by following the same process as explained in section 4.2. The classification results from the three classes were chosen.

After the classification process, boundaries were drawn around Makoko (Lagos) and Paraisopolis (Vila Andrade) slums, respectively by visual perception using the edit tool (create features). With the prior knowledge of the location of the slums in the study area from the VHR drone imagery and orthophoto respectively, the classification results (rasters) were clipped with the created polygon (boundaries) using the “extract by mask tool” (see fig 47 and 48).

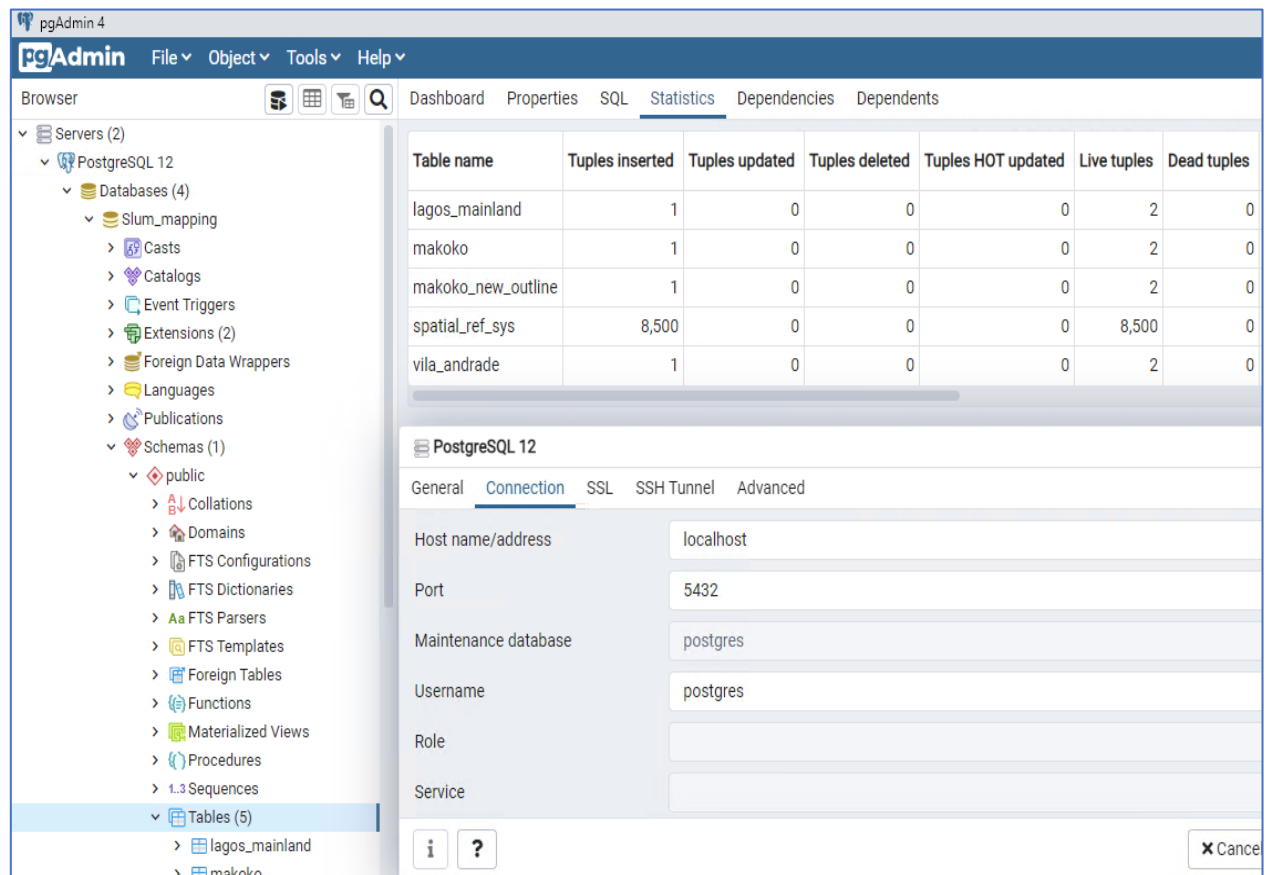
5 WEB APPLICATION DEVELOPMENT

This chapter explained the processes involved to build the web application. As described in the workflow diagram (see fig 6), the web application required to visualize the classification result was created following the outlined processes as described below.

5.1 Setting up PostgreSQL/PostGIS database

PostgreSQL database was set up to house the vector data (administrative boundary). PostgreSQL is a free and open-source object-relational database designed with the capability of storing large data. Being a very robust and flexible database system, it utilizes SQL (Structured Query Language) for its operation and can accommodate data in different formats which are expanded with extensions and dependencies. Storing spatial data on PostgreSQL requires a PostGIS extension. PostGIS is open-source software that provides supports for geographic data or objects in a PostgreSQL database.

This study utilized the localhost PostgreSQL/PostGIS database from a dedicated computer system at the Department of Geoinformatics, Palacky University Olomouc (UPOL). The computer was made available to aid the creation of a database and publishing of data. PostgreSQL was accessed using the pgAdmin4 tool and a new database named “Slum_mapping” was created. PostGIS extension was added to the database using the query tool within pgAdmin4. With the database up and running, the vector data were uploaded using the PostGIS shapefile loader as shown in fig 32. The uploaded data were checked by navigating to the schema “Public” on the pgAdmin interface within the database (see fig 31).



The screenshot displays the pgAdmin 4 interface. On the left, the 'Servers' tree shows 'PostgreSQL 12' with a sub-server 'Slum_mapping'. Under 'Slum_mapping', there are 'Databases (4)', 'Schemas (1)', and 'Tables (5)'. The 'Tables (5)' folder is expanded, showing 'lagos_mainland' and 'makoko'. The main pane shows the 'Statistics' tab for the 'lagos_mainland' table, displaying a table with columns: Table name, Tuples inserted, Tuples updated, Tuples deleted, Tuples HOT updated, Live tuples, and Dead tuples. Below this, the 'PostgreSQL 12' connection properties are shown, with the 'Connection' tab selected. The connection details include: Host name/address: localhost, Port: 5432, Maintenance database: postgres, Username: postgres, Role: (empty), and Service: (empty).

Table name	Tuples inserted	Tuples updated	Tuples deleted	Tuples HOT updated	Live tuples	Dead tuples
lagos_mainland	1	0	0	0	2	0
makoko	1	0	0	0	2	0
makoko_new_outline	1	0	0	0	2	0
spatial_ref_sys	8,500	0	0	0	8,500	0
vila_andrade	1	0	0	0	2	0

Fig 31 The database connection and the uploaded shapefiles on PgAdmin (PostgreSQL) (Source: Author)

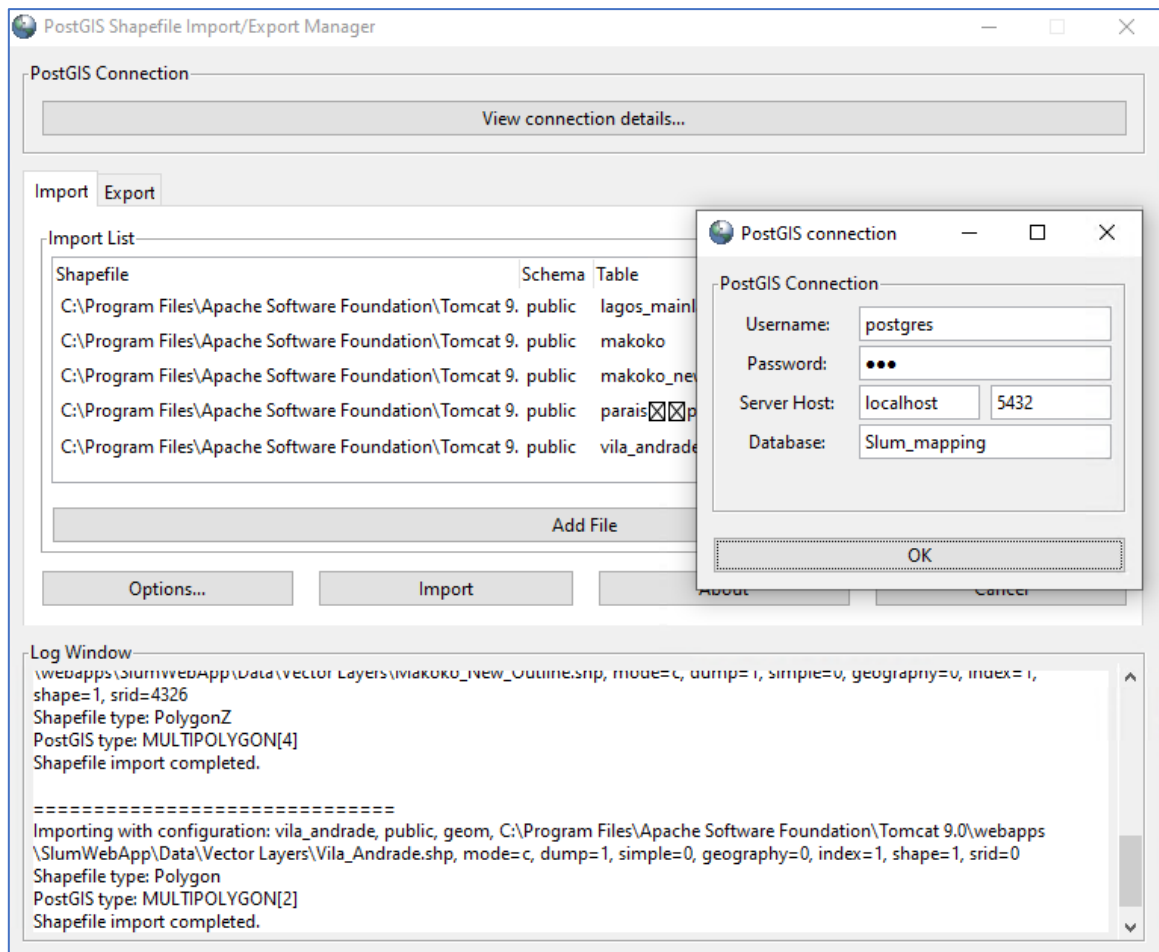


Fig 32 Uploading boundary shapefiles with PostGIS 3 shapefile loader (Source: Author)

5.2 Publishing Web Services on Geoserver

The study areas' classification results and the administrative boundaries were published as web services using the Geoserver. Geoserver is an open-source Java-based software server used for viewing, editing, sharing and publishing geospatial data following open standards (OGC, 2021). It fosters data interoperability and implements Open Geospatial Consortium (OGC) standard protocols such as Web Feature Service (WFS), Web Map Service (WMS), Web Map Tile Service (WMTS), Web Coverage Service (WCS), Web Processing Service (WPS) which can be consumed in any interoperable web application environment. This study requires the data to be published as WFS (shapefile) and WMS (GeoTIFF); hence Geoserver suits the need for the data publishing necessary for the implementation of the web application (see fig 33).

Due to the unavailability of a public server for the Geoserver, the localhost server was used with the data being published on the computer that was used for the database creation at the Department of Geoinformatics, Palacky University Olomouc. The Geoserver was installed and accessed using the designated login details and a new workspace named "Slum-mapping" was created. The workspace housed and organized the data that was published on Geoserver.

A new store was created for each raster data, which connects the data source for the published raster data. In this store section, the raster (GeoTIFF) data source was navigated from the computer directory and was published accordingly. Raster style was

created for the data that displayed the data legend and was selected during the data publishing process.

The PostGIS database was connected to the Geoserver to foster publishing the vector data. This was achieved by creating a new vector store and the PostGIS database was selected. A vector style was created with a polygon legend and applied to the published vector data. The layer preview was clicked to view the published data and the WMS/WFS RESTful URL for the published data were selected which were later used in the web application environment (see fig 34).

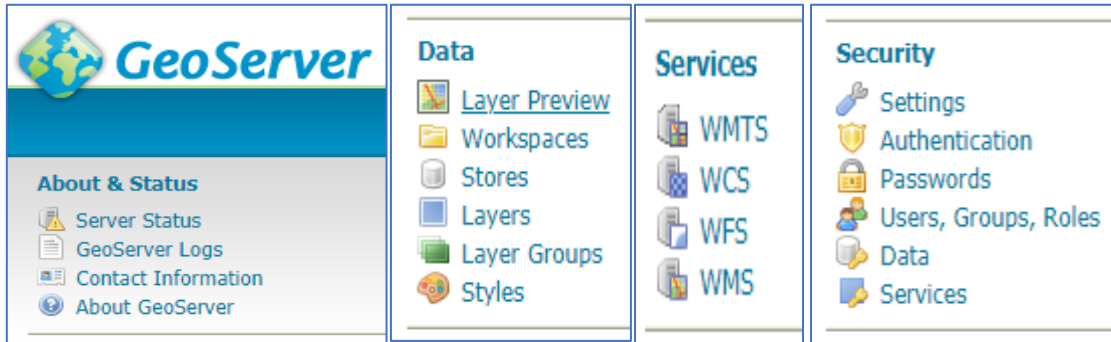


Fig 33 The Geoserver Environment (Source: Author)

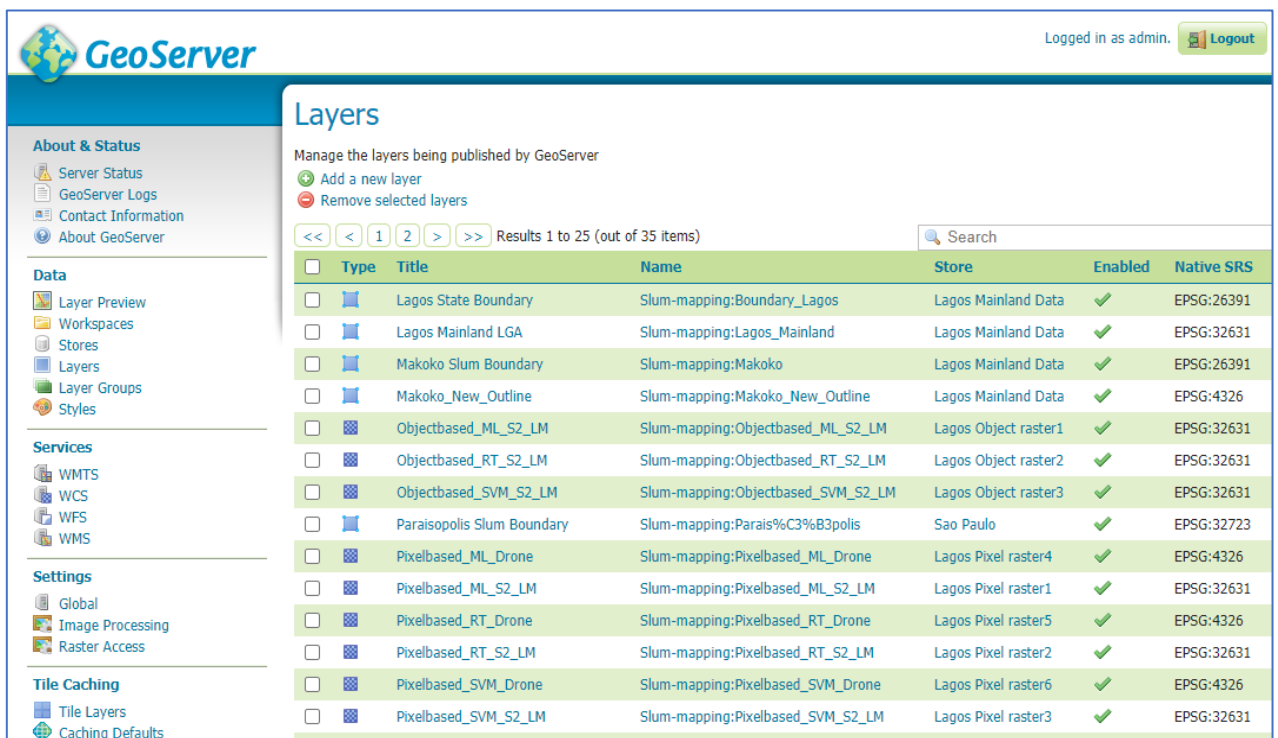


Fig 34 Section of the published data on Geoserver Environment (Source: Author)

5.2.1 Web App Creation on Leaflet

The web application was developed with the leaflet library. Leaflet is an open-source Java library employed for creating and interacting with map data on the web. It displays vector data, raster data and markers. While leaflet is embedded with major features, some advanced features on leaflet can be extended with plugins such as a Geoserver plugin (Agafonkin, 2021).

Visual studio code (VS code), being a text and code editor, was used to access the Leaflet library. The library, which contained the Hypertext Markup Language framework

(HTML), Cascading Style Sheets (CSS), JavaScript library, was downloaded from the leaflet official web page (<https://leafletjs.com/download.html>). A folder was created on the computer system named “SlumWebApp” in which the library was unzipped into the folder. VS code editor was launched and the created folder was opened to access the library from the code editor (see fig 35). HTML framework was created with connection to the CSS file (leaflet.css) and JavaScript (leaflet.js).

Geoserver requires a plugin for its usage in the leaflet because it is an advanced web platform feature. The Geoserver plugin was downloaded and added into the web app folder for easy connection and linkage into the code editor. The WFS/ WMS RESTful URLs were integrated into the leaflet code to visualise the published data on the web application. Other plugins such as full screen, minimap etc. were also downloaded and integrated into the code accordingly.

```

225 Lagos_Mainland_Boundary.addTo(map);
226
227 //Raster Images
228 var Pixel_ML_S2_LM = L.Geoserver.wms("http://158.194.94.29:8081/geoserver/wms", {
229   layers: "slum-mapping:Pixelbased_ML_S2_LM",
230   transparent: true,
231   attribution: "Mapping and Monitoring Slums Using Geoinformation Technologies",
232 });
233
234 var Pixel_RT_S2_LM = L.Geoserver.wms("http://158.194.94.29:8081/geoserver/wms", {
235   layers: "slum-mapping:Pixelbased_RT_S2_LM",
236   transparent: true,
237 });
238
239 var Pixel_SVM_S2_LM = L.Geoserver.wms("http://158.194.94.29:8081/geoserver/wms", {
240   layers: "slum-mapping:Pixelbased_SVM_S2_LM",
241   transparent: true,
242 });
243 Pixel_SVM_S2_LM.addTo(map);
244
245 var Object_ML_S2_LM = L.Geoserver.wms("http://158.194.94.29:8081/geoserver/wms", {
246   layers: "slum-mapping:Objectbased_ML_S2_LM",
247   transparent: true,
248 });
249
250 var Object_RT_S2_LM = L.Geoserver.wms("http://158.194.94.29:8081/geoserver/wms", {
251   layers: "slum-mapping:Objectbased_RT_S2_LM",
252   transparent: true,
253 });
254
255 var Object_SVM_S2_LM = L.Geoserver.wms("http://158.194.94.29:8081/geoserver/wms", {
256   layers: "slum-mapping:Objectbased_SVM_S2_LM",

```

Fig 35 Using the leaflet library in the VS code environment (Source: Author)

Scale bar, zoom control, legend, layers, base maps and imprint information were added to the web application as part of the core map elements. Different base maps (Imagery, Streetmap, Grayscale, Topographic etc.) were added to the map to have a different view about the study areas hence enabled a sound understanding of the study area’s terrain and relief characteristics. Two web applications were developed, one for each study areas i.e. Lagos Mainland LGA and Vila Andrade (see fig 36 and 37), due to their different locations and to facilitate easy access for the user.

The web applications showcased the classification results, administrative boundaries with well descriptive layers and legends. Five base maps were attached to the web application which allows user to toggle their preferred basemap. On the left side of the web map, there exists a sidebar that can be toggled on and off with an easy button. The sidebar contained other information about the results, the thesis website and a Github repository created for this study.

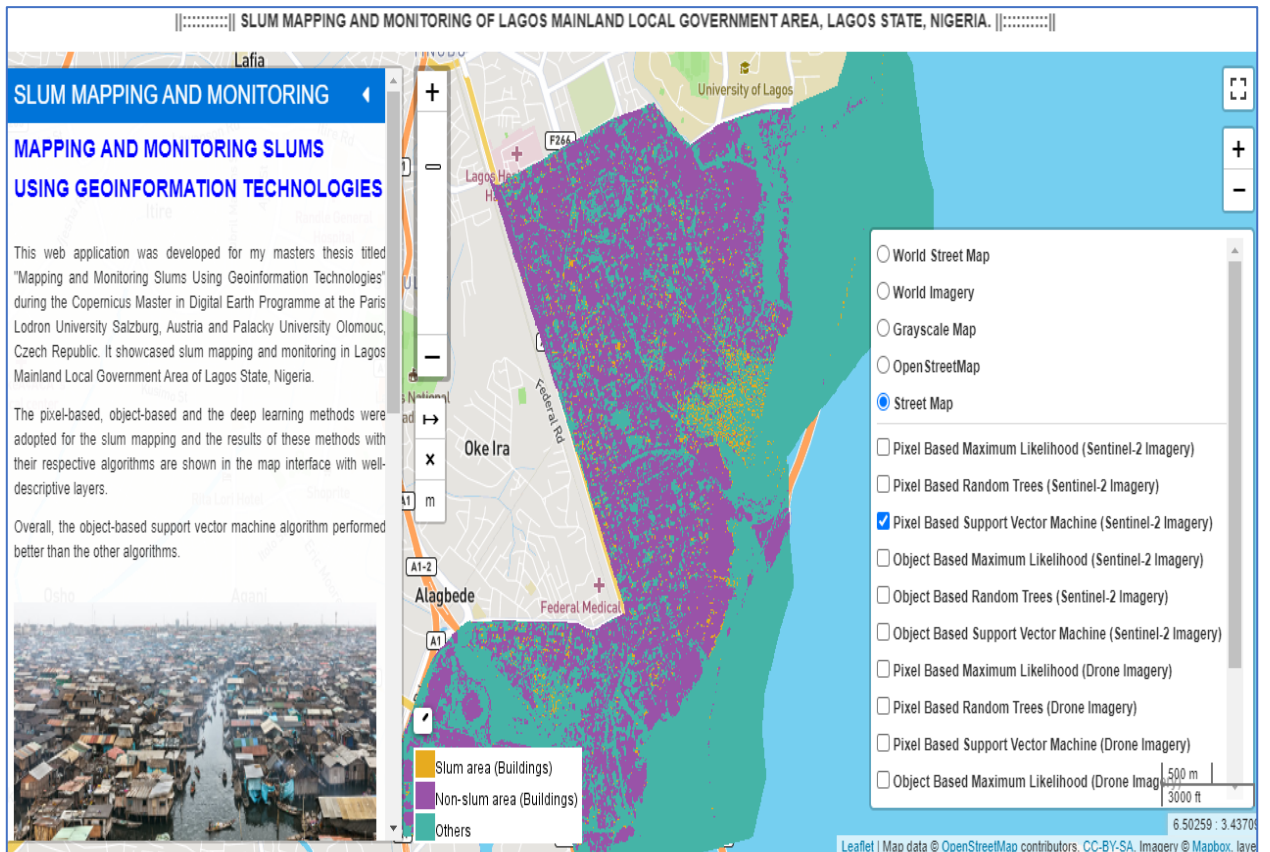


Fig 36 Web application visualizing the results of the Lagos Mainland LGA (Source: Author)

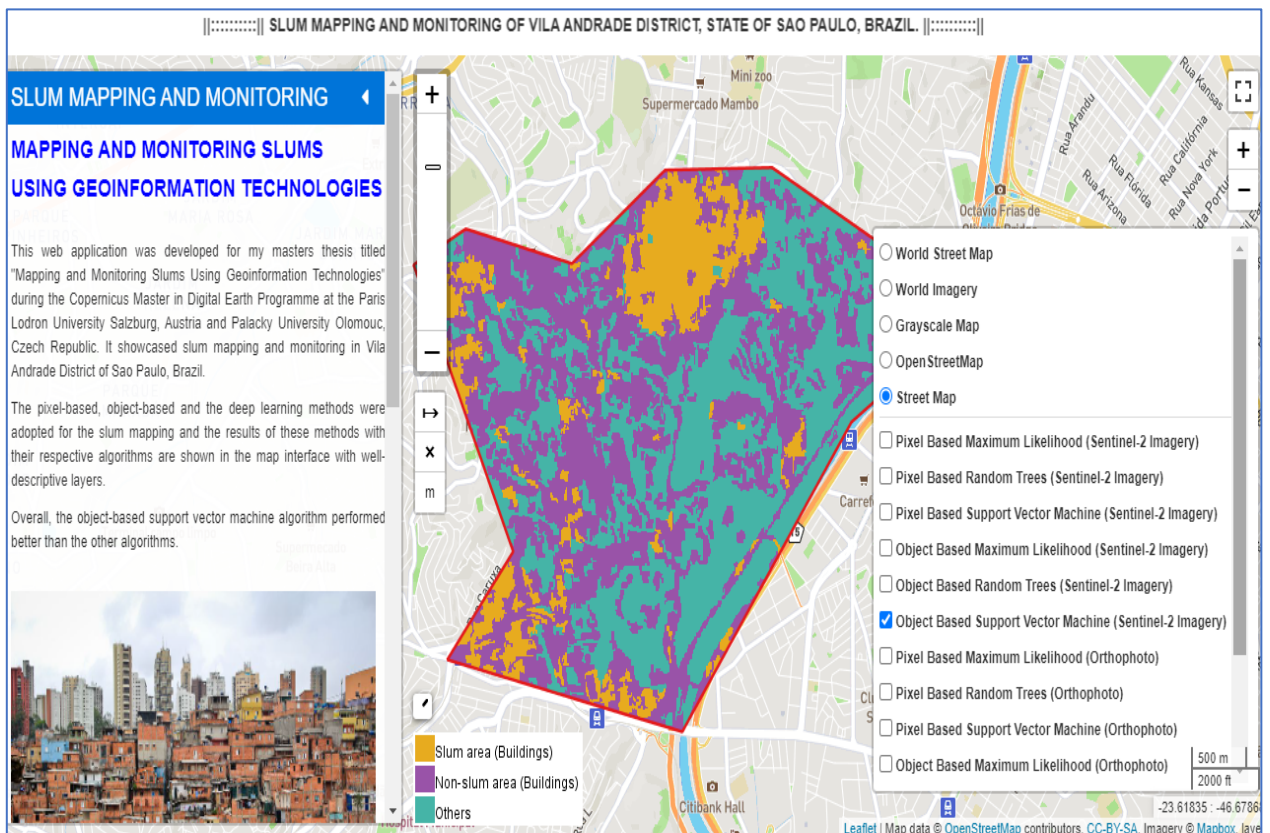


Fig 37 Web application visualizing the results of the Vila Andrade District (Source: Author)

6 RESULTS

This chapter displayed and summarised the results of the thesis. The results of the pixel-based, object-based and deep learning methods were evaluated. The performance of the algorithms in properly delineating slum areas from other classes from the study areas were accessed and evaluated. The comparison and accuracy assessment of the applied algorithms was achieved based on the error matrix (confusion matrix) and the percentage of these accuracies were highlighted. The displayed results in this chapter are the classification results obtained after class merging (i.e. three classes (slums {buildings}, non-slums {buildings} and others)) since they are the final results.

The results followed the sequence of the pixel-based classification of the Sentinel-2 imagery of both study areas, the drone imagery and the orthophoto. Then the object-based and deep learning classification results followed suit respectively. Since there is good knowledge about the morphologies and location of the slums within the study areas based on familiarity with Lagos Mainland, Nigeria (study area 1) and visual perception of Vila Andrade, Brazil (study area 2) from the orthophoto, the results are therefore analysed.

6.1 Results of the pixel-based classification

The pixel-based method employed the spectral properties of the imagery for the classification. Having successfully carried out the classifications using the pixel-based method on all datasets, the results are presented in fig 38-41. In fig 38, the classification from the Sentinel-2 imagery of Lagos Mainland showed that the ML algorithm had a lot of misclassification with noticeably misclassifying non-slum areas as slum areas, whereas the RT and SVM algorithms had good classifications to some degree.



Fig 38 Pixel-based classification result from Sentinel-2 imagery of Lagos Mainland

As shown in fig 39, the location of the slum in Vila Andrade was classified correctly with the SVM algorithm. However, some locations on the imagery were misclassified as slum areas. The RT algorithm performed better than all other algorithms in this result and the ML algorithm categorized the major part of the study area into “Other class”.

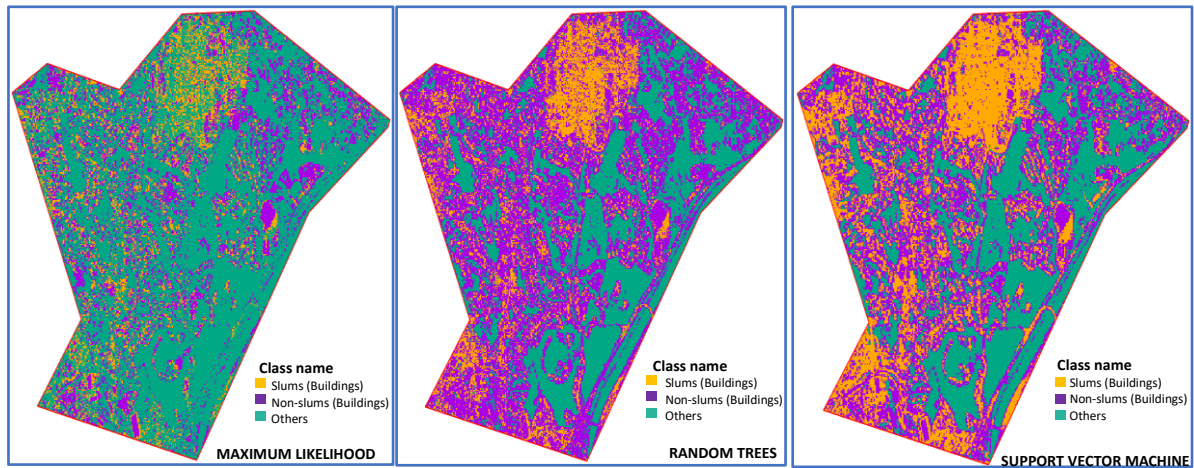


Fig 39 Pixel-based classification result from Sentinel-2 imagery of Vila Andrade

In fig 40, the result from the SVM algorithm had the best prediction with a kappa statistics of 0.662 as shown in table 8. The RT algorithm performed averagely and had some misclassifications with the prediction of non-slum areas as slums hence it has a kappa statistics of 0.514. On the other hand, the ML algorithm assigned lots of pixels as "Other Class" and had an accuracy of 0.431. It was observed that the colour and structure of the rooftops of the buildings in some part of the non-slums areas are homogenous with the slum areas. This might have huge effects on the result of the algorithms.

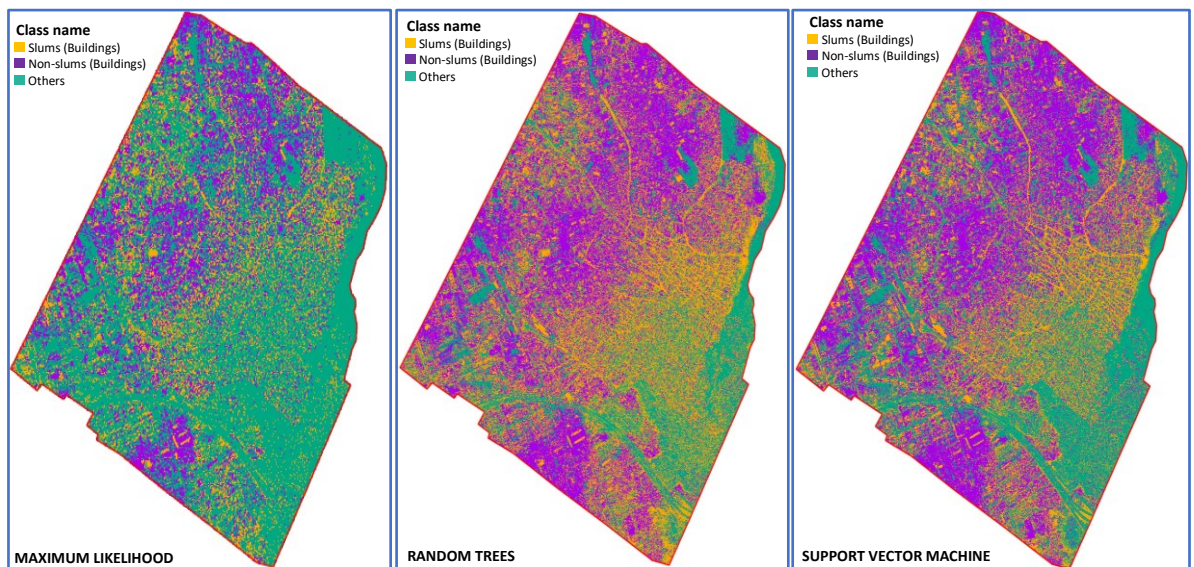


Fig 40 Pixel-based classification result from drone imagery of Makoko and environs

It was perceived that the bottom right and bottom right of the orthophoto of Vila Andrade has built structures that are homogenous to the slums, although distinct heterogeneity was noticed in other parts of the orthophoto. This observation was possible due to the spatial resolution of the orthophoto (12cm), which facilitated clear visualization of the study area. Figure 41 shows that all algorithms perceived these regions as slums however the ML algorithm overpredicted its classification.

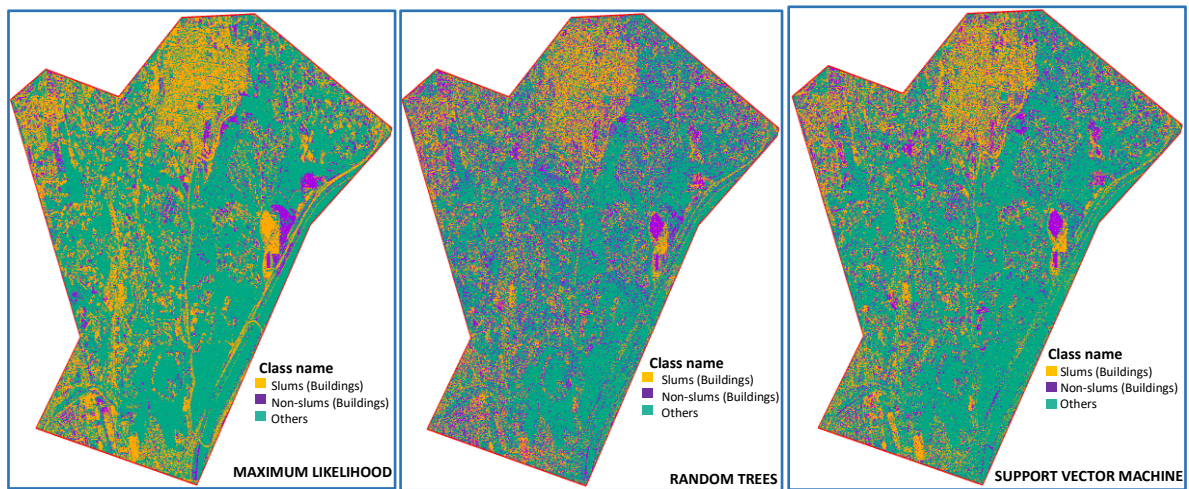


Fig 41 Pixel-based classification result from orthophoto of Vila Andrade

6.2 Results of the object-based classification

The object-based method applied the spatial and spectral characteristics for its classification. The imagery were segmented using the mean shift segmentation with the befitting parameters after having confirmed the best parameters for the segmentation process. As shown in fig 42, there were overprediction and underprediction by the three algorithms but the ML algorithm overpredicted more than the other algorithms. Slum class were assigned to non-slums areas with the RT algorithm also assigning road class (other class) as slums.

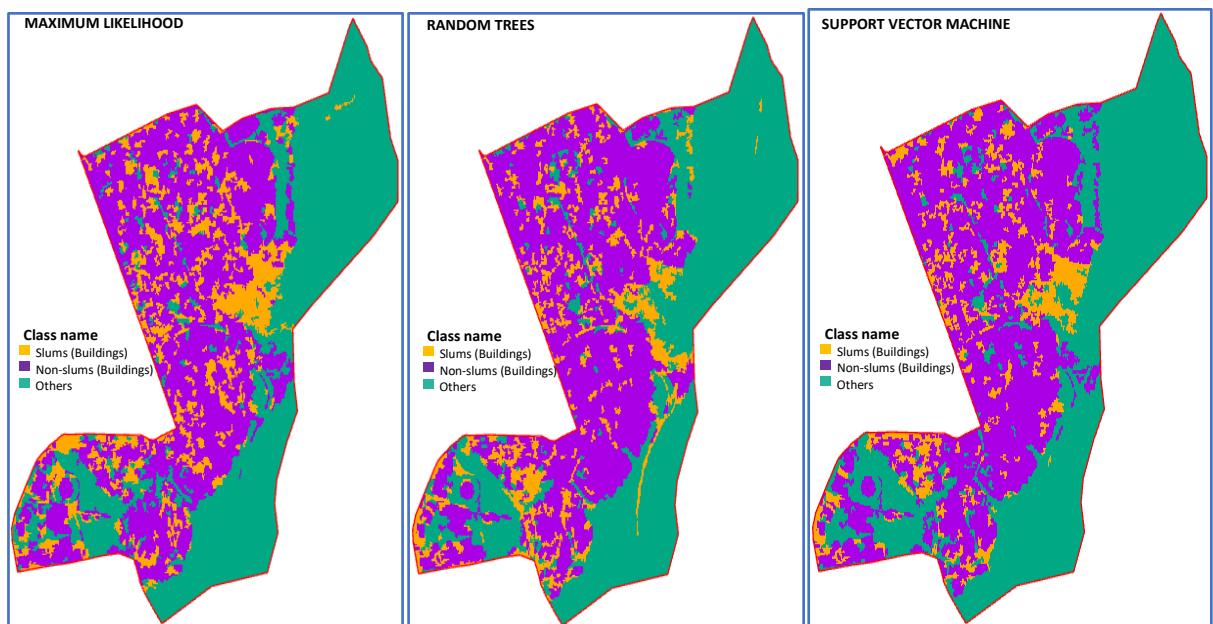


Fig 42 Object-based classification result from Sentinel-2 imagery of Lagos Mainland

The same observation as fig 42 reflected in the results shown in fig 43 but the ML algorithm had huge misclassification with user accuracy, producer accuracy and kappa statistics of 0.450, 0.543 and 0.264 respectively (see table 7). On the other hand, the SVM algorithm was able to discriminate the Paraisopolis slum distinctly with few misclassifications while RT algorithm performed averagely.

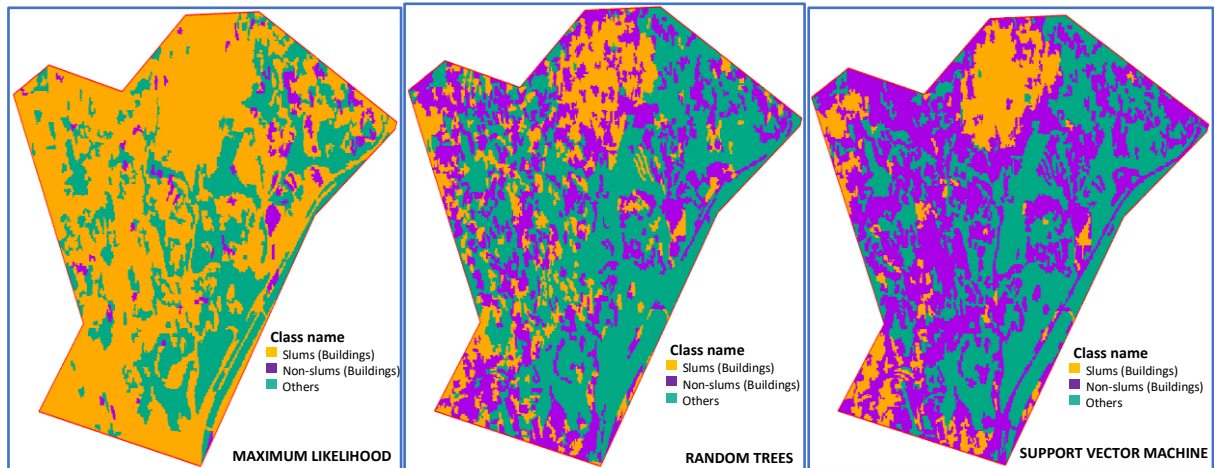


Fig 43 Object-based classification result from Sentinel-2 imagery of Vila Andrade

The object-based classification result of the drone imagery indicates that the SVM algorithm outperformed the other algorithms with user accuracy of 0.865, producer accuracy of 0.857 and kappa statistics of 0.776 as presented in table 8. The RT algorithm perceived some part of the water class (other class) as slums and the ML algorithm classified most buildings of Makoko slums into "Others class" as shown in fig 44.

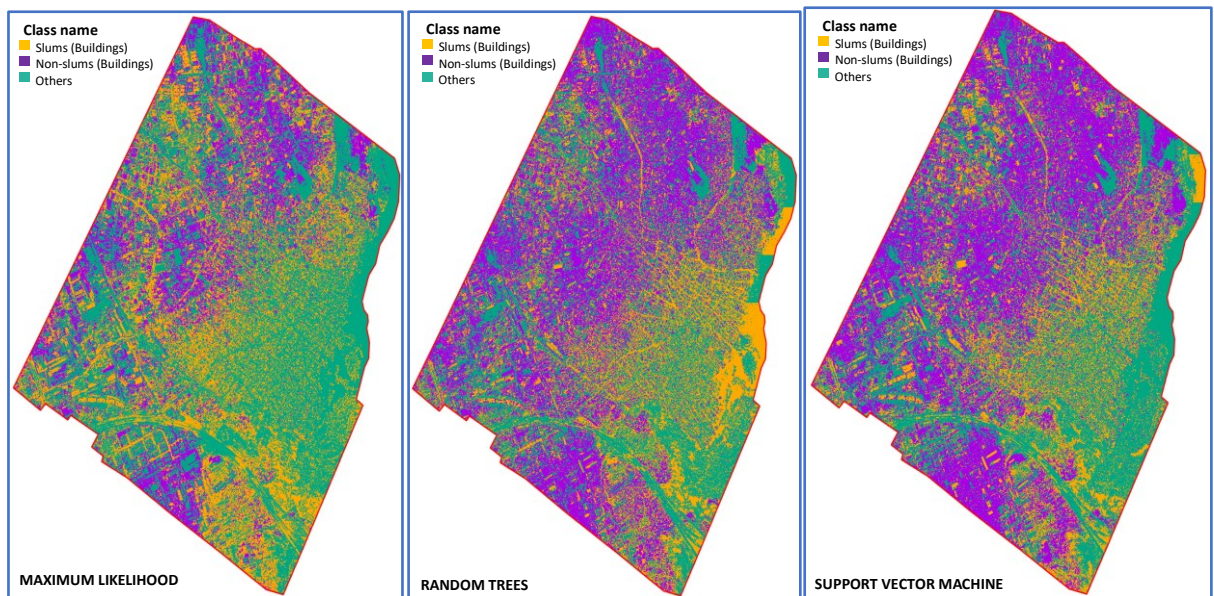


Fig 44 Object-based classification result from drone imagery of Makoko and environs

In the middle right of the results in fig 45, there was a certain building that belongs to non-slum areas and was classified as slums by the three algorithms. These misclassifications occurred because the building had similar rooftops (colour) that resembled that of the slum area; hence the algorithm perceived it as a slum building. Aside from this observation, the SVM algorithm performed much better with good discrimination of the slums, non-slum areas and others class (water, vegetation and road). The RT algorithm perceived water class (other class) as slum shown in the middle right and bottom right of the RT algorithm result. Furthermore, the ML algorithm detected and categorized majorly non-slum areas as slums.

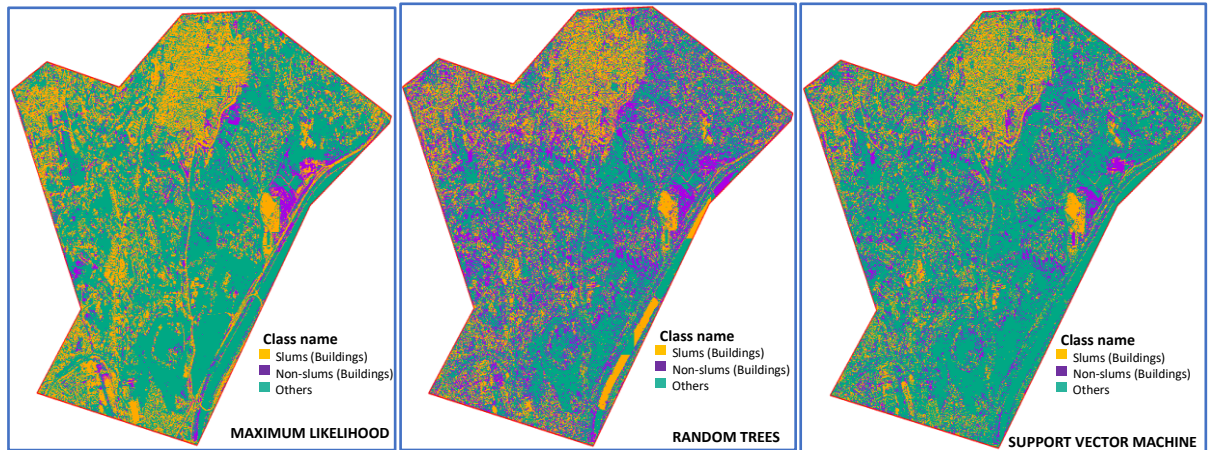


Fig 45 Object-based classification result from orthophoto of Vila Andrade

6.3 Results of the deep learning classification

The deep learning classification was carried out on drone imagery and orthophoto. Many attempts were made to classify the Sentinel-2 imagery but were unsuccessful. The U-Net model was attempted to be trained with the selected training samples for the Sentinel-2 imagery, but the process failed. Hence, the Sentinel-2 imagery was not classified with the deep learning classification. The result shown in this section were that of the drone imagery and the orthophoto with three (3) classes.

The drone imagery classification showed a false-positive and false-negative result. The false-positive implies that it classified the study area majorly as non-slums when such should not be the case, while the false negative in this regard means the model was unable to indicate the presence of other class and hence perceived them as their true classes (see fig 46a). In figure 46a, the algorithm detected and classified the slum and non-slum areas into the non-slum areas with the slum area existing as a point in the result. Furthermore, the vegetation class did not appear in the classification result (see appendix 2 for deep learning classification result with five (5) classes).

Fig 46b showcased the classification result from the orthophoto with good discrimination of the slum areas, non-slum areas and partially the vegetation areas however the water class was omitted from the classification result (see appendix 2).

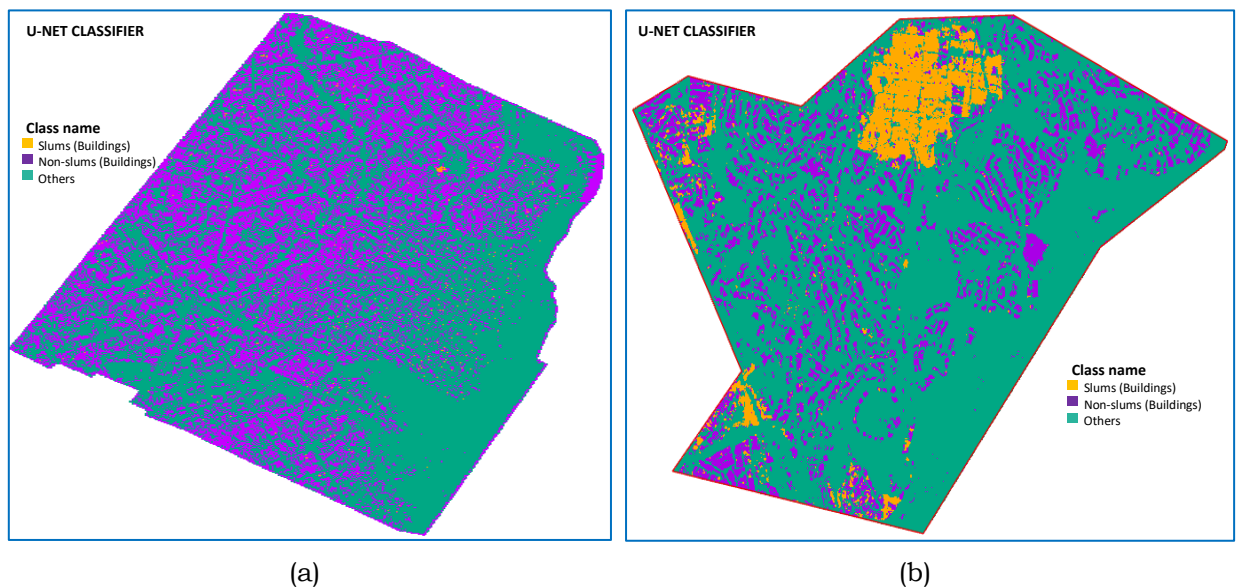


Fig 46 Deep learning classification result of the drone imagery and the orthophoto

6.4 Comparison of Algorithms

To determine the best algorithm for slum mapping and monitoring from the analysis, the results from the algorithms were compared and evaluated. The comparison was carried out based on the ability of each algorithm to achieve reliable classification result which was measured by the time consumption (processing time) and the site-specific accuracy assessment including error (confusion) matrix (user accuracy, producer accuracy and kappa statistics).

In principle, an algorithm is very effective if the user accuracy, producer accuracy, and kappa statistics of the classification are 1 (i.e. 100%). This implies that the algorithm performed at its best and handled the positive and negative classes. Hence, the algorithm solved the issue of overpredicting and underpredicting a certain class by ignoring another class in the classification.

As explained in section 4.4.2, the algorithms' accuracy was analyzed and compared categorically based on their classification methods as explained below.

6.4.1 Comparison of algorithms in the classification of Lagos Mainland Sentinel-2 imagery

Table 6 presented the accuracy result of the algorithms from the pixel and object-based methods of the Lagos Mainland Sentinel-2 imagery. The SVM algorithm performed better in both methods than other algorithms with an accuracy (kappa statistics) of 57.7% and 48.8%, respectively although the pixel-based SVM showed a better result than the object-based SVM in the classification as shown in fig 42 and 45. The RT algorithm had a similar result to the SVM algorithm with an accuracy of 54.6% and 47.1% for the pixel and object-based methods. In terms of processing time, the object-based method consumed more time than the pixel-based method (see table 11).

Table 6 Accuracy results of the pixel and object-based methods for Lagos Mainland Sentinel-2 imagery

Lagos Mainland (Pixel-based method)			
	User accuracy	Producer accuracy	Kappa statistics
Maximum likelihood (ML)	0.643	0.653	0.476
Random trees (RT)	0.746	0.693	0.546
Support vector machine (SVM)	0.763	0.714	0.577
Lagos Mainland (Object-based method)			
	User accuracy	Producer accuracy	Kappa statistics
Maximum likelihood (ML)	0.620	0.616	0.427
Random trees (RT)	0.656	0.643	0.471
Support vector machine (SVM)	0.682	0.660	0.488

6.4.2 Comparison of algorithms in the classification of Vila Andrade Sentinel-2 imagery

As shown in fig 38 and 43, the ML algorithm overpredicted in the classification results, especially in figure 38 where it categorized most of the study area as slums, hence has an accuracy of 40.1% and 26.4% for the pixel and object-based methods respectively. In the pixel-based method, the random trees algorithm outperformed the SVM algorithm. Classes that belongs to non-slums were classified as slums in the classification result of the SVM algorithm than that of the RT algorithm. The object-based method on the other

hand showed that the SVM algorithm performed better than the RT algorithm with an accuracy of 67.4% (see table 7).

Table 7 Accuracy results of the pixel and object-based methods for Vila Andrade Sentinel-2 imagery

Vila Andrade (Pixel-based method)			
	User accuracy	Producer accuracy	Kappa statistics
Maximum likelihood (ML)	0.576	0.552	0.401
Random trees (RT)	0.743	0.764	0.585
Support vector machine (SVM)	0.735	0.764	0.572
Vila Andrade (Object-based method)			
	User accuracy	Producer accuracy	Kappa statistics
Maximum likelihood (ML)	0.450	0.543	0.264
Random trees (RT)	0.701	0.698	0.547
Support vector machine (SVM)	0.812	0.806	0.674

6.4.3 Comparison of algorithms in the classification of Makoko & environs Drone imagery

The object-based method outperformed the pixel-based method in the classification result of the drone imagery, as shown in table 8. The SVM algorithm had a better performance in classifying the classes than the ML algorithm and the RT algorithm. The ML algorithm of the pixel-based method gave more attention to the “Other class” (majorly the road class). The object-based SVM algorithm with an accuracy of 77.6% was the best accuracy in this regard.

Table 8 Accuracy results of the pixel and object-based methods for Makoko Drone imagery

Makoko & environs (Pixel-based method)			
	User accuracy	Producer accuracy	Kappa statistics
Maximum likelihood (ML)	0.645	0.611	0.431
Random trees (RT)	0.689	0.675	0.514
Support vector machine (SVM)	0.775	0.774	0.662
Makoko & environs (Object-based method)			
	User accuracy	Producer accuracy	Kappa statistics
Maximum likelihood (ML)	0.533	0.532	0.288
Random trees (RT)	0.679	0.679	0.513
Support vector machine (SVM)	0.865	0.857	0.776
Makoko & environs (Deep learning method)			
U-Net algorithm	0.351	0.476	0.234

6.4.4 Comparison of algorithms in the classification of Vila Andrade orthophoto

Table 9 presents the accuracy assessment of the classification results from the Vila Andrade orthophoto. The SVM algorithms of both methods had an accuracy above 70%, although the object-based method SVM outperformed the pixel-based method. The RT algorithms misclassified the water class (other class) as slums, although the results obtained were better than that of the ML algorithms. The ML algorithm had its highest accuracy so far compared to the ML algorithm results of the other imagery. Some misclassifications were also observed in the ML algorithm results as road class (others

class) were classified as slums (see fig 41). As for the processing time, the SVM algorithms consumed more time with less time observed for the ML algorithms (see table 10).

Table 9 Accuracy results of the pixel and object-based methods for Vila Andrade orthophoto

Vila Andrade (Pixel-based method)			
	User accuracy	Producer accuracy	Kappa statistics
Maximum likelihood (ML)	0.784	0.785	0.682
Random trees (RT)	0.774	0.787	0.690
Support vector machine (SVM)	0.806	0.845	0.714
Vila Andrade (Object-based method)			
	User accuracy	Producer accuracy	Kappa statistics
Maximum likelihood (ML)	0.714	0.761	0.567
Random trees (RT)	0.708	0.724	0.582
Support vector machine (SVM)	0.846	0.847	0.780
Vila Andrade (Deep learning method)			
U-Net algorithm	0.974	0.968	0.953

6.4.5 Comparison of processing time used by the algorithms

The processing time for each algorithm to complete its task was as detailed in table 10. It is important to note that the time taken has to do with some factors: the type of imagery used, the extent of the study area, the computer configuration (computer memory), and proficiency of the operator in image classification. For the processing and analysis, this study utilized a DELL computer system with the following configurations: (Intel Core i5, 64-bit Windows 10 Pro operating system, 16GB ROM, 500GB memory, central processing unit (CPU) of 2.30GHz).

The object-based method took more processing time than the pixel-based method with the SVM algorithm of both methods consuming more time than the other algorithms. The deep learning method on the other hand used a huge amount of processing time for its classification. The computer system used for this study runs on a CPU (Central Processing Unit) which has significant effects on the processing time as a computer system with GPU (Graphics Processing Unit) is highly recommended for faster processing time.

Table 10 Processing time of all methods and the algorithms

Imagery	Required time in hours			
	Sentinel-2 imagery		Drone imagery	Orthophoto
Algorithms (Methods) / Study Area	(Lagos Mainland)	(Vila Andrade)	(Makoko & Environs)	(Vila Andrade)
ML (Pixel-based)	0.5	0.5	1.5	1.6
RT (Pixel-based)	0.7	0.8	1.8	2
SVM (Pixel-based)	0.7	0.8	1.9	2.2
ML (Object-based)	1.5	1.4	3	3
RT (Object-based)	1.8	1.6	4	6
SVM (Object-based)	2	2	5	7
U-Net (Deep learning)	----	-----	52	55

In a nutshell, the comparison of the performance of the algorithms indicates the following facts: First, the SVM algorithm of the pixel and object-based methods had better predictions with an overall accuracy of 63.1% and 68% respectively, although few misclassifications were observed. The RT algorithms of both methods had more misclassifications in all cases and had an overall accuracy of 58.4% and 52.8% for the pixel and object-based methods.

The pixel-based and object-based ML algorithms could not handle the overprediction and underprediction effects hence had overall accuracies of 49.8% and 38.7% respectively. The ML algorithms overpredicted the slums in the classification results thereby categorized non-slum buildings as slum buildings (see fig 38 and 43), most especially in fig 43 where it had the lowest user accuracy, producer accuracy and kappa statistics. The SVM algorithm consumed more processing time than the RT and ML algorithms in both methods but the deep learning model used lots of processing time to achieve the classification.

The deep learning classification had an overall accuracy of 60%. The result obtained for the drone imagery in fig 46a showed misclassifications hence predicted the slum area as non-slums areas but the algorithm performed optimally in the orthophoto (see fig 46b). Noteworthy, the deep learning algorithm did not achieve any result with the Sentinel-2 imagery.

6.5 Result of the Slum change monitoring

To calculate the slum extents (number of pixels that contained the slum area class), the values in the count column of the clipped raster attribute table were extracted and multiplied by the pixel size of the Sentinel-2 imagery (which is 10*10).

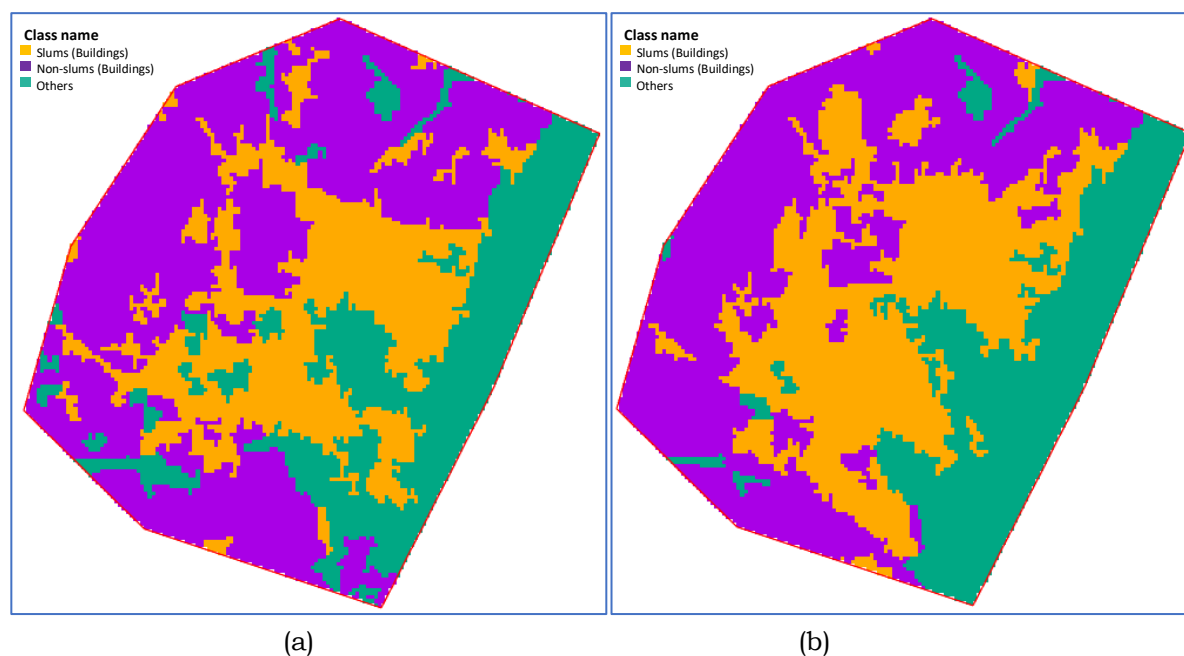


Fig 47 Clipped raster of Lagos Mainland Sentinel-2 imagery for slum change calculation.

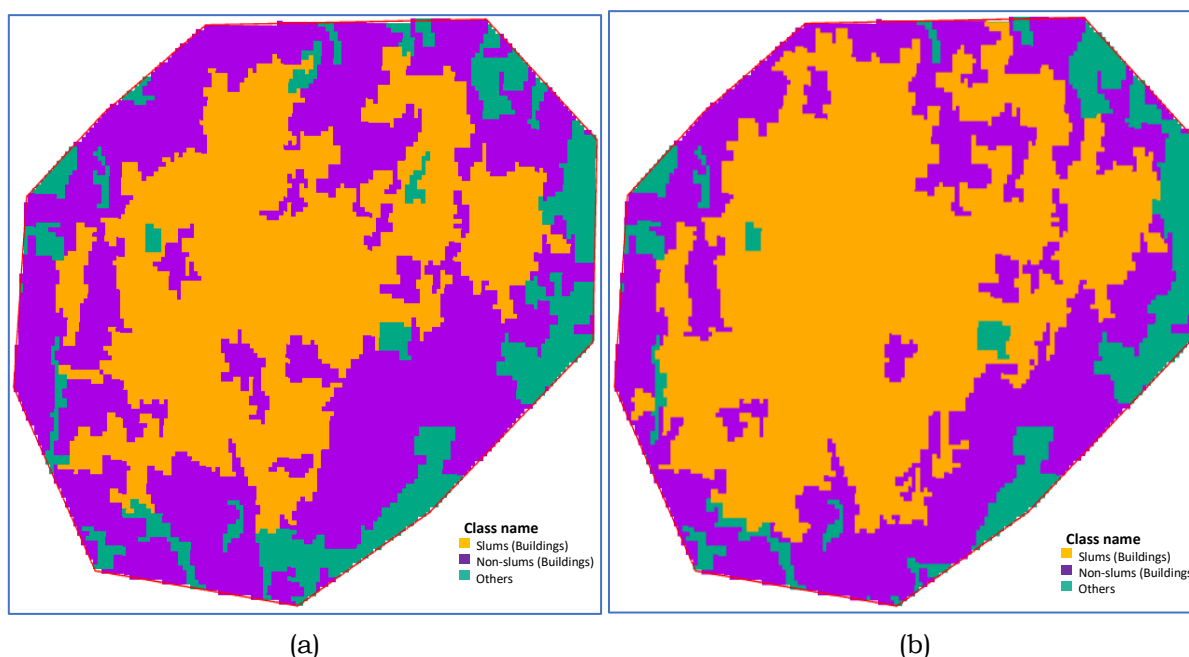


Fig 48 Clipped raster of Vila Andrade Sentinel-2 imagery for slum change calculation.

Figure 47a and 47b displayed the clipped rasters for the first set (01-01-2020) and the second set (26-12-2020) of Lagos Mainland Sentinel-2 imagery. The slum change was calculated as shown in table 11.

Table 11 The slum change calculation for Lagos Mainland

Acquisition date	Pixel count (PC)	Pixel size (PS) = (10*10)	Slum extent in m ² (SE) = (PC * PS)	Slum extent in hectares (SE) / 10000
01-01-2020	4304	100	430400	43.04
26-12-2020	5348	100	534800	53.48

Slum change (Dec. 2020 – Jan. 2020) = (53.48 – 43.04) hectares = 10.44 hectares

It was observed that the Makoko slum has grown by 10.44 hectares.

The clipped rasters from the first set (08-12-2019) and the second set (07-11-2020) of Vila Andrade Sentinel-2 imagery are shown in fig 48a and 48b. The same process was followed to detect the slum change in Vila Andrade (see table 12).

Table 12 The slum change calculation for Vila Andrade

Acquisition date	Pixel count (PC)	Pixel size (PS) = (10*10)	Slum extent in m ² (SE) = (PC * PS)	Slum extent in hectares (SE) / 10000
08-12-2019	5641	100	564100	56.41
07-11-2020	7427	100	742700	74.27

Slum change (Dec. 2019 – Nov. 2020) = (74.27 – 56.41) hectares = 17.86 hectares

The calculation above shows that the Paraisopolis slum has grown by 17.86 hectares within the period of observation.

Fig 49 presents the graphical representation of the study areas' slum changes and the difference obtained from the analysis.

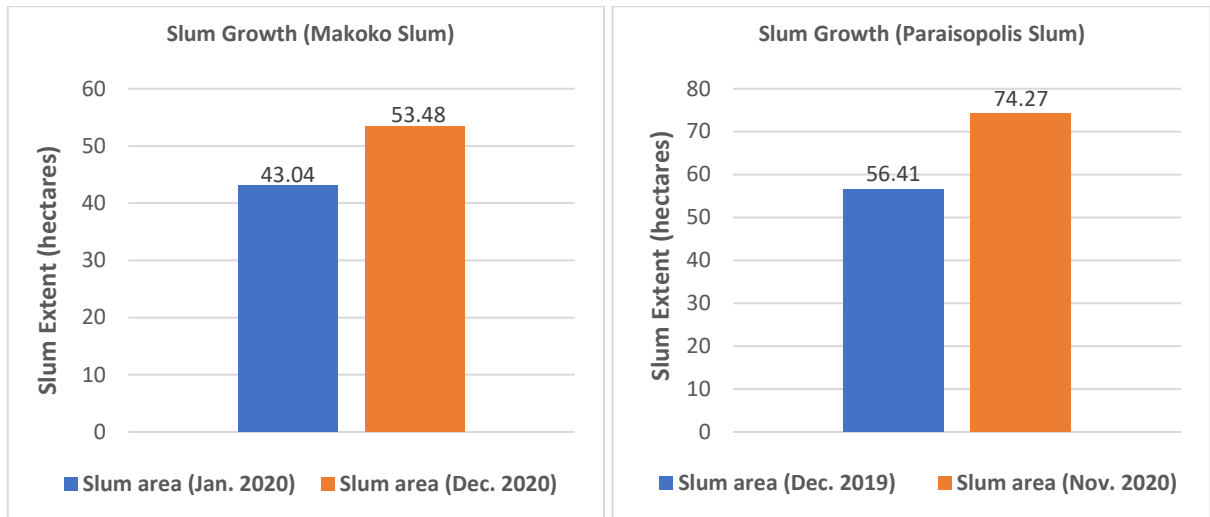


Fig 49 Graphical Representation of the Slum Growth for the study areas

During the analysis, some observations were discovered. These observations were from the Sentinel-2 imagery of the two study areas, thereby affected the slum change results.

1. Even though the Sentinel-2 imagery of both years were of the same platform (Sentinel 2B), the RGB colours (pixel colours) differs.
2. There was shift in some positions on the two imagery even though the imagery are of the same projection system.

6.6 Pixel Counts Calculation

The algorithms were further analyzed by calculating the pixels which each algorithm allocated to each class against the pixel counts as existed in the reference data. To achieve this, the reference data was rasterized using the “Polygon to raster tool” in the ArcGIS Pro. In the attribute table, the pixel count of the classes existed in the count column which were then saved as the reference pixel counts and used to plot the reference pixel count graphs as shown in fig 50 and 51.

Each reference dataset has a different number of pixels due to their difference in spatial resolution. For the Sentinel-2 imagery (10m resolution) of Lagos Mainland and Vila Andrade, their pixel counts were 158223 and 105307 pixels respectively while the drone imagery (4.9cm) and orthophoto (12cm) has 1156970589 and 731227937 pixels respectively. The reference graphs were compared to the graphs created from the classification result. It was deduced that the SVM algorithm performed better in allocating the features to their respective classes (most especially the slum area, which is the main focus of this study) than the ML and RT algorithms. In the orthophoto, the DL U-Net algorithm had the nearest percentage in terms of allocating the slum to its class than all other algorithms. Appendix 3 analyzed further the graphical representation of the classification results.

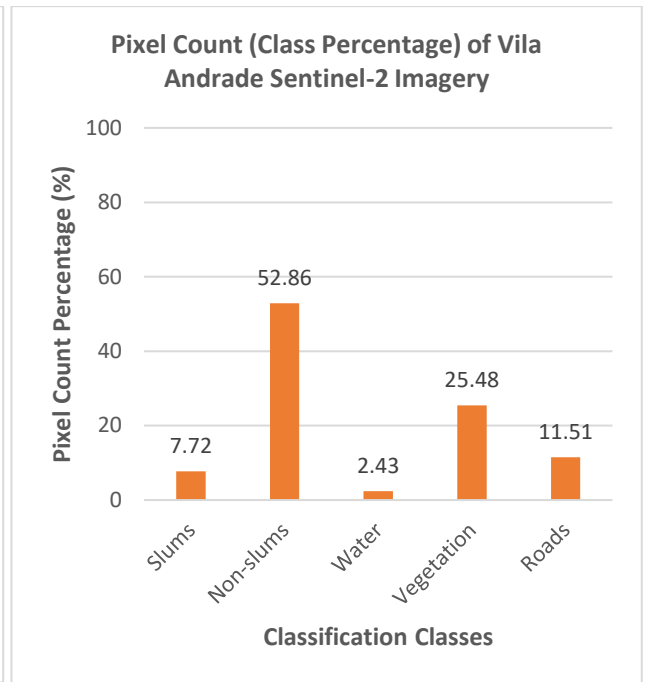
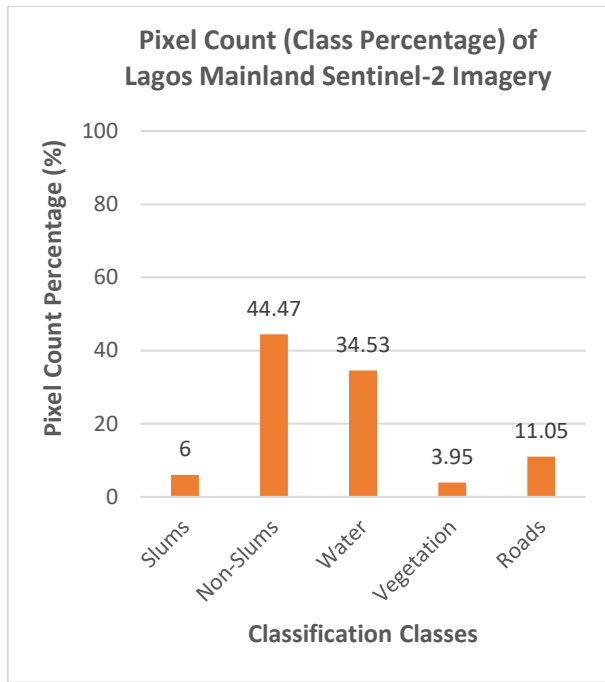


Fig 50 Pixel Counts of Sentinel-2 Imagery of Lagos Mainland (L) and Vila Andrade (R)

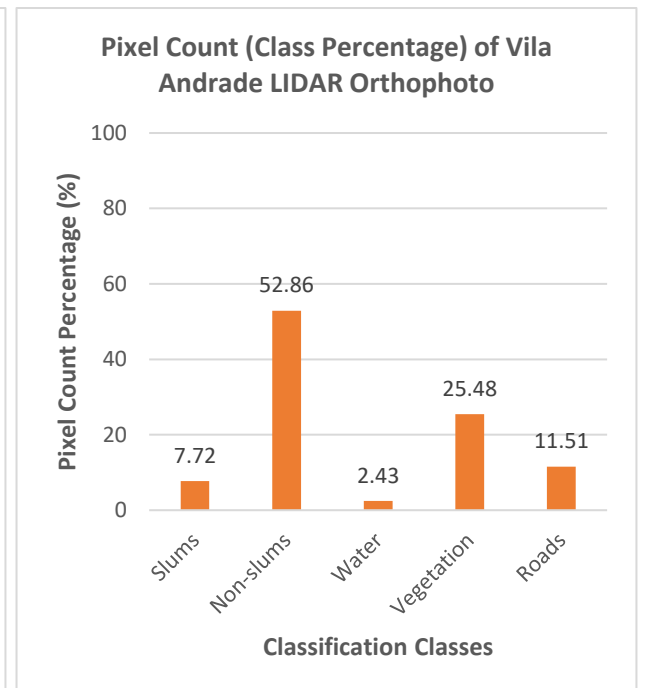
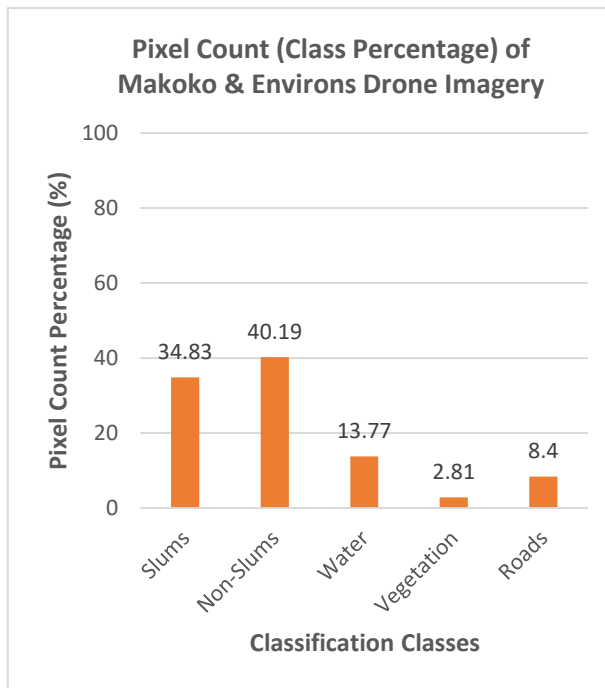


Fig 51 Pixel Counts of Drone Imagery of Makoko (L) & Orthophoto of Vila Andrade (R)

7 DISCUSSION

Slum proliferation has been a major issue for world urbanization. Determining the actual extent (delineation) of slums and the number of occupants (slum dwellers) poses more difficulty due to its continual growth. With the world population being estimated by the UN to grow more with 2.5 billion people in the next three decades of which a larger portion of this population will live in slum areas, it is evident that the current world slums need to be properly mapped to effectively control the growth which will foster slum upgrading to support the achievement of Sustainable Development Goals (SDGs) No. 11 of the UN.

This thesis demonstrated the capability of Sentinel-2 imagery for mapping and monitoring slums due to its free access and global coverage however, with the issue of cloud covers, there is a limitation as to choosing imagery for a particular date if all imagery within such date is not cloud-free. Noteworthy, three bands (B2, B3, B4) out of the 13 available spectral bands with 10m spatial resolution were adopted for this study. The spectral bands with 20m and 60m spatial resolutions are not suitable for slum mapping due to their low spatial resolutions, which might challenge the classification algorithms in detecting slum from such data. Also, another highlight of the Sentinel-2 imagery is its availability in an archived mode which can be downloaded from the Copernicus open access hub, thereby facilitated the slum change detection carried out in this thesis.

Also, VHR imagery acquired from drone and LIDAR platforms are very reliable source of information for slum mapping as demonstrated in this thesis. With such imagery, the slum areas were vividly located by visual interpretation and good knowledge of differentiating between slums and non-slum areas. The classification obtained from these data outclassed that of the result from the Sentinel-2 imagery due to their spatial resolution of 4.9cm (drone imagery) and 12cm (orthophoto) as the algorithms were able to classify the data concisely.

Initially, the DEM, DSM and building footprints were proposed as part of the data needed for this study but the available DEM and DSM for the study areas were the global DEM and DSM with 30m resolution. Such resolution is not suitable for slum mapping. Also, the OSM data was proposed for the building footprints, but the available data on OSM did not cover the study area; hence they were not suitable for the study.

The deep learning classification was not achieved on the Sentinel-2 imagery due to the unavailability of land cover data of the study area with slum classes. Many attempts were made to train the DL model with the Sentinel-2 imagery using the selected polygon samples but were unsuccessful. The DL U-Net algorithm was trained with the training samples on the drone imagery and the orthophoto. The drone imagery and orthophoto were classified successfully but overprediction and underprediction were observed from the result of the drone imagery. Also, only four (4) classes were detected from the orthophoto as the algorithm could not detect the water class but performed better in the slum area.

The result analysis from this study showed that the pixel-based and object-based SVM algorithms outclassed the maximum likelihood and random trees of both methods in all classifications. However, the object-based SVM performed better than the pixel-based SVM in the study areas. Furthermore, the findings showed that the DL U-Net algorithm could not detect the Makoko slum on the drone imagery but worked better on slums that existed on land (i.e. Paraisopolis slum in Vila Andrade) hence the algorithm

is not suitable for slums that are located on the water. To achieve a very accurate result for the DL classification, the DL model would need to be trained with lots of training data.

The result from the slum change showcased the capability of Sentinel-2 imagery for slum change monitoring and detection. The study noticed some observations regarding the difference in the RGB colours of the two imageries and displacement of features in some positions on the imagery which affected the result. Therefore, the study concludes that because slums are usually located within urban areas which in some cases has similar building morphology with urban buildings, slum change monitoring would require VHR imagery.

It is important to note that none of the algorithms could optimally map out the slum area in the study areas without little or more misclassifications, although the results obtained would suffice as a cornerstone for further research. The algorithms find it very hard to distinctly map the slum area from the non-slum area due to similar characteristics between the two classes, such as building type and structure, roof type and colour, spacing between buildings, etc.

This study can serve as a basis for mapping slums on water area as no study has fully showcased detecting and mapping Makoko slums. Furthermore, datasets like DEM, DTM and DSM can be used together with the imagery to improve the accuracy of the results. Including the elevation data would help identify the distinctive morphology of slum buildings. Building footprints could be used to estimate the population density of the slum area; OSM data can serve this purpose, although due to its crowdsourcing operations, it has been observed that not all buildings have been successfully mapped however, building footprints can be extracted from VHR imagery.

Since slums is a global challenge, this study suggests that slum areas should be added as a global land cover class and be separated from urban areas (buildings) when generating an updated global land cover as this study could not find land cover data with slum classes for the chosen study areas that can be used as either training data or reference data during the classification process.

In this time of Covid-19 pandemic where large gathering is discouraged, and social distancing might be difficult to achieve in slum areas due to the nature of the slum settlements, being able to determine the location of slums and the actual population of slum dwellers in a particular slum would afford the concerned bodies to make necessary plans and policies to curb the disease from spreading within the slum areas and beyond which can also serve the purpose of preparedness for the future epidemic. Therefore, this can be achieved with GIS and Remote Sensing coupled with the population census of the area in consideration.

This study has demonstrated the potentialities of Geoinformation technologies in the context of slum mapping. Over time, various datasets and methods have been adopted to map slums but developing a globally formalized standard methodology that would effectively map, detect and monitor the growth of slums from different regions (continents) with different slum morphology and characteristics still poses a big challenge but with the technological advancement, it is believed that this can be achieved. This methodology would be such that can facilitate near-real-time or periodic slum monitoring.

The outlooks would expand further on slum mapping, upgrading, and control, focusing on slums built on land and water or very close to the waterline area.

8 CONCLUSION

The principal goal of this thesis was to map and monitor slums using geoinformation technologies. The partial aims were to develop a test methodology for mapping and monitoring slums using open data, to leverage satellite imagery, geophysical datasets and complementary data for slum detection within different cities, to evaluate the functionalities of different algorithms and determine which algorithm provides the best result and to monitor the slum growths in the context of curbing disease outbreak.

Two study areas with different slum morphology and relief characteristics were chosen for this thesis to test whether the algorithms can map and monitor slums with different slum characteristics. The first study area was Lagos Mainland local government in Lagos, Nigeria in which Makoko slum (majorly built on water (Lagos lagoon) with sticks and woods shelters) is one of the settlements in this region. The second study area was Vila Andrade district in Sao Paulo, Brazil, which housed the Paraisopolis slum (one of the most populated slums in Brazil). In this study, three imagery were used: the Sentinel-2 imagery being the major dataset, the drone imagery, and orthophoto.

To achieve the aim of this thesis, the workflow was categorized into data acquisition, processing and analysis and finally, web application development. The data were acquired from their available platforms. Sentinel-2 imagery of the study areas were acquired from the Copernicus open access hub web portal, DJI Mavic Pro was leveraged to acquire the drone imagery of the first study area, the orthophoto of the second study area was downloaded in tiles from the Sao Paulo open access Geosampa web page and lastly, the administrative boundaries of the study areas were downloaded from GADM open portal.

The data processing and analysis involved image mosaicing, image classification, and slum change detection using the ArcGIS Pro software due to its robustness and capability for numerous GIS applications. The supervised image classification in the classification wizard of the ArcGIS Pro which housed the classification methods (pixel-based and object-based) and classification algorithms (maximum likelihood (ML), random trees (RT) and support vector machine (SVM)) was used for the image classification process.

Before the classification proper, the drone images were mosaiced and also the orthophoto since they were captured in tiles. Classification schema was created with five (5) classes (slum (buildings), non-slum (buildings), water, vegetation and roads) and training samples (polygon) were selected from the imagery, respectively. The algorithms were trained with the training sample, the trained algorithms were applied to classify the imagery and the classes were reclassified into three (3) i.e. slums (buildings), non-slums (buildings) and others (the water, vegetation and roads were combined).

Foremost, the analysis was achieved on the Sentinel-2 imagery of the study areas with the pixel-based method. At the same time, the algorithms (ML, RT, SVM) were applied respectively for the classification. Afterwards, the same training samples were used to classify the Sentinel-2 imagery with the object-based method using the same algorithms as that of the pixel-based method.

To determine whether the algorithms can map slums from different datasets (imagery) while checking their performances, pixel and object-based classification were carried out on the drone imagery and the orthophoto individually with the same training datasets as explained above.

The deep learning (DL) classification was the third method and was carried out on the drone imagery and the orthophoto. DL classification has a separate workflow in ArcGIS Pro which followed the sequence of preparing the training data, training the deep learning model and lastly classify the imagery with the trained model. Using the same

training samples from the supervised classification, the deep learning model (U-Net model) was trained and was applied to classify the drone imagery. The orthophoto was classified with the same process.

The finding of this study showed that the pixel-based and object-based SVM algorithms outperformed other algorithms for all datasets however the object-based SVM had good prediction with an overall accuracy of 68% over the pixel-based SVM (63.1%). The RT algorithm for both pixel and object-based methods had accuracies of 58.4% and 52.8% respectively followed by the ML algorithm with overall accuracies of 49.8% and 38.7% for both methods. The deep learning classification had an overall accuracy of 60%.

This study can be used as a test methodology for mapping and monitoring slums in other locations however to improve the accuracy of the results, more input data (DEM, DSM, land cover data) are evident.

LIST OF FIGURES

Fig 1 Makoko Slum in Lagos Mainland, Nigeria.....	13
Fig 2 Study Area 1 (Lagos mainland local government, Nigeria).....	14
Fig 3 Paraisópolis Slum in Vila Andrade, Brazil.....	14
Fig 4 Study Area 2 (Vila Andrade district, Brazil).....	15
Fig 5 Section view of the Sentinel-2 (L), drone imagery (M) and Makoko orthophoto (R) used for this study.....	15
Fig 6 Thesis workflow diagram.....	17
Fig 7 Traditional pixel-based image classification workflow.....	22
Fig 8 General framework of object-oriented image system.....	22
Fig 9 Framework of the RS image intelligent interpretation system.....	23
Fig 10 The homepage of the Copernicus open access hub.....	27
Fig 11 Searching the S-2 Lagos Mainland (Study area 1) on the open access hub portal.....	27
Fig 12 Searching the S-2 Vila Andrade (Study area 2) on the open access hub portal.....	28
Fig 13 Sample of the drone images of the buildings in Slum (L) and Urban areas (R).	28
Fig 14 The homepage of the Geo Sampa web portal.....	29
Fig 15 Vila Andrade imagery tiles on the web portal.....	29
Fig 16 Sample of the orthophoto of the buildings in Slum (L) and Urban areas (R).....	30
Fig 17 GADM homepage	30
Fig 18 Selection of study areas in shapefile format from GADM web portal.....	31
Fig 19 The classification wizard structure in ArcGIS Pro.....	32
Fig 20 Clipped Sentinel-2 imagery of Lagos mainland (L) and Vila Andrade (R).....	33
Fig 21 The mosaiced drone imagery (L) and orthophoto (R).....	33
Fig 22 Pixel and object-based classification workflow.....	33
Fig 23 The five classes (L) and the reclassified three classes (R).....	34
Fig 24 The selected training samples for the classification process.....	35
Fig 25 Sample of a generic random tree.....	36
Fig 26 Sample of a linear support vector machine.....	37
Fig 27 Deep learning classification workflow.....	38
Fig 28 U-Net architecture.....	38
Fig 29 The deep learning classification process for the Makoko drone imagery.....	39
Fig 30 The reference dataset for the study areas.....	40
Fig 31 The database connection and the uploaded shapefiles on PgAdmin (PostgreSQL)...42	
Fig 32 Uploading boundary shapefiles with PostGIS 3 shapefile loader.....	43
Fig 33 The Geoserver Environment.....	44
Fig 34 Section of the published data on Geoserver Environment.....	44
Fig 35 Using the leaflet library in the VS code environment.....	45
Fig 36 Web application visualizing the result of the Lagos Mainland LGA.....	46
Fig 37 Web application visualizing the result of the Vila Andrade District.....	46
Fig 38 Pixel-based classification result from Sentinel-2 imagery of Lagos Mainland..	47

Fig 39 Pixel-based classification result from Sentinel-2 imagery of Vila Andrade.....	48
Fig 40 Pixel-based classification result from drone imagery of Makoko and environs....	48
Fig 41 Pixel-based classification result from orthophoto of Vila Andrade.....	49
Fig 42 Object-based classification result from Sentinel-2 imagery of Lagos Mainland...	49
Fig 43 Object-based classification result from Sentinel-2 imagery of Vila Andrade.....	50
Fig 44 Object-based classification result from drone imagery of Makoko and environs..	50
Fig 45 Object-based classification result from orthophoto of Vila Andrade.....	51
Fig 46 Deep learning classification result of the drone imagery and the orthophoto.....	51
Fig 47 Clipped raster of Lagos Mainland Sentinel-2 imagery for slum change calculation.	55
Fig 48 Clipped raster of Vila Andrade Sentinel-2 imagery for slum change calculation.	56
Fig 59 Graphical Representation of the Slum Growth for the study areas.....	57
Fig 50 Pixel Counts of Sentinel-2 Imagery of Lagos Mainland (L) and Vila Andrade (R)..	58
Fig 51 Pixel Counts of Drone Imagery of Makoko (L) & Orthophoto of Vila Andrade (R...)	58

LIST OF TABLES

Table 1 Sentinel-2 imagery acquisition dates and the band combination used.....	16
Table 2 Attribute information about the acquired drone imagery.....	16
Table 3 Frequency of methods versus main focus for slum mapping using VHR imagery	25
Table 4 Sample of the result of confusion matrix accuracy assessment.....	40
Table 5 Set of Sentinel-2 imagery used for the change detection.....	41
Table 6 Accuracy results of the pixel and object-based methods for Lagos Mainland Sentinel-2 imagery.....	52
Table 7 Accuracy results of the pixel and object-based methods for Vila Andrade Sentinel- 2 imagery.....	53
Table 8 Accuracy results of the pixel and object-based methods for Makoko Drone imagery.....	53
Table 9 Accuracy results of the pixel and object-based methods for Vila Andrade orthophoto.....	54
Table 10 Processing time of all methods and the algorithms.....	54
Table 11 The slum change calculation for Lagos Mainland.....	56
Table 12 The slum change calculation for Vila Andrade.....	56

REFERENCES AND INFORMATION SOURCES

- ADDINK, E., VAN COILLIE, F. (2010). *Object-based Image Analysis | GIM International* [online]. [cit. 2021-01-14] Available online: <<https://www.gim-international.com/content/article/object-based-image-analysis>>.
- AGAFONKIN V. (2021). *Leaflet - a JavaScript library for interactive maps*. [online] [cit. 2021-04-24] Available online: <<https://leafletjs.com/>>.
- ARANTXA H. (2019). Paraisópolis, Brazil. A city of favelas aiming to be egalitarian, sustainable and accessible. [online] [cit. 2021-04-01] Available online: <<https://tomorrow.city/a/paraisopolis-brazil-a-city-of-favelas-aiming-to-be-egalitarian-sustainable-and-accessible>>.
- ASTRIUM (2012). *Pléiades Imagery User Guide* [online]. Geoinformation Services (October 2012 - V 2.0) [cit. 2020-12-26]. Available online: <<https://www.intelligence-airbusds.com/en/8718-user-guides>>.
- AYO, B. (2020). *Integrating OpenStreetMap Data and Sentinel-2 Imagery for Classifying and Monitoring Informal Settlements*. A Master Thesis Dissertation submitted in February 2020 at the Master Program in Geospatial Technologies at Universidade Nova de Lisboa, Portugal.
- BLASCHKE, T. (2010). Object Based Image Analysis for Remote Sensing. *ISPRS Journal of Photogrammetry and Remote Sensing* (Vol. 65, Issue 1, pp. 2–16). <https://doi.org/10.1016/j.isprsjprs.2009.06.004>.
- DARE, P. M., FRASER, C. S. (2001). Mapping informal settlements using high resolution satellite imagery. *International Journal of Remote Sensing*, 22(8), 1399–1401. <https://doi.org/10.1080/01431160120654>.
- DUQUE, J. C., PATINO, J. E., BETANCOURT, A. (2017). Exploring the Potential of machine learning for automatic slum identification from VHR imagery. *Remote Sensing*, 9(9), 1–23. <https://doi.org/10.3390/rs9090895>.
- EMEKA, IFEYINWA (2020). *Makoko, Lagos: The World's Largest Floating City* [online]. [cit. 2021-01-15] Available online: <<https://heydipyourtoesin.com/makoko-lagos-worlds-largest-floating-city/>>.
- ERDAS (1999). ERDAS Field Guide. In E. Inc. (Ed.), *Fifth Edition, Revised and Expanded* (Fifth, pp. 1–672).
- ESA (2013). *The Operational Copernicus Optical High Resolution Land Mission (Sentinel-2)* [online]. pg. 1–2. [cit. 2021-01-14] Available online: <www.esa.int/copernicus>.
- ESRI (2021a). *2D, 3D & 4D GIS Mapping Software | ArcGIS Pro* [online]. [cit. 2021-01-05] Available online: <<https://www.esri.com/en-us/arcgis/products/arcgis-pro/overview>>
- ESRI (2021b). *Accuracy Assessment—ArcGIS Pro | Documentation* [online]. [cit. 2021-04-06] Available online:<<https://pro.arcgis.com/en/pro-app/latest/help/analysis/image-analyst/accuracy-assessment.htm>>.
- ESRI (2021c). *How U-net works? | ArcGIS for Developers*. ArcGIS API for Python [online]. [cit. 2021-03-18] Available online: <<https://developers.arcgis.com/python/guide/how-unet-works/>>.
- ESRI (2021d). *The Image Classification Wizard—ArcGIS Pro | Documentation* [online]. [cit. 2021-02-02] Available online: <<https://pro.arcgis.com/en/pro-app/latest/help/analysis/image-analyst/the-image-classification-wizard.htm>>.

- FOODY, G. M. (2002). *Status of land cover classification accuracy assessment*. *Remote Sensing of Environment* Vol. 80, 185–201. doi.org/10.1016/S0034-4257(01)00295-4.
- GROHMANN, C. H. (2019). *Free LiDAR data for São Paulo City* [online]. [cit. 2021-02-22] Available online: <https://spamlab.github.io/blog/pmsp_lidar/>.
- GUO, L., CHEHATA, N., MALLET, C., BOUKIR, S. (2011). Relevance of airborne lidar and multispectral image data for urban scene classification using Random Forests. *ISPRS Journal of Photogrammetry and Remote Sensing*, 66(1), 56–66. <https://doi.org/10.1016/j.isprsjprs.2010.08.007>.
- HOFMANN, P. (2001). Detecting Informal Settlements From Ikonos Image Data Using Methods of Object Oriented Image Analysis – An Example From Cape Town (South Africa). *Remote Sensing of Urban Areas*, 35 (January 2001), 107–118.
- IBRAHIM, M. R., TITHERIDGE, H., CHENG, T., HAWORTH, J. (2018). *predictSLUMS: A new model for identifying and predicting informal settlements and slums in cities from street intersections using machine learning*. *Computers, Environment and Urban Systems*, Volume 76, 2019, pp. 31-56, ISSN 0198-9715, doi.org/10.1016/j.compenvurbsys.2019.03.005.
- JEREMY ZHANG (2019). *UNet — Line by Line Explanation* [online] - *Towards Data Science*. [cit. 2021-04-02] Available online: <<https://towardsdatascience.com/unet-line-by-line-explanation-9b191c76baf5>>
- KOHLI, D., SLIUZAS, R., KERLE, N., STEIN, A. (2011). An ontology of slums for image-based classification. *Computers, Environment and Urban Systems*, 36(2), 154–163. <https://doi.org/10.1016/j.compenvurbsys.2011.11.001>.
- KOHLI, D., SLIUZAS, R., STEIN, A. (2016). Urban slum detection using texture and spatial metrics derived from satellite imagery. In *Journal of Spatial Science* (Vol. 61, Issue 2, pp. 405–426). <https://doi.org/10.1080/14498596.2016.1138247>.
- KUFFER, M., PFEFFER, K., SLIUZAS, R. (2016). *Slums from Space — 15 Years of Slum Mapping Using Remote Sensing*. <https://doi.org/10.3390/rs8060455>.
- LANG, S., BLASCHKE, T. (2006). Bridging Remote sensing and GIS – *What are the main supportive pillars?* First international conference on Object-Based Image Analysis (OBIA 2006).. *International Archives of Photogrammetry, Remote Sensing and Spatial Information Sciences*. XXXVI.
- LEONITA, G., KUFFER, M., SLIUZAS, R., PERSELLO, C. (2018). Machine learning-based slum mapping in support of slum upgrading programs: The case of Bandung City, Indonesia. *Remote Sensing*, 10(10). <https://doi.org/10.3390/rs10101522>.
- LILLESAND T. M., KIEFER R. W. (2000). *Remote Sensing and Image Interpretation* (4th ed.). John Wiley and Sons Inc. ISBN-13: 978-0471255154.
- MAHABIR, R., CROITORU, A., CROOKS, A. T., PEGGY, A., STEFANDIS, A. (2018a). *A Critical Review of High and Very High-Resolution Remote Sensing Approaches for Detecting and Mapping Slums: Trends, Challenges and Emerging Opportunities*. <https://doi.org/10.3390/urbansci2010008>.
- MAHABIR, R., CROITORU, A., CROOKS, A. T., PEGGY, A., STEFANDIS, A. (2018b). Detecting and mapping slums using open data: a case study in Kenya. *International Journal of Digital Earth*, 13(6), 683–707. <https://doi.org/10.1080/17538947.2018.1554010>.
- MAKINDE, E. O., SALAMI, A. T., OLALEYE, J. B., OKEWUSI, O. C. (2016). Object Based and Pixel Based Classification Using Rapideye Satellite Imager of ETI-OSA, Lagos, Nigeria. *Geoinformatics FCE CTU*, 15(2), 59–70. <https://doi.org/10.14311/gi.15.2.5>.

- MAPASYST. (2019). *Geospatial Technology - What's the difference between a supervised and unsupervised image classification?* [online] [cit. 2021-02-03] Available online: <<https://mapasyst.extension.org/whats-the-difference-between-a-supervised-and-unsupervised-image-classification/>>.
- MATHER, P. (1987). *Computer Processing Methods of Remotely-Sensed Images*. St Edmundsbury Press Ltd, Bury St Edmunds, Suffolk, Wiley and Sons.
- METHU, S. (2014). *Postcards from home: Documenting Nigeria's floating community - CNN* [online] [cit. 2021-04-02] Available online: <<https://edition.cnn.com/2014/12/24/world/africa/nigeria-makoko-photograph-sulayman-afose/>>.
- MO, D. K., LIN, H., LI, J., SUN, H., XIONG, Y. M. (2007). Design and implementation of a high spatial resolution remote sensing image intelligent interpretation system. *Data Science Journal*, 6(SUPPL.). <https://doi.org/10.2481/dsj.6.S445>.
- MOUNTRAKIS, G., IM, J., OGOLE, C. (2011). Support Vector Machines in remote sensing: A review. *ISPRS Journal of Photogrammetry and Remote Sensing*, 66(3), 247–259. <https://doi.org/10.1016/j.isprsjprs.2010.11.001>.
- MUNDHE, N. (2019). *Identifying and mapping of slums in pune city using geospatial techniques*. ISPRS - International Archives of the Photogrammetry, Remote Sensing and Spatial Information Sciences. XLII-5/W3. 57-63. [10.5194/isprs-archives-XLII-5-W3-57-2019](https://doi.org/10.5194/isprs-archives-XLII-5-W3-57-2019).
- MYINT, S. W., GOBER, P., BRAZEL, A., GROSSMAN-CLARKE, S., WENG, Q. (2011). Per-pixel vs. object-based classification of urban land cover extraction using high spatial resolution imagery. *Remote Sensing of Environment*, 115(5), 1145–1161. <https://doi.org/10.1016/j.rse.2010.12.017>.
- OGC (2021). *Open Source Geospatial Foundation: GeoServer*. [online] [cit. 2021-04-22] Available online: <<http://geoserver.org/>>.
- OTTAVIANNI, J. (2020). *Mapping Makoko: A Community Stating its Right to Exist* [online]. [cit. 2020-12-20] Available online: <<https://www.urbanet.info/mapping-makoko-a-community-stating-its-right-to-exist/>>.
- PATIL, M. B., DESAI, C. G., UMRIKAR, B. N. (2012). Image Classification Tool for Land Use / Land Cover Analysis : A Comparative Study of Maximum Likelihood. *International Journal of Geology, Earth, and Environmental Sciences*, 2(3), 189–196.
- RAGHAVENDRA, S., DEKA, P. C. (2014). Support vector machine applications in the field of hydrology: A review. *Applied Soft Computing Journal*, 19, 372–386. <https://doi.org/10.1016/j.asoc.2014.02.002>.
- RANGUELOVA, E., WEEL, B., ROY, D., KUFFER, M., PFEFFER, M., LEES, M. (2018). *Pixel Image based classification of slums, built-up and non-built-up areas in Kalyan and Bangalore, India*. *European Journal of Remote Sensing*. 52. 1-22. <https://doi.org/10.1080/22797254.2018.1535838>.
- RAVINE NEWS (2018). *Makoko slum in Lagos, Nigeria*. [online] [cit. 2021-01-09] Available online: <<https://es-la.facebook.com/1933992096851171/posts/makoko-slum-in-lagos-nigeria-is-the-worlds-largest-floating-city-dubbed-the-veni/2651254115124962/>>.
- REUß, F. (2017). *Detection of favelas in Brazil using texture parameters and machine learning*. Master Thesis at Graz University of technology, Austria. January 2017, 1–94.
- RICHARDS, J. (2013). *Remote Sensing Digital Image Analysis* (pp. 99–125). https://doi.org/10.1007/978-3-642-30062-2_4.

- RODRIGUEZ-GALIANO, V. F., CHICA-OLMO, M., ABARCA-HERNANDEZ, F., ATKINSON, P. M., JEGANATHAN, C. (2012). Random Forest classification of Mediterranean land cover using multi-seasonal imagery and multi-seasonal texture. *Remote Sensing of Environment*, 121, 93–107. <https://doi.org/10.1016/j.rse.2011.12.003>.
- RONNEBERGER O., FISCHER, P., BROX, T. (2015). U-Net: Convolutional Networks for Biomedical Image Segmentation. *IEEE Access*, 9, 16591–16603. <https://doi.org/10.1109/ACCESS.2021.3053408>.
- ROY, D., BERNAL, D., LEES, M. (2019). An exploratory factor analysis model for slum severity index in Mexico City. *Urban Studies*, 57(4), 789–805. <https://doi.org/10.1177/0042098019869769>.
- ROY, D., PALAVALLI, B., MENON, N., KING, R., PFEFFER, K., LEES, M., SLOOT, P. M. A. (2018). Survey-based socio-economic data from slums in Bangalore, India. *Scientific Data*, 5, 1–9. <https://doi.org/10.1038/sdata.2017.200>.
- SAFAVIAN, S. R., LANDGREBE, D. (1991). *A Survey of Decision Tree Classifier Methodology. A Survey Of Decision Tree Classifier Methodology 1*. 21(3), 660–674.
- SANKESARA, H. (2019). *U-Net - Introducing Symmetry in Segmentation* [online]. Towards Data Science. [cit. 2021-04-02] Available online: <<https://towardsdatascience.com/u-net-b229b32b4a71>>.
- SCIKIT-LEARN (2020). *Support Vector Machines — scikit-learn 0.24.1 documentation* [online]. [cit. 2021-04-01] Available online <<https://scikit-learn.org/stable/modules/svm.html>>.
- SHEKHAR, S. (2012). Detecting Slums From Quick Bird Data in Pune Using an Object Oriented Approach. *ISPRS - International Archives of the Photogrammetry, Remote Sensing and Spatial Information Sciences*, XXXIX-B8(September), 519–524. <https://doi.org/10.5194/isprsarchives-xxxix-b8-519-2012>.
- SHEKHAR, S. (2014). Mapping for change: participatory approaches in slum planning. *Indian Cartographer*, XXXIV.
- SHELHAMER, E., LONG, J., DARRELL, T. (2017). Fully Convolutional Networks for Semantic Segmentation. In *IEEE Transactions on Pattern Analysis and Machine Intelligence* (Vol. 39, Issue 4, pp. 640–651). <https://doi.org/10.1109/TPAMI.2016.2572683>.
- SLIUZAS, R. V., KERLE, N., KUFFER, M. (2008). Object-oriented mapping of urban poverty and deprivation. In *Proceedings of the 4th EARSeL Workshop on Remote Sensing for Developing Countries in Conjunction with GISDECO 8: June 4-7, 2008, Istanbul, Turkey/European Association of Remote Sensing Laboratories (EARSeL)*, 12p.
- SLIUZAS, R., KUFFER, M., GEVAERT, C., PFEFFER, K. (2017). *Slum mapping From space to unmanned aerial vehicle based approaches*. *Joint Urban Remote Sensing Event (JURSE)*, 2017, pp. 1-4, doi: 10.1109/JURSE.2017.7924589.
- TESFAY, M. W. (2018). *A comparison of single class learning and expert system object-oriented classification for mapping slum settlements in Addis Ababa city, Ethiopia*. A Master Thesis Dissertation submitted in February 2018 at the Master Program in Geospatial Technologies at Universidade Nova de Lisboa, Portugal.
- TUCKER, C. J., GRANT, D. M., DYKSTRA, J. D. (2004). NASA's global orthorectified landsat data set. *Photogrammetric Engineering and Remote Sensing*, 70(3), 313–322. <https://doi.org/10.14358/PERS.70.3.313>.

UN-HABITAT (2003). United Nations Human Settlements Programme: The Challenges of Slums (Global Report of Human Settlements 2003). In *Analytical Biochemistry* (Vol. 238, Issue 1). Earthscan Publications Ltd. www.unhabitat.org.

UN-HABITAT (2007). Twenty First Session of the Governing Council: What are Slums and why do they exist. *Sustainable Urbanization: Local Action for Urban Poverty Reduction, Emphasis on Finance and Planning: Twenty First Session of the Governing Council 16 - 20 April 2007, Nairobi, Kenya What*, 7623151–7623153.

UNITED NATIONS (2019). *World Urbanization Prospects The 2018 Revision: Department of Economic and Social Affairs*.

VAPNIK V. N., CHERVONENKIS A. YA. (1971). *On the Uniform Convergence of the Relative Frequencies of Events to their Probabilities*. *XVI*(2), 264–280.

VILICIC, F., BERGAMO, G., PAOLA DE SALVO, M., DUARTE, S. (2009) [online]. *Violence in Paraisópolis, the second largest slum in the city*. [cit. 2021-01-12] Available online: <<https://vejasp.abril.com.br/cidades/violencia-em-paraisopolis-segunda-maior-favela-da-cidade/>>.

VOŽENÍLEK, V. Diplomové práce z geoinformatiky. Edition ed. Olomouc: Vydavatelství Univerzity Palackého, 2002.

WEEKS, J. R., HILL, A., STOW, D., GETIS, A., FUGATE, D. (2007). Can we spot a neighborhood from the air? Defining neighborhood structure in Accra, Ghana. In *GeoJournal* (Vol. 69, Issues 1–2, pp. 9–22). <https://doi.org/10.1007/s10708-007-9098-4>.

WIKIPEDIA (2020). *List of Lagos State local government areas by population* [online]. [cit. 2021-01-08] Available online: <https://en.wikipedia.org/wiki/List_of_Lagos_State_local_government_areas_by_population>.

WIKIPEDIA (2021a). *Paraisópolis (São Paulo neighborhood)* [online] [cit. 2021-04-02] Available online: <[https://pt.wikipedia.org/wiki/Paraisópolis_\(bairro_de_São_Paulo\)#cite_note-par-2](https://pt.wikipedia.org/wiki/Paraisópolis_(bairro_de_São_Paulo)#cite_note-par-2)>.

WIKIPEDIA (2021b). *U-Net* [online] [cit. 2021-04-02] Available online: [cit. 2021-04-02] Available online: <<https://en.wikipedia.org/wiki/U-Net>>.

WIKIPEDIA (2021c). *Vila Andrade* [online] [cit. 2021-02-01] Available online: <https://pt.wikipedia.org/wiki/Vila_Andrade>.

WORLDPOPULATIONREVIEW (2021). *Lagos Population 2021 (Demographics, Maps, Graphs)*. [online] [cit. 2021-03-11] Available online: <<https://worldpopulationreview.com/world-cities/lagos-population>>.

YAN G., (2003). Pixel based and object oriented image analysis for coal fire research. *International Institute for Geo-Information and Earth Observation (TIC), Master*, 93. www.itc.nl/library/papers_2003/msc/ereg/gao_yan.pdf.

ZHOU, H., WANG, X., SCHAEFER, G. (2011). Mean shift and its application in image segmentation. *Studies in Computational Intelligence*, 339(61401413), 291–312. https://doi.org/10.1007/978-3-642-17934-1_13.

ATTACHMENTS

LIST OF ATTACHMENTS

Bound attachments:

Appendix 1: Results of pixel-based classifications for five classes

Appendix 2: Results of object-based and deep learning classifications for five classes

Appendix 3: Graphs showing the pixel count of classification results of the pixel-based method

Appendix 4: Graphs showing the pixel count of classification results of the object-based method

Appendix 5: Graphs showing the pixel count of classification results of the deep learning-based method

Free attachments

Appendix 6: Poster

Appendix 7: USB Pen Drive

USB Pen Drive Structure

Directories:

Analysis

Data

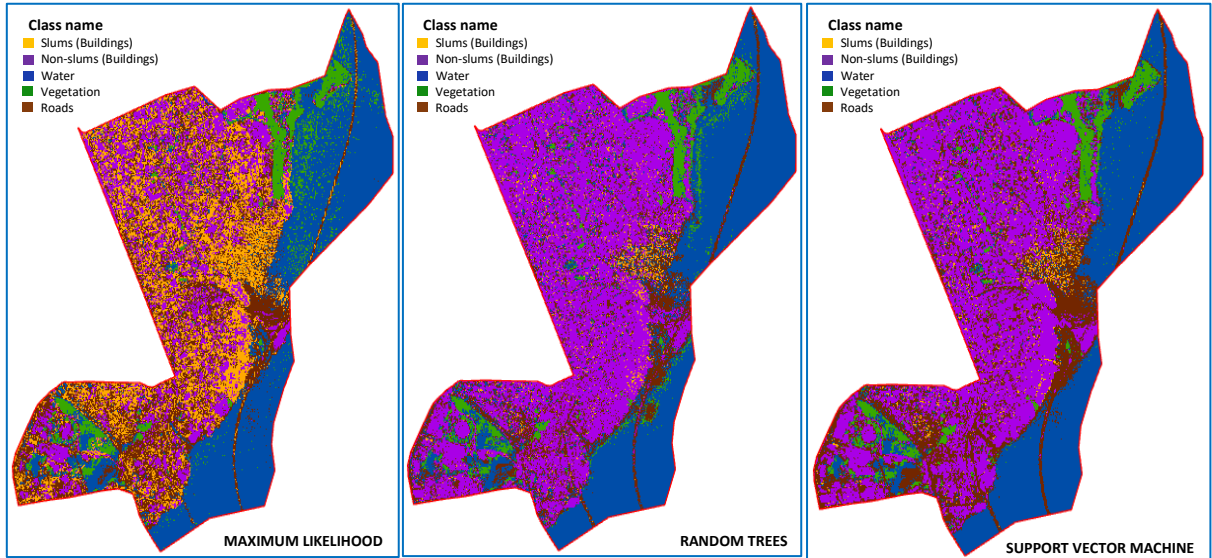
Poster

Text

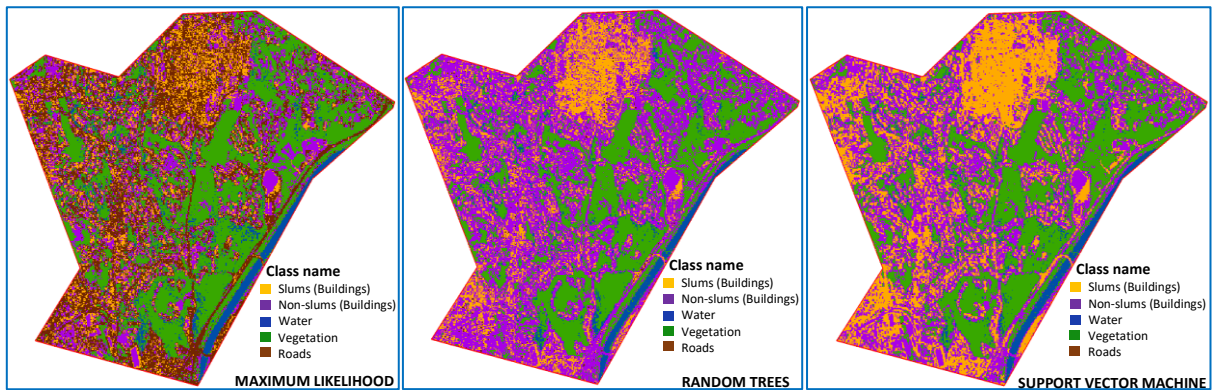
Website

APPENDIX 1

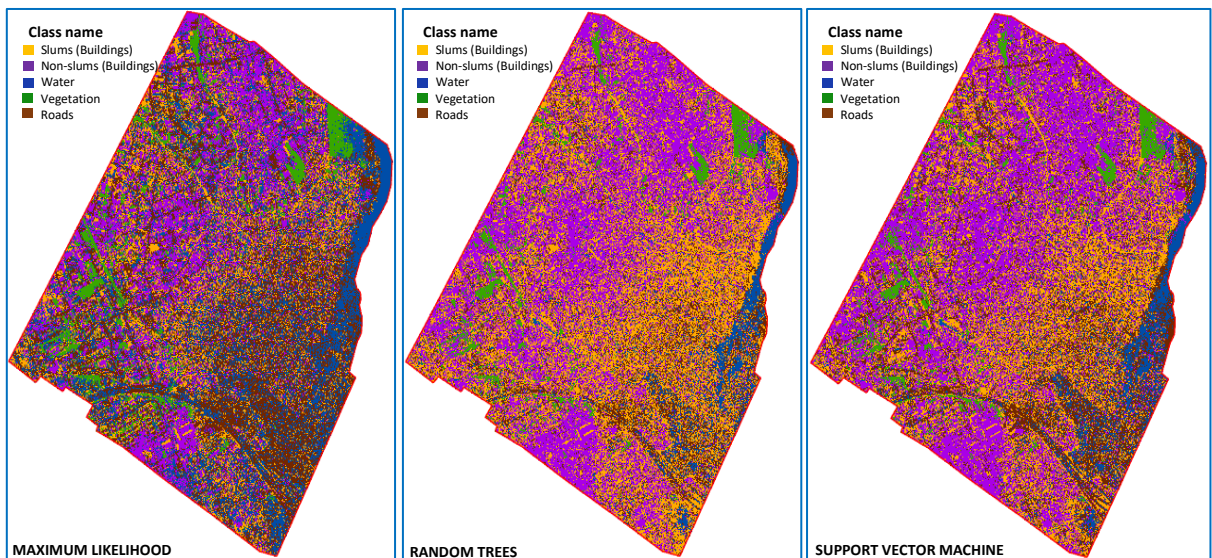
Results Of Pixel-Based Classifications For Five Classes



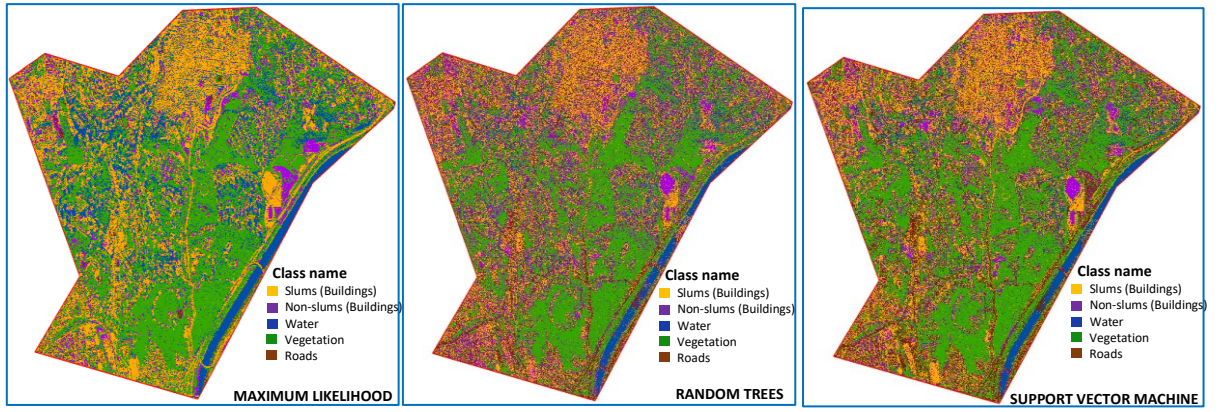
Pixel-based classification result from Sentinel-2 imagery of Lagos Mainland (5classes)



Pixel-based classification result from Sentinel-2 imagery of Vila Andrade (5classes)



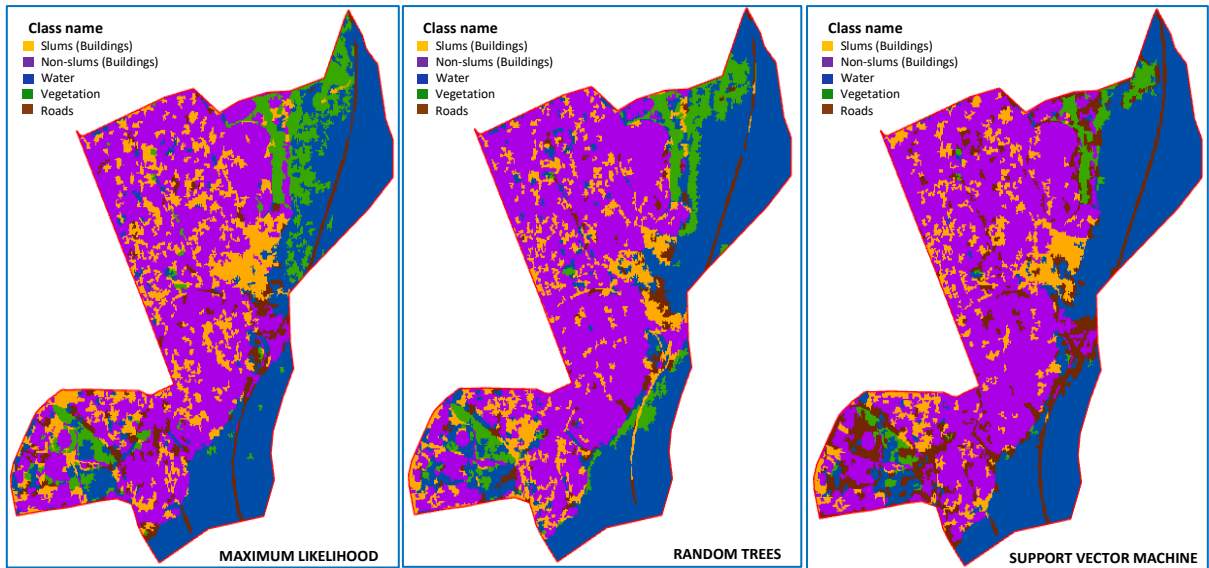
Pixel-based classification result from Drone Imagery of Makoko and environs (5classes)



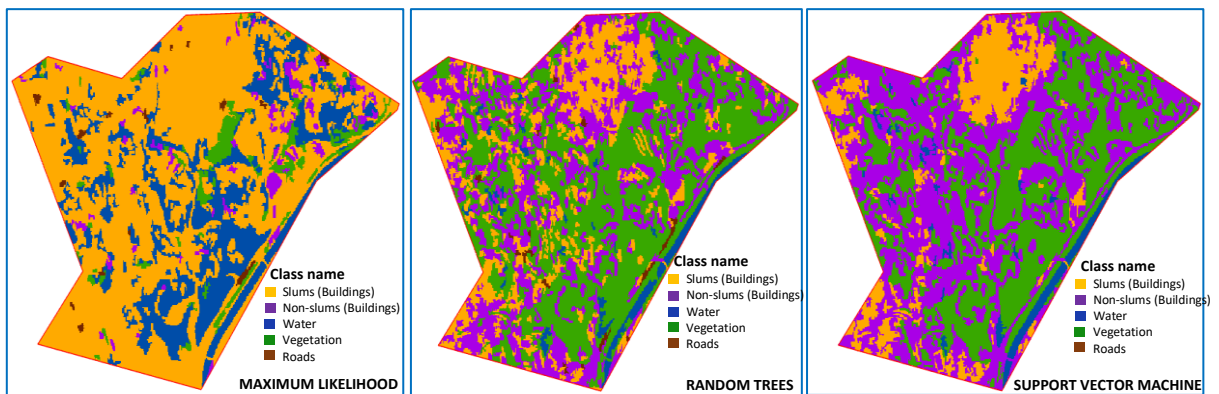
Pixel-based classification result from Orthophoto of Vila Andrade (5classes)

APPENDIX 2

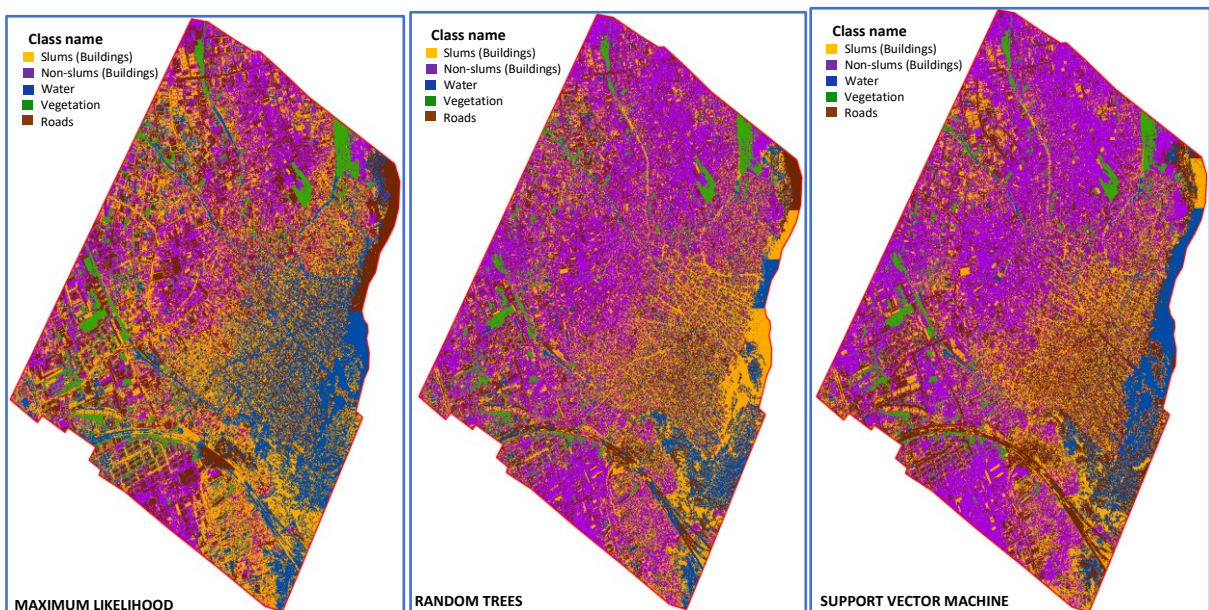
Results Of Object-Based Classifications For Five Classes



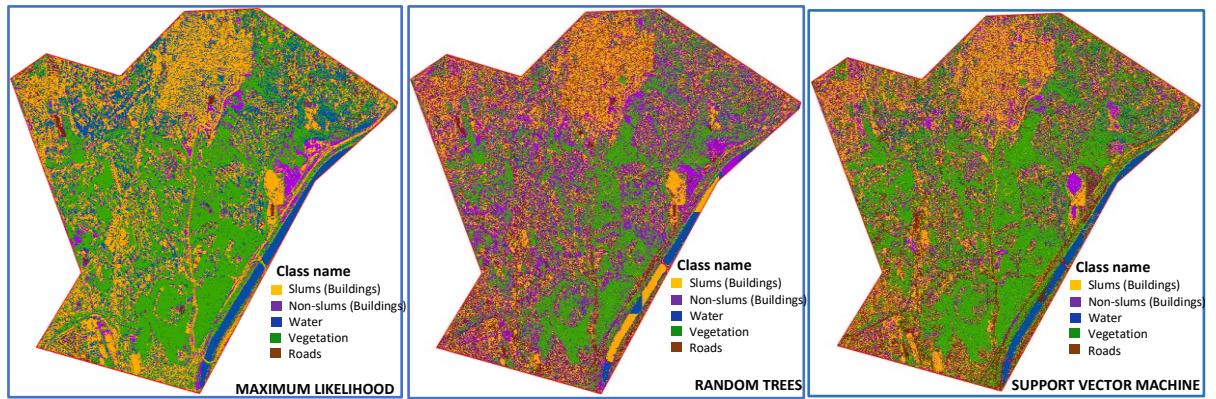
Object-based classification result from Sentinel-2 imagery of Lagos Mainland (5classes)



Object-based classification result from Sentinel-2 imagery of Vila Andrade (5classes)

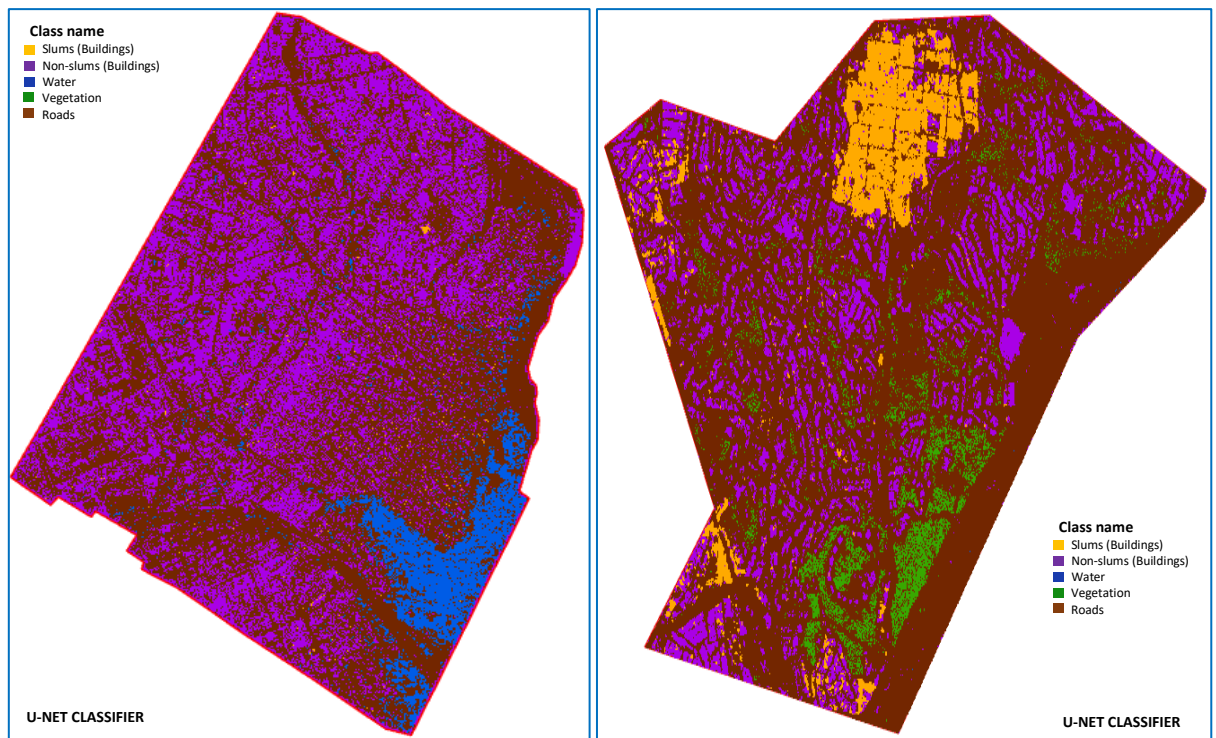


Object-based classification result from Drone Imagery of Makoko and environs (5classes)



Object-Based Classification Result From Orthophoto Of Vila Andrade (5classes)

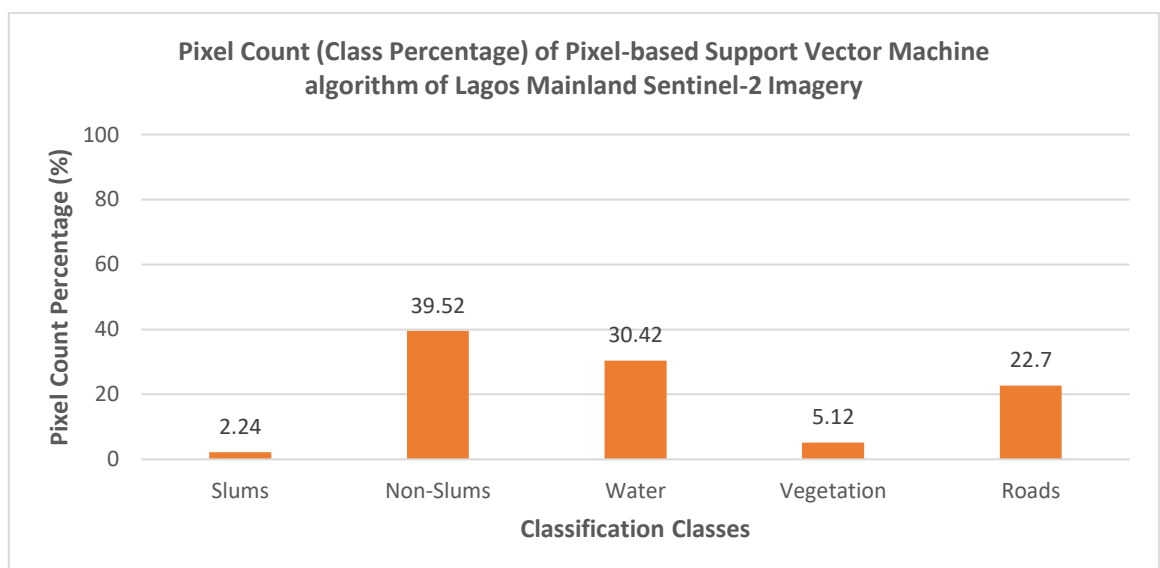
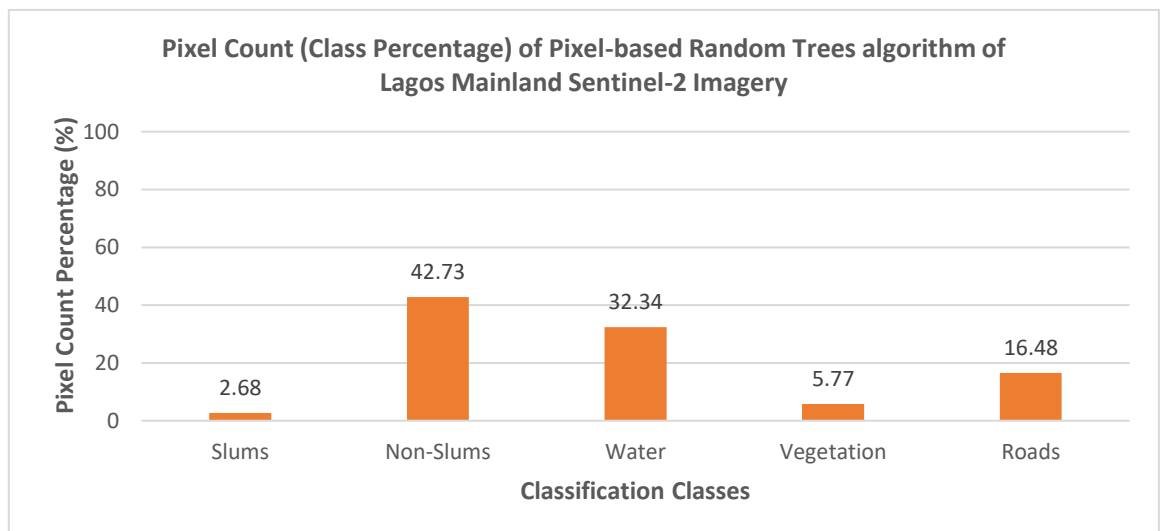
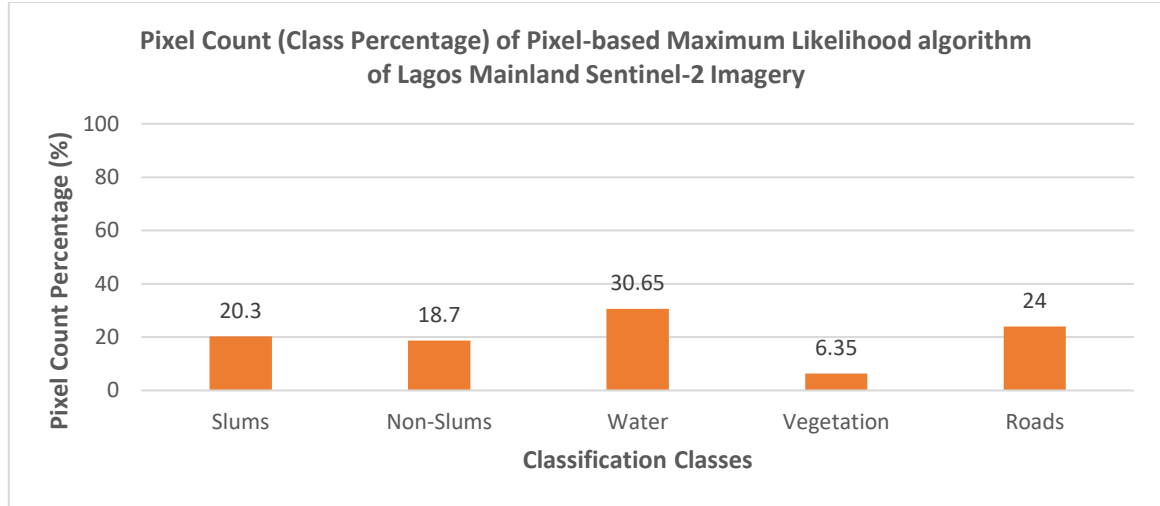
Results Of Deep Learning Classifications For Five Classes



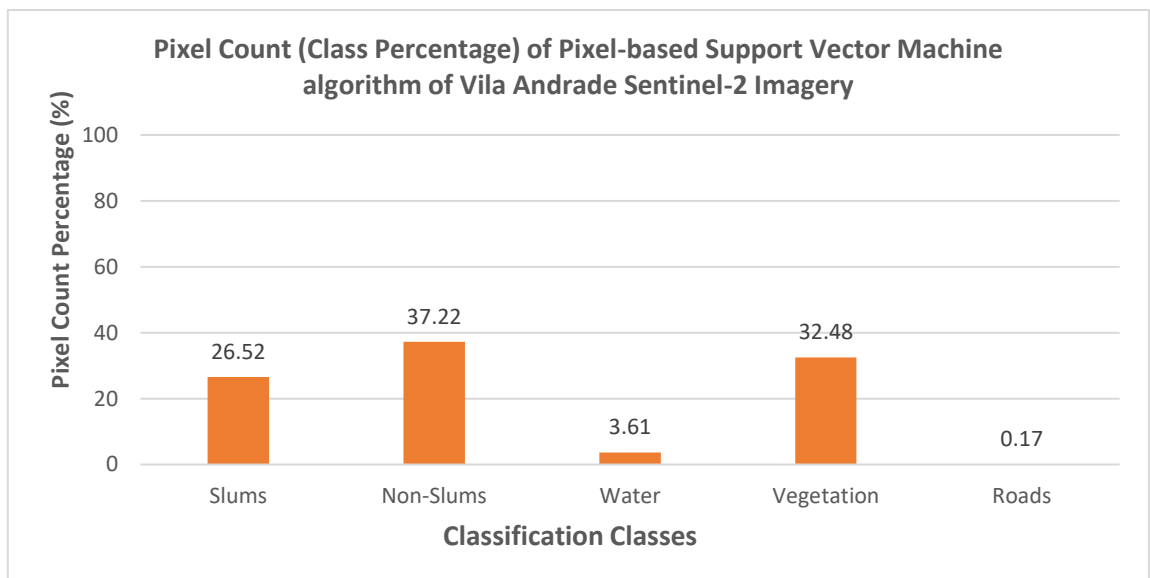
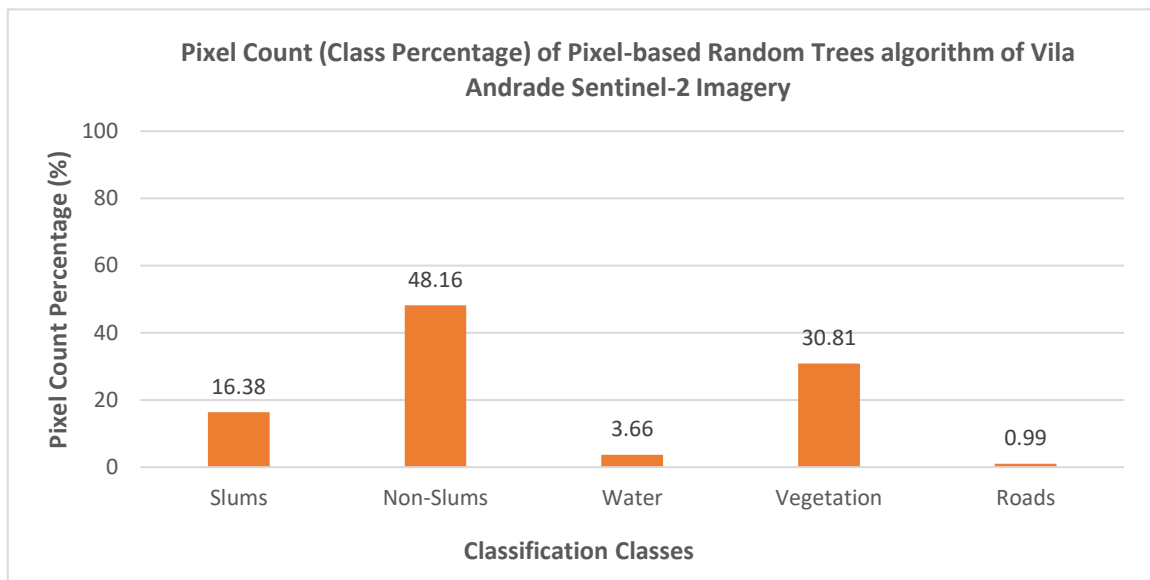
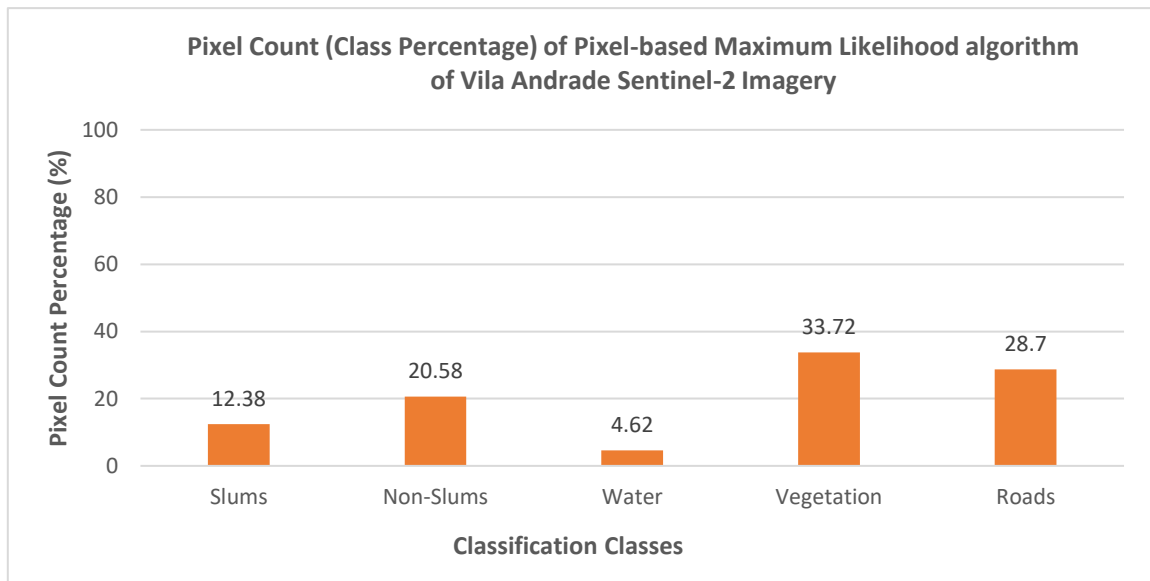
APPENDIX 3

Graphs showing the pixel count of classification results of the pixel-based method

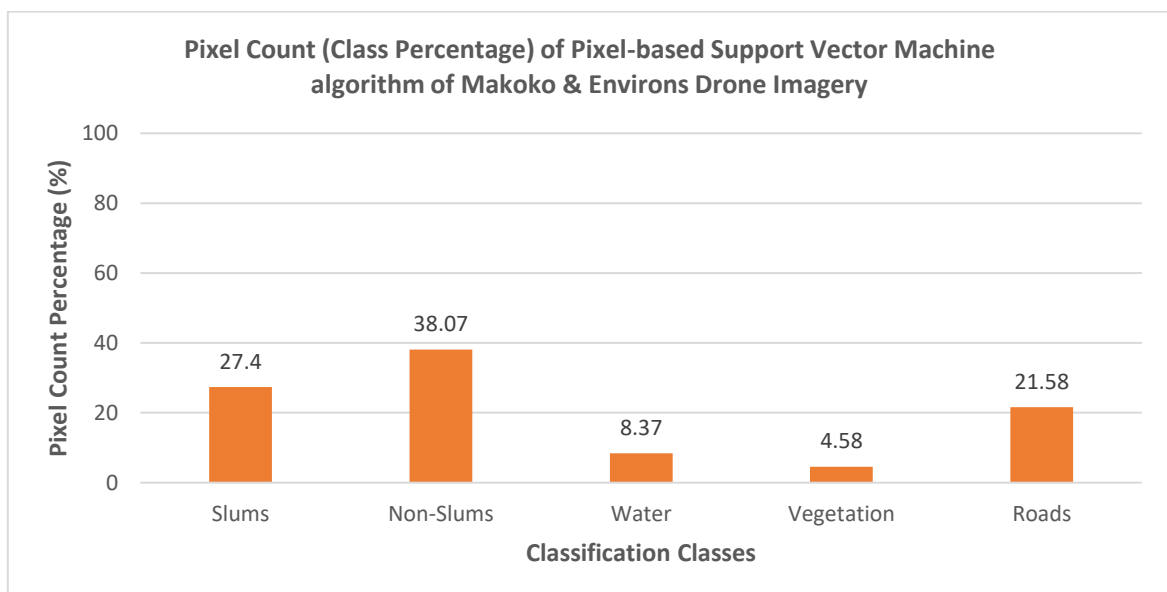
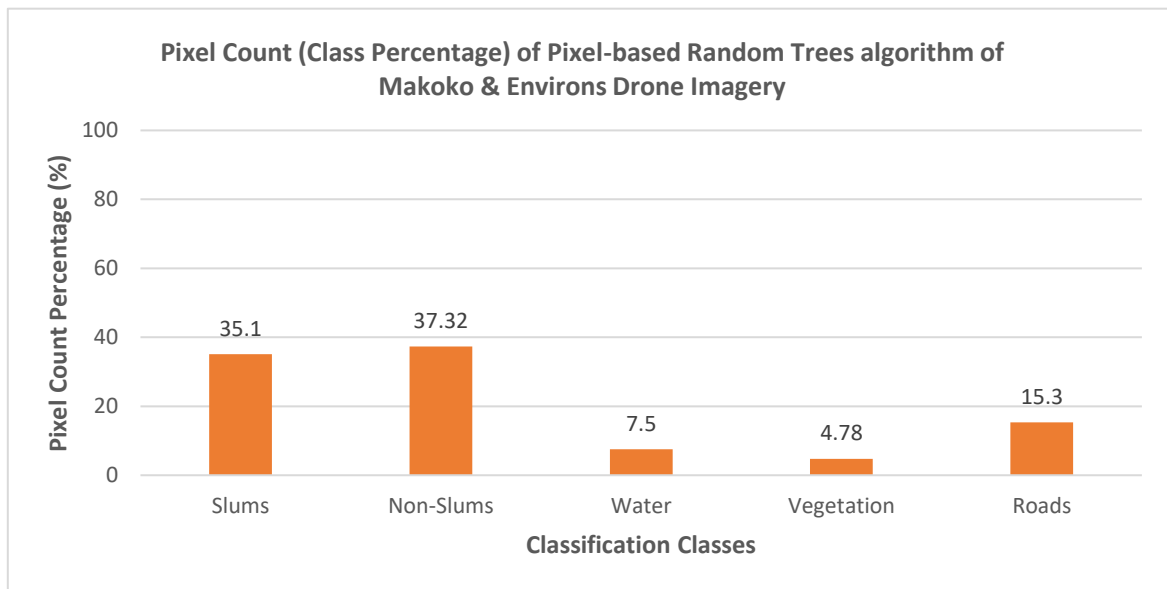
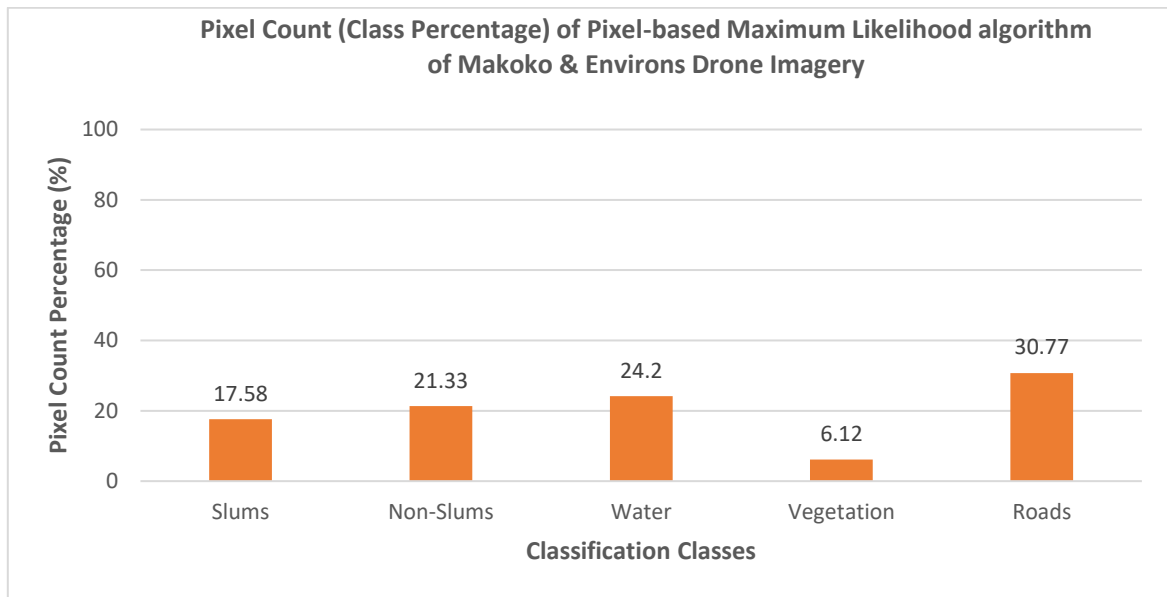
- **Sentinel-2 Imagery of Lagos Mainland**



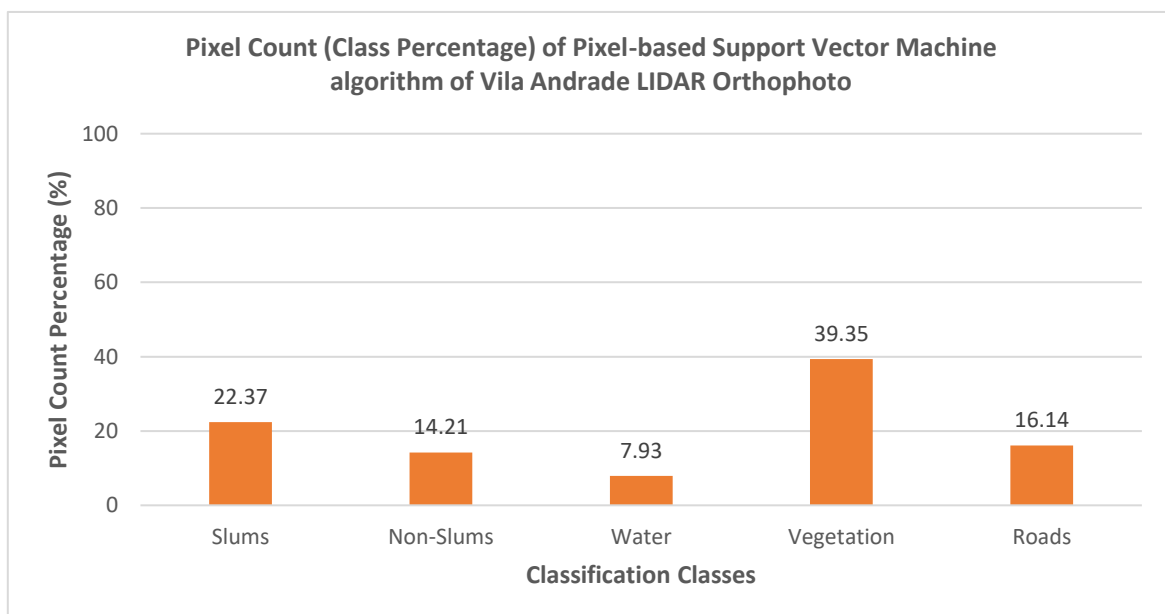
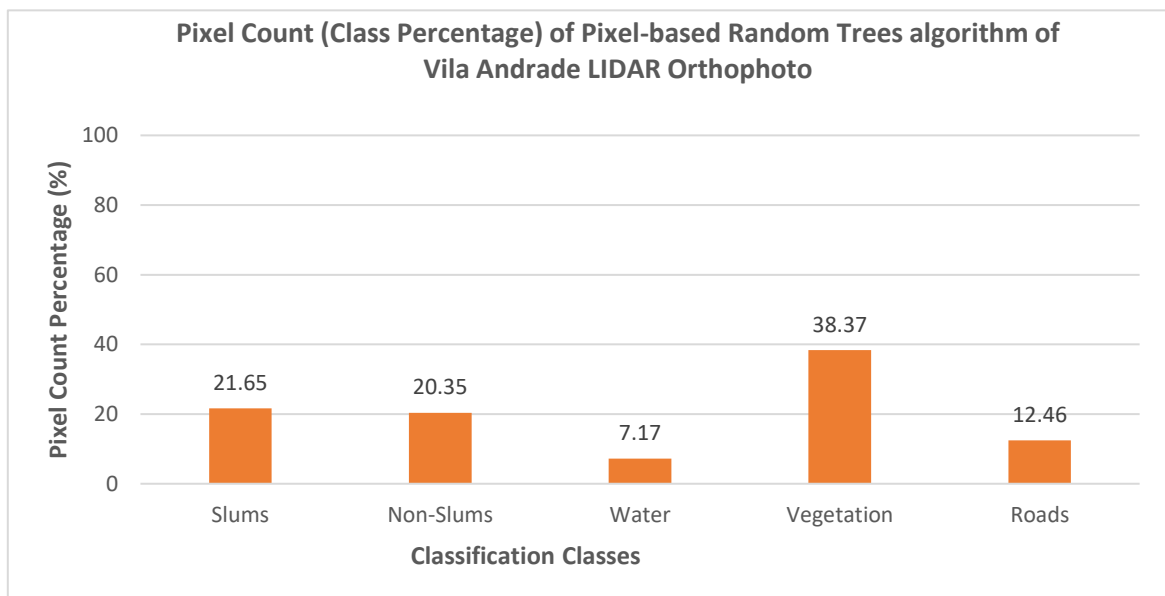
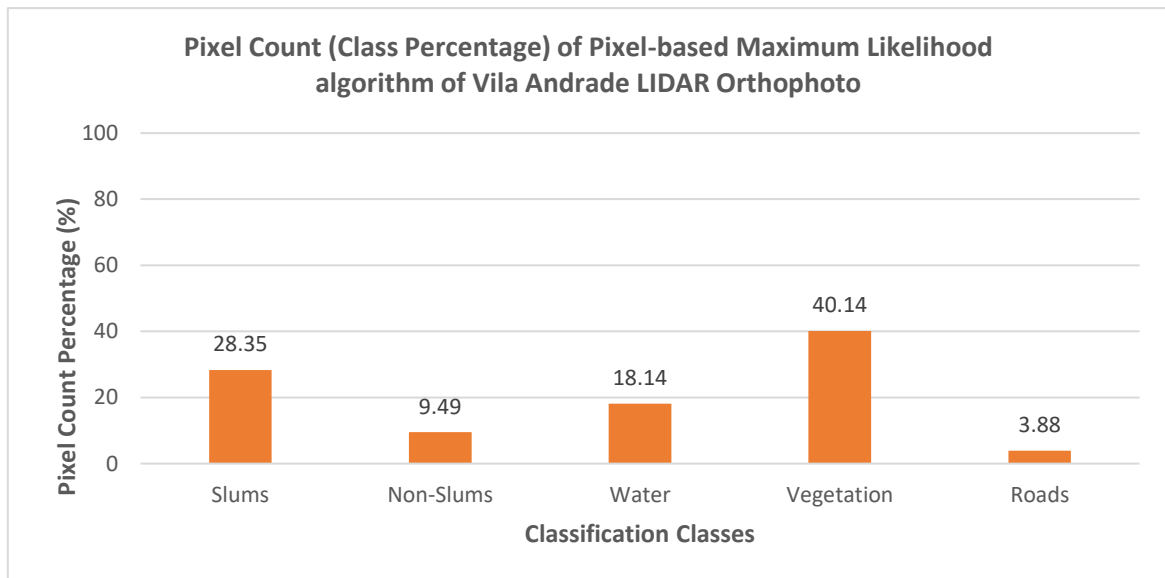
- **Sentinel-2 Imagery of Vila Andrade**



- **Drone Imagery of Makoko and Environs**



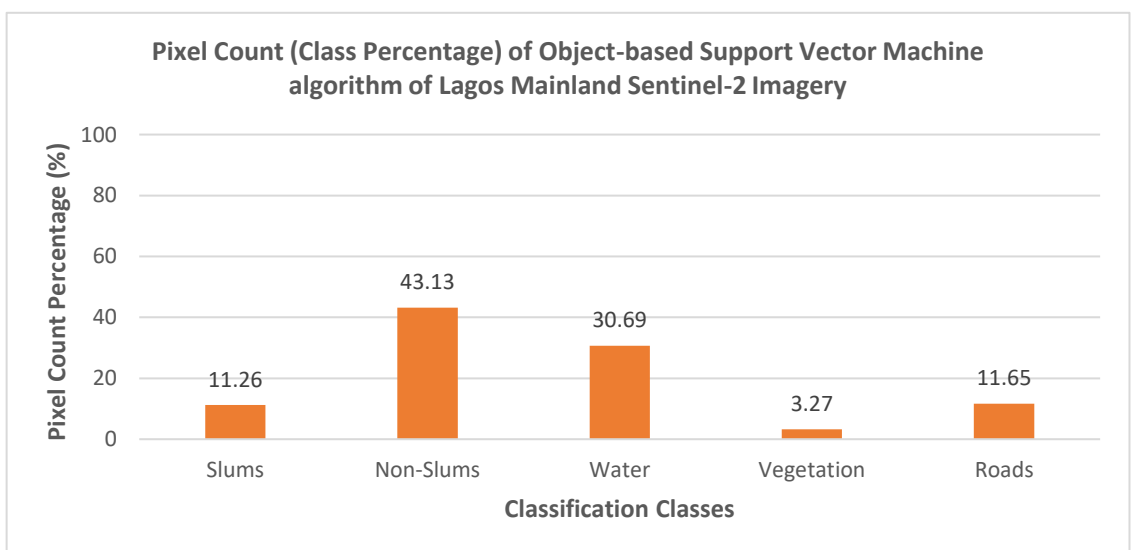
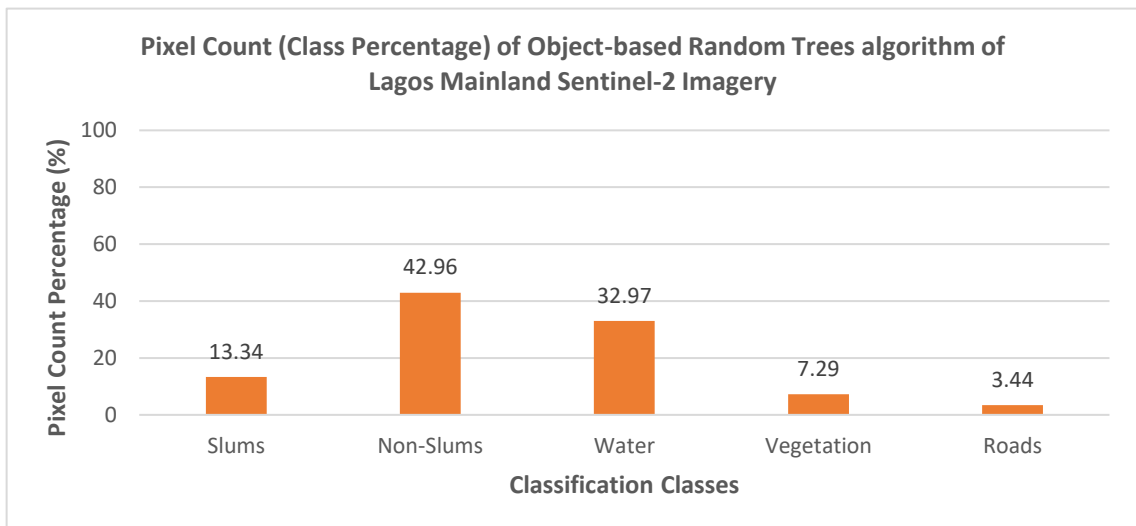
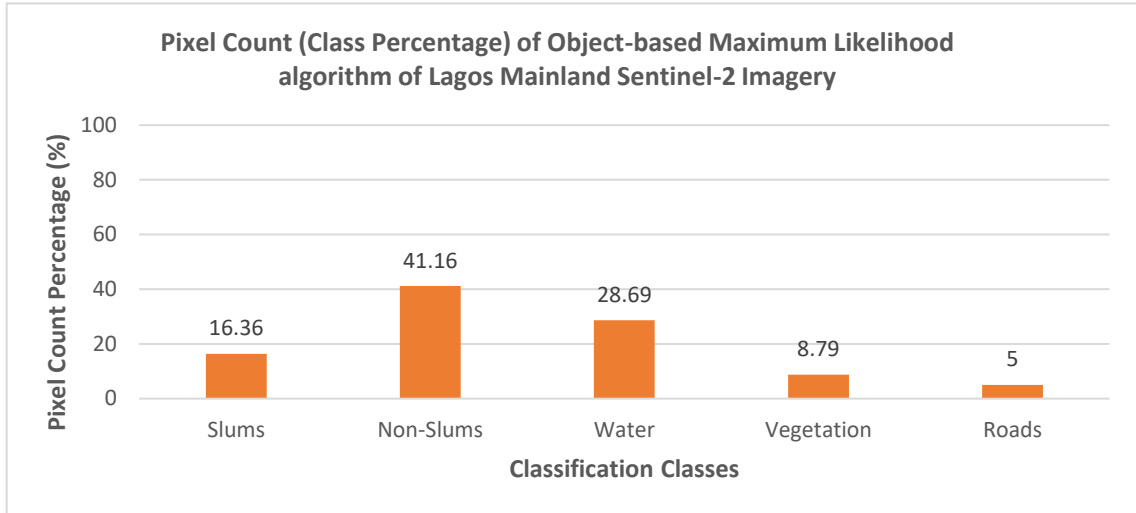
- **Orthophoto of Vila Andrade**



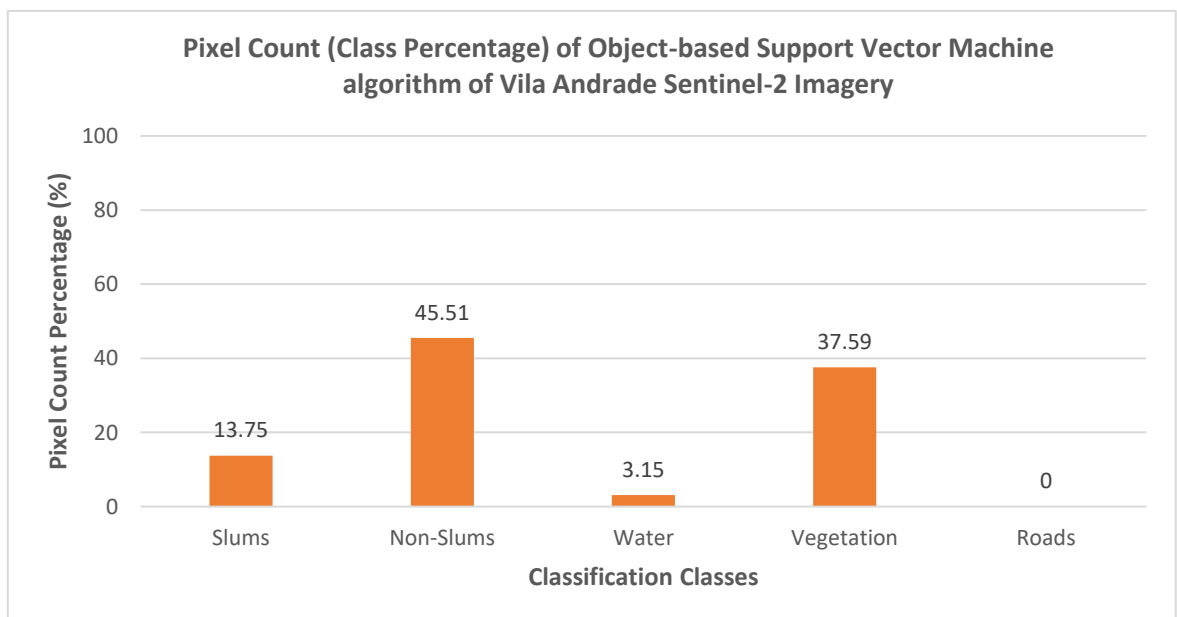
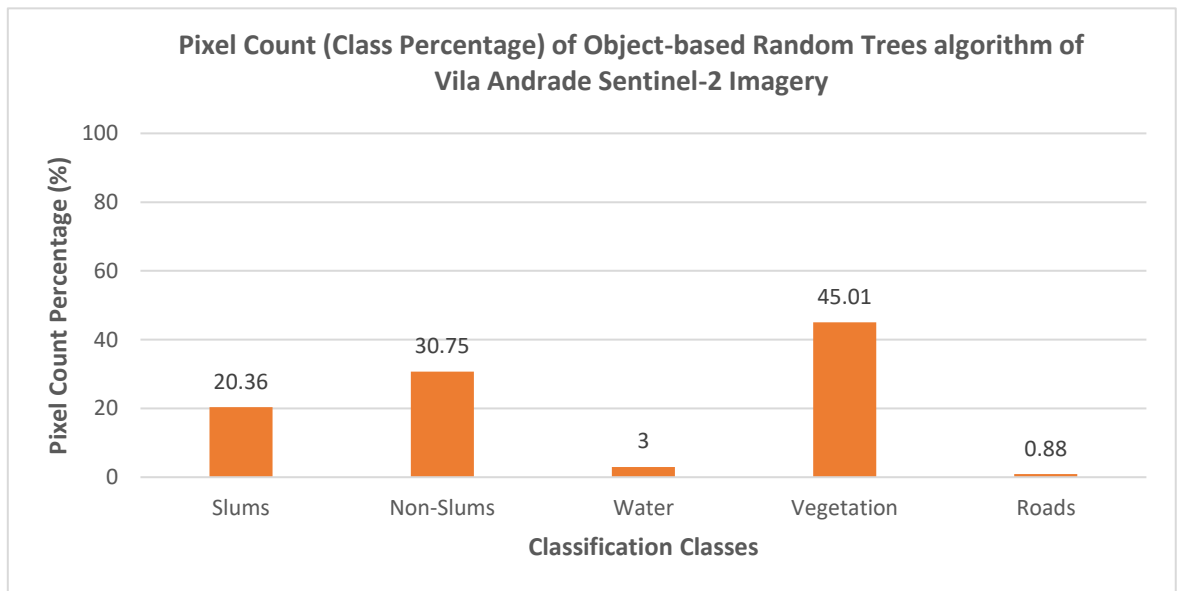
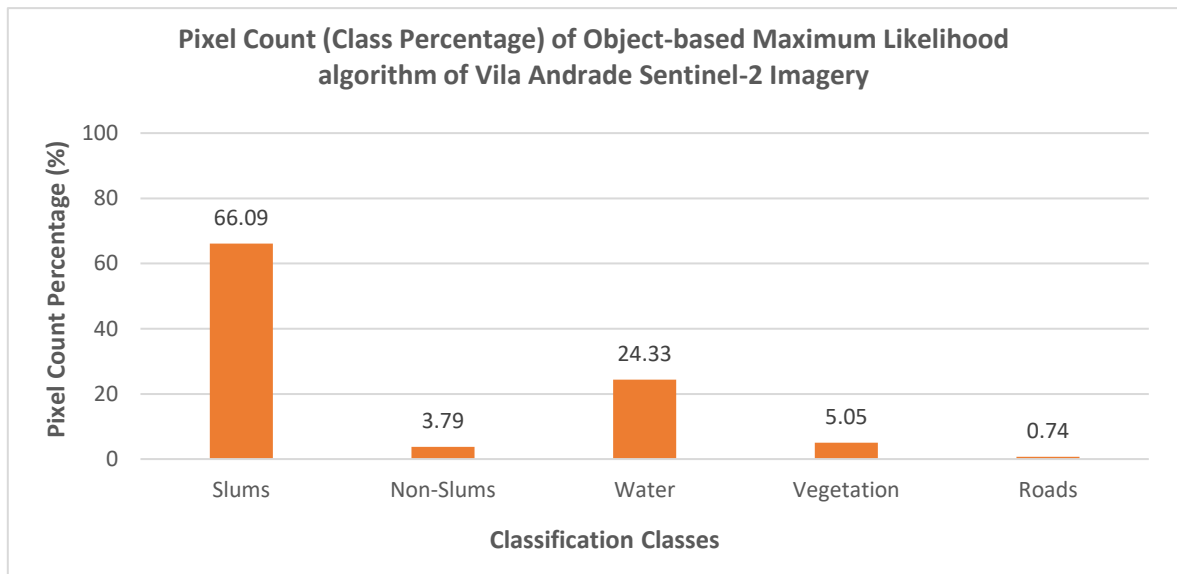
APPENDIX 4

Graphs showing the pixel count of classification results of the object-based method

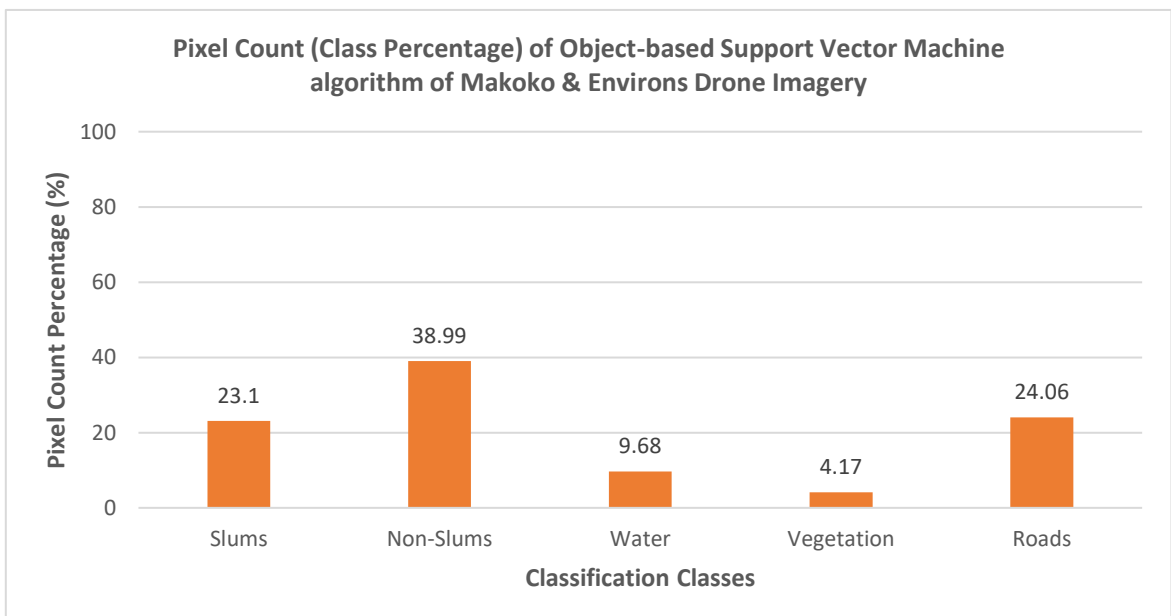
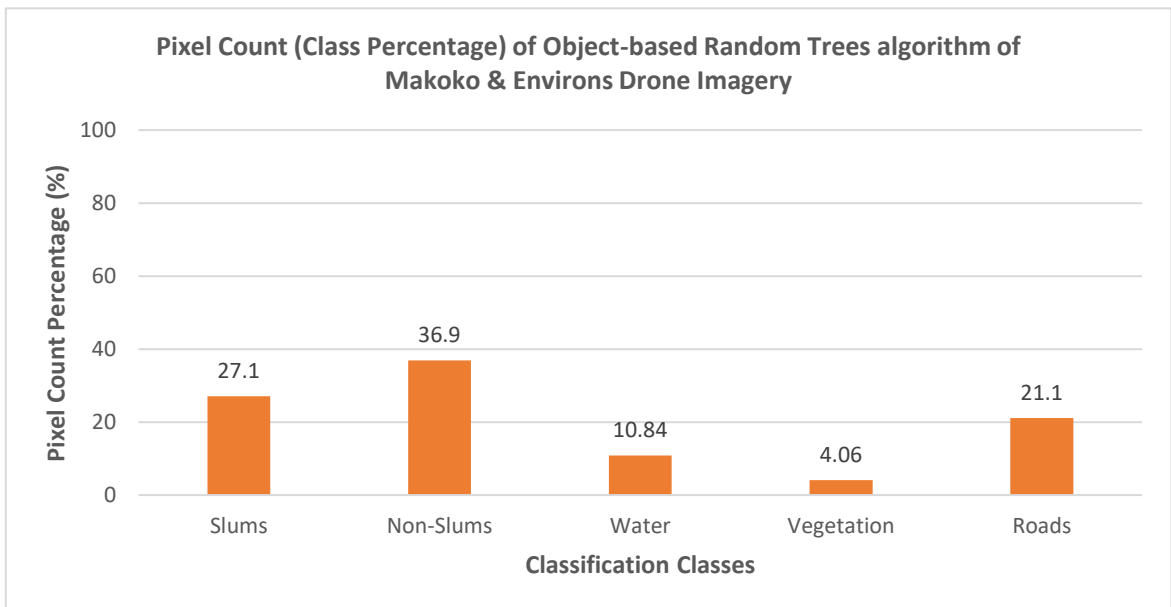
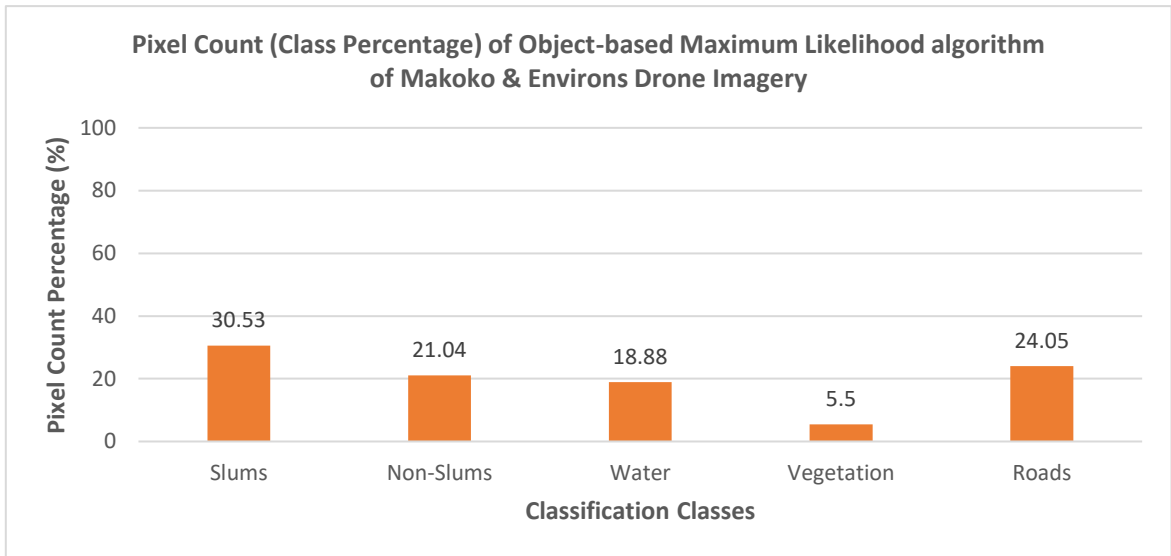
- **Sentinel-2 Imagery of Lagos Mainland**



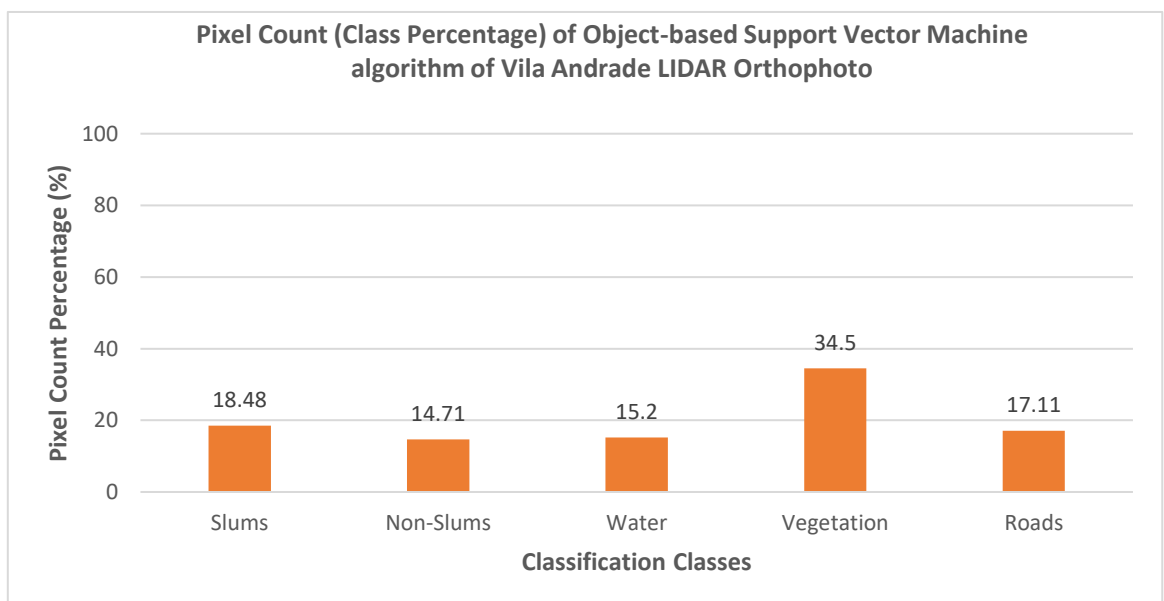
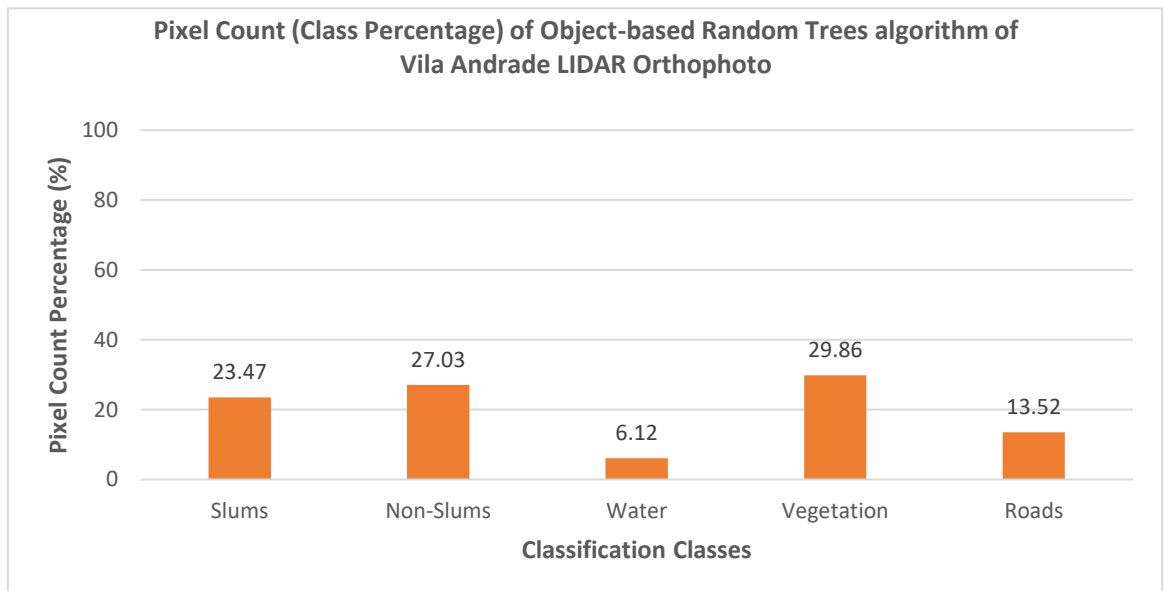
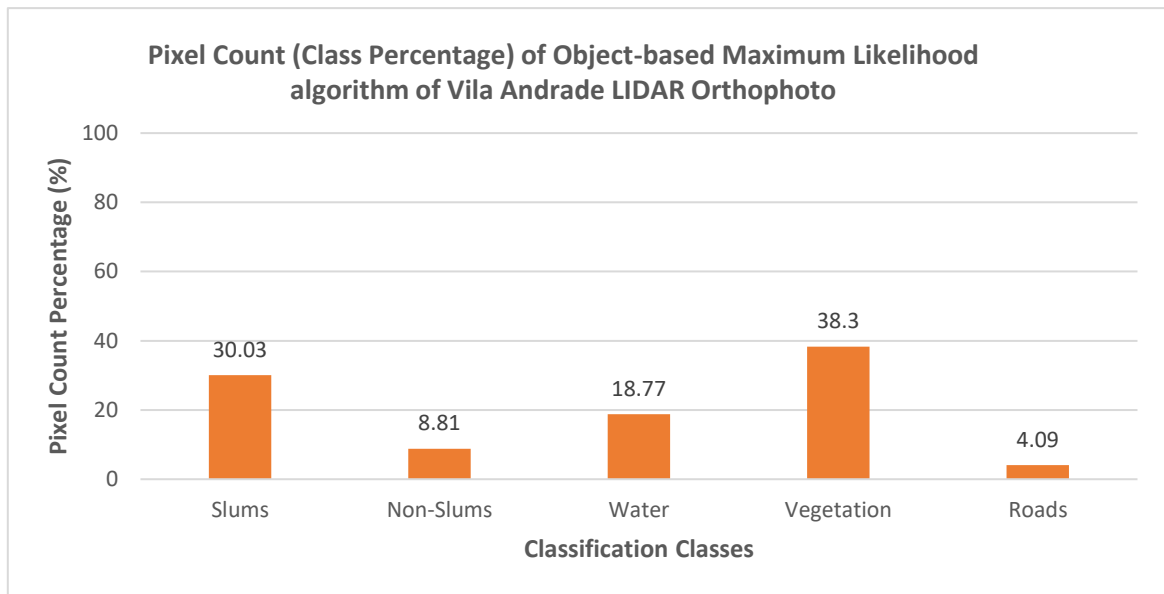
- **Sentinel-2 Imagery of Vila Andrade**



- **Drone Imagery of Makoko and Environs**



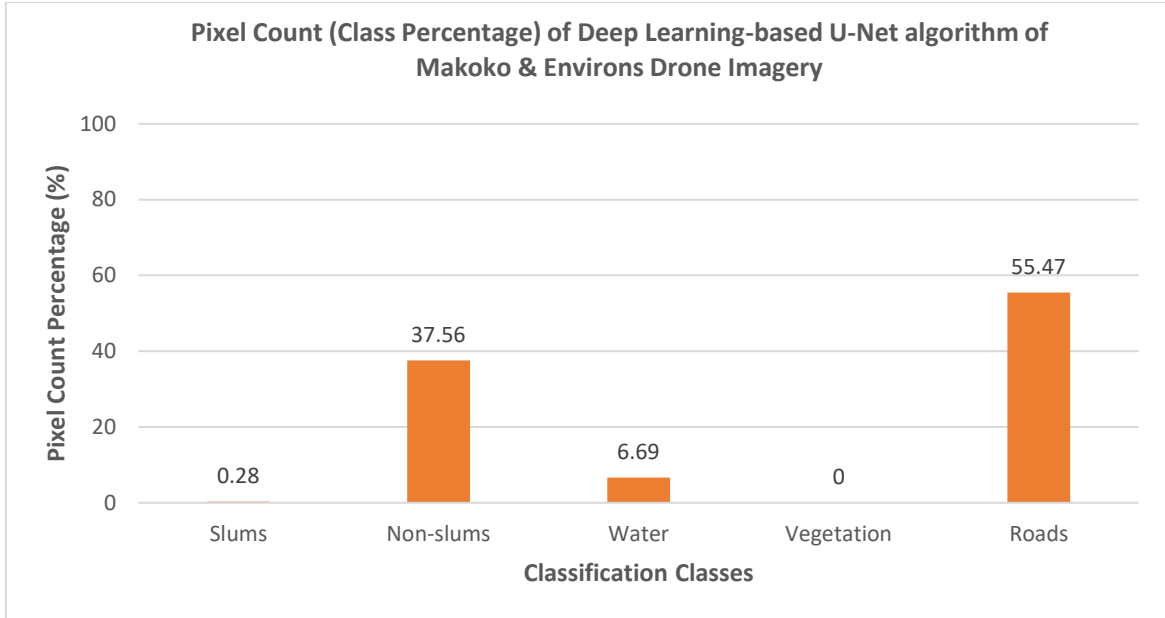
- **Orthophoto of Vila Andrade**



APPENDIX 5

Graphs showing the pixel count of classification results of the deep learning-based method

- **Drone Imagery of Makoko and Environs**



- **Orthophoto of Vila Andrade**

